Power Quality Assessment & Mitigation in Distribution System
(A Case Study at Adama Spinning Factory)

By: Henock Habte

A Thesis Submitted to the

Department of Electrical and Computer Engineering

School of Electrical Engineering and Computing

Presented in Partial Fulfillment of the Requirements for the Degree of

Masters of Science in Electrical Engineering (Power Engineering)

Office of Graduate Studies

Adama Science and Technology University

Adama

May, 2018

Power Quality Assessment & Mitigation in Distribution System

(A Case Study at Adama Spinning Factory)

By: Henock Habte

Advisor: Dr. Tafesse Asrat

Co-advisor: Milkias Berhanu

A Thesis Submitted to the

Department of Electrical and Computer Engineering

School of Electrical Engineering and Computing

Presented in Partial Fulfillment of the Requirements for the Degree of

Masters of Science in Electrical Engineering (Power Engineering)

Office of Graduate Studies

Adama Science and Technology University

Adama

May, 2018

APPROVAL SHEET

We, the undersigned, members of the Board of Examiners of the final open defense by Henock Habte, have read and evaluated his thesis entitled "Power Quality Assessment & Mitigation in Distribution System (A Case Study at Adama Spinning Factory)" and examined the candidate.

This is, therefore, to certify that the thesis has been accepted in partial fulfillment of the requirement of the Degree of Masters of Science in Electrical Engineering (Power Engineering).

Supervisor/Advisor	Signature	Date
Chairperson	Signature	Date
Internal Examiner	Signature	Date
External Examiner	Signature	Date

DECLARATION OF STUDENT AND ADVISOR

I hereby declare that this MSc Thesis is my original work and has not been presented for a degree in any other university, and all sources of material used for this thesis have been duly acknowledged.

Name: ____

Signature: ____________________________________

This MSc Thesis has been submitted for examination with my approval as thesis advisor.

Name: ____

Signature: ____________________________________

Date of Submission: _____________

ACKNOWLEDGEMENT

First of all I would like to thank my advisor Dr. Tafesse Asrat and Co-advisor Ato Milkias Berhanu for their guidance, support and motivation for completing this thesis work.

I would like to express my deepest thanks to all the management staffs of Adama Spinning Factory especially to Ato Tadesse Ayele, Engineering and Technic Manager and Ato Getu Shimeles, Electrical Maintenance Division Head of the factory. Without their willingness and help, it was not possible to regularly attend my courses and complete my MSc.

I extend my sincere thanks to all Adama Spinning Factory Electrical Maintenance staffs for their kind help in recording the measurement data of the factory day and night.

I am grateful to my families and friends for their continuous support.

TABLE OF CONTENTS

LIST OF TABLES

TABLE **PAGE**

LIST OF FIGURES AND ILLUSTRATIONS

FIGURES **PAGE**

LIST OF ABBREVIATIONS AND SYMBOLS

IEEE - Institute of Electrical and Electronics Engineers

IEC - International Electro-technical Commission

DVR - Dynamic Voltage Restorer

DSTATCOM - Distribution Static Synchronous Compensator

THD_I / THD_V - Total Harmonic Distortion current/voltage

TDD - Total Demand Distortion

EMC - Electromagnetic Compatibility

ESA - Ethiopian Standards Agency

NECE - National Electro-technical Committee of Ethiopia

CMDB - Central Main Distribution Board

ASD - Adjustable Speed Drives

PFC - Power Factor Controller

PCC - Point of Common Coupling

CT - Current Transformer

CPD - Custom Power Devices

VSI - Voltage Source Inverter

SRF - Synchronous Reference Frame

IRP - Instantaneous Reactive Power

MOSFET - Metal Oxide Field Effect Transistor

IGBT - Insulated Gate Bipolar Transistor

V_h - rms Voltage at Harmonic Order h

I_h - rms Current at Harmonic Order h

I_L - Maximum Demand Load Current

f_r - Resonant Frequency

I_{sc} - Short Circuit Current

Z_{sc} - Short Circuit Impedance

I_{pri}/I_{sec} - Primary/Secondary Current of Transformer

Z_{tr} - Transformer Impedance

R_{tr} - Series Resistance of Transformer

X_{tr} - Series Leakage Reactance of Transformer

I_{FL} - Full Load Current

$\%Z_{tr}$ - Percentage Impedance of Transformer

$\%X_{tr}$ - Percentage Reactance of Transformer

P_D - Load Average Kilowatt Demand

V_r - Rated Voltage at the Fundamental Frequency

V_α/I_α - Instantaneous α-axis Voltage/Current on the orthogonal α-β Coordinate

V_β/I_β - Instantaneous β-axis Voltage/Current on the orthogonal α-β Coordinate

p - Instantaneous Active Power

q - Instantaneous Reactive Power

$\bar{p}/\bar{q}$ - Average (dc) Component of the Instantaneous Active/Reactive Power

$\tilde{p}/\tilde{q}$ - Oscillating Component of the Instantaneous Active/Reactive Power

P_{loss} - Active Power Loss

V_s - Source Voltage

I_s - Source Current

I_{load} - Load Current

I_{ref} - Reference Current

I_{comp} - Compensator (DSTATCOM) Output Current

m_a - Modulation Index

V_{DC} - Direct Current (DC) Link Voltage of VSI

V_{ph} - Phase Voltage

V_{LL} - Line to Line Voltage

ABSTRACT

Investigation and monitoring of power quality is necessary to maintain accurate operation of sensitive equipment in an industrial environment. This paper presents the assessment and mitigation of power quality problem in Adama Spinning Factory. Monitoring of voltage and current harmonic distortion levels up to the 11^{th} order on the four distribution transformers of the factory's electrical network is carried out using DELAB NV8s PFC measuring equipment. Even though this equipment is primarily intended for automatic power factor controlling using 3-phase capacitor banks, they also have a capability to measure %THD and individual harmonic distortion up to 11^{th} order for voltage and current. The measured voltage and current harmonic distortion levels are compared with the IEEE 519-2014 and IEC 61000-2-2 / -3-4 international standards. The harmonic voltage distortion level in the factory has found to be well under the limits set by these standards while the current harmonic distortion levels on three of the transformers exceeds the standard limits with a maximum $\%THD_I$ value of up to 43.8%. Moreover, the power factor level of the factory on the utility meter found to be below 0.9, the minimum limit not to be penalized by the utility.

For mitigating the current harmonic distortion level in the factory a Distribution Static Synchronous Compensator (DSTATCOM) in current control mode is proposed. DSTATCOM is a shunt connected device, designed to inject unbalanced and harmonically distorted current to distribution line to eliminate unbalance or distortions in the load current. Instantaneous reactive power (IRP) based control theory is used to generate the reference currents. The distribution network of the factory is modeled in MATLAB's SIMULINK environment by considering the distribution transformer impedances, the power factor capacitor banks and the linear RL load. The non-linear loads are modeled as ideal harmonic current sources of 3^{rd} to 11^{th} order harmonics with amplitude of the maximum measured harmonic amplitude. The performance of the proposed DSTATCOM is evaluated by simulating the distribution network with and without DSTATCOM. The simulation results show that the source current becomes pure sinusoidal and in-phase with the source voltage within 0.02 seconds (one cycle) after the introduction of the DSTATCOM in the system.

Key words: *Power Quality, Harmonic Distortion, Power Quality Standards, Custom Power Devices, DSTATCOM, Instantaneous Reactive Power Theory, MATLAB/SIMULINK*

CHAPTER 1

INTRODUCTION

1.1 Background

The wide spread use of modern power electronic technologies in industrial, commercial and residential equipment has raised the awareness of power quality issues over the last few years. The use of electronically controlled and energy efficient machineries in modern manufacturing industries make them sensitive to small deviation in the supply power quality. Thus, in recent years, to realize the reduction of adverse effects and added costs related to power quality problem in distribution network, conducting a power quality problem assessment in industries is becoming a requirement.

The increasing concern on power quality issues by different stakeholders has driven the requirement for standards that defines different power quality disturbances, describe measuring methods and how the different power quality parameters are calculated and interpreted. Different international standards have been proposed by a number of standard organizations. The power quality related international standards, formulated by the Institute of Electrical and Electronics Engineers (IEEE) and International Electro-technical Commission (IEC), are the most widely used standards in the field.

Starting from the time of awareness and identification of power quality problems a lot of conventional solutions have been proposed and implemented to protect end used equipments and also utility power system equipments. The evolution of power electronics controller devices has given to the birth of custom power applications, in which a wide range of flexible controllers using power electronics components are utilized to improve the power quality at distribution level. The term Custom Power Device (CPD) refers to the use of power electronic controllers for distribution systems to enhance the quality and reliability of power that is delivered to customers.

In Ethiopia, the manufacturing sector is growing in recent years. But the power interruption is continuing to be a day to day occurrence. As a result quality of power is interpreted only as continuity of the supplied power and both the utility and consumes are focusing only on the power quality disturbances related to interruptions. But due to increased number of non-linear consumer loads connected to the distribution system, other types of power quality disturbances like harmonic distortions are likely to present in the system. A lot of power quality assessments have to be conducted at different parts of the power system in order to evaluate the power quality level and take proper mitigation actions. In this thesis work a power quality problem assessment will be done on Adama Spinning Factory distribution system, and a proper way of mitigating the problem will be proposed.

1.2 Statement of the Problem

Adama Spinning Factory is located in Adama city and has started operation in 2008 with new technologically advanced and sensitive manufacturing machineries and equipments. As every electric consumer in Ethiopia, the factory is facing a lot of problems due to low level of power quality and reliability of the supplied electric power. The extensive use of power electronic based devices like adjustable speed drives (ASD) in the factory creates current harmonic distortions in the system, which in turn distorts the supplied voltage. Moreover, the connection of new electric consumers to the distribution system is changing the characteristics of the distribution system from time to time. The combined consequence of these facts makes the factory more prone to power quality and reliability problems. As the factory's weekly/monthly performance reports [18] show, the factory is facing a lot of problems as a result of power quality disturbances which includes failure of expensive electronic printed boards and ASD (inverters), repeated burn out of electric motors, software corruption and also a repeated fire accident in the power factor correcting unit. In order to identify and characterize the existing power quality disturbances precisely; and to select and apply a proper solution to mitigate the disturbances which exceeds the standard limits set by standard organizations, power quality assessment has to be carried out in the factory. Therefore, this thesis work will try to address the power quality related problems by carrying out a power quality assessment on the factory and proposing a way to mitigate them, which in effect helps the factory to stay competitive in the market by reducing costs.

1.3 Objective

The general objective of this thesis work is to investigate the Adama Spinning Factory distribution network for power quality problems and propose a mitigation technique, if power quality disturbance levels outside recommended standard limits are found in the system.

The specific objectives of the project include:

- To investigate power quality problems in Adama Spinning Factory distribution network and to compare the level of disturbances with international/national standards.
- To simulate and analyze the distribution network of Adama Spinning Factory using collected data.
- To propose mitigation technique, if there exist power quality disturbance levels which exceed recommended standard limits, and simulate the distribution network with the proposed technique to see its performance.

1.4 Motivation

Adama spinning factory is one of the largest factories in Adama city with sophisticated electronic and electro-mechanical equipments. I was one of the staff member and electrical section head for the last couple of years in which I got best opportunity to closely investigate the overall electrical phenomenon of the factory. During those times, I came to see and observe many electrical problems which are the consequences of power quality problems.

An investigation of power quality problem had been carried out in the factory in 2010 by [2], in which a tuned shunt passive filter is proposed and designed to compensate the current harmonic distortion presented on the system at that time. Since then there have been a lot of changes on the utility and factory side, which changes the overall characteristic and performance of the factory's distribution network. On the factory side, there was an expansion project in 2011, to increase its production capacity by 35%. This expansion project includes installation of machineries with total additional installed capacity of about 1107.04 KVA and to accommodate this, one additional 800KVA distribution transformer is installed in the factory. On the utility side, the capacity of the substation supplying the factory has upgraded its capacity by installing one 50MVA step down transformer to accommodate the increasing demand of electricity in the city. Moreover, the factory's load is transferred to a new feeder line in 2016. As a result, the proposed mitigation techniques by [2] may not be applicable for the present distribution network of the factory. Therefore, the researcher is interested to further assess the power quality problems on the currently existing distribution system of the factory and propose a proper way of mitigation to bring additional benefit for the factory in terms of continuous and reliable operation.

1.5 Significance of the Study

In recent years, industries are trying to optimize their process to stay competitive in the production of their particular product. Hence, the significance of this study, in particular, is to help Adama Spinning factory in minimizing the costs incurred in its process due to power quality problem. The outcome of this study is mainly useful for the factory, to become aware of the quality of the electric power utilized by its production machineries and equipment; and most importantly, by implementing the proposed solution of this study, the factory can reduce downtime, off-standard products and thus production loss by limiting the effects of power quality problems.

Moreover, the study encourages industries and/or researchers to conduct a power quality investigation in different distribution networks and take corrective actions to enhance the quality of power used by consumers. As a result, industries will become profitable and competitive in the global market, which in turn contributes a lot to the country's economic growth.

1.6 Scope of the Study and Methodology

In this study voltage and current harmonic distortion levels, which are among the most common power quality disturbances in modern distribution system, were investigated in Adama Spinning Factory's distribution network. Data was initially gathered by reviewing different papers and standards. Additional data were collected by reviewing different electrical installation documents and weekly/monthly performance reports of the factory and also through discussion with the factory engineers. DELAB NV8s instrument was used to measure the voltage and current harmonic distortion level of the factory's distribution network. Analysis and comparison of the measurement data with the IEEE 519-2014 and IEC 61000-2-2 / -3-4 recommended harmonic distortion limits was carried out.

The factory distribution network was modeled in the MATLAB/SIMULINK environment. The model includes the distribution transformers, power factor correcting capacitors with anti-resonant reactors, linear and nonlinear loads of the factory distribution network. A DSTATCOM in current control mode was proposed as a mitigation technique and simulation of the factory distribution network with proposed DSTATCOM is done to see its performance.

1.6 Organization of the Thesis

This thesis presents the power quality assessment carried out on Adama Spinning Factory distribution network in which measurement of harmonic distortion level, comparison of the measurement data with international standards and simulation of the network with proposed mitigation technique are briefly discussed. The thesis is organized in to six chapters.

Chapter one, as the introductory part of this research paper, contains the background, statement of the problem, objectives, motivation and significance of the study.

Chapter two presents the summary of the research papers and publication reviewed. This chapter also presents a brief definition of different power quality phenomena with possible ways of mitigation techniques. The available international standards and the availability of national standards on power quality are discussed.

Chapter three describes the general overview of Adama spinning Factory. The electrical distribution network of the factory is presented in detail. How the electrical power is distributed; what kinds of linear and non-linear electrical loads are connected to the distribution network and what kinds of power quality related problems are commonly faced in the factory are addressed in detail. Description of the monitoring equipment used for this study is also presented in this chapter.

This chapter also presents how the distribution network of the factory is modeled in MATLAB SIMULINK environment and how different parameters are gathered and calculated for preparing the model. The IEEE and IEC international standards related to harmonic distortions are presented in this chapter.

Chapter four comprises measurement results together with interpretation and discussion of the results obtained.

Chapter five presents a brief description of the proposed current harmonic mitigation technique and simulation of the distribution network with the proposed solution. Simulation results and discussion of the distribution network with and without the proposed mitigation technique is also presented.

Chapter six is dedicated for findings and conclusions of the study. Recommendation for future work is also presented in this chapter.

CHAPTER TWO

LITERATURE REVIEW

2.1 Reviewed Studies and Papers

Both electric utilities and end users of electric power are becoming increasingly concerned about the quality of electric power and a lot of research works and case studies have been done on the issue of electric power quality in different parts of the world. There are many relevant papers written relating to the scope of this project. Furthermore, an investigation of power quality problem has been conducted by Milkias Berhanu [2] in 2010, on Adama Spinning Factory. Preliminary description and results of some research works, which are reviewed while preparing this research paper, is presented below.

Milkias Berhanu [2] in 2010 has done an investigation of power quality problems in distribution network of Adama Spinning Factory. This thesis work focuses only on harmonic current distortion level of factory's distribution network and it was compared with the power quality standard levels stated on IEEE-1159 and IEC-61000. Out of the four distribution transformer, monitoring of harmonic current distortion level was carried out only on three of them due to measurement device problem on one of the transformer. The research work tries to find out the parallel resonance frequency of the network by considering all the PFC capacitors. Then, the paper proposes a tuned passive filter to mitigate the current harmonics which was above the standard limits set by IEEE and IEC. Moreover, PSpice software was used for simulation of the network with and without the proposed tuned passive filter. The simulation results on this paper show that the addition of shunt tuned passive filter on the distribution network reduces the distortion of the current waveform significantly. The simulation was done by considering all the available PFC capacitor banks in the system, but in actual scenario the capacitor banks are switched in to and out of the system automatically based on the power factor level of the system. This will make the electrical characteristics of the network to change dynamically and affect the performance of the proposed tuned passive filters.

Hussein Mohamed El-Eissawi Fathi [3], in 2012, has done a PhD thesis submitted to Al-Azhar University, on power quality Assessment of Egypt 2nd Testing Research Reactor (ETRR-2) center. Measurement and analysis of different power quality disturbances like transients, voltage sag, voltage swell, flicker, harmonics, voltage unbalance and frequency deviations have been done on the distribution system. The paper tries to compare the measured data with international standards and also propose and design mitigation mechanisms for the disturbances which exceed standard limits. For the disturbances captured during measurement a single tuned passive filter, Dynamic Voltage Restorer (DVR) and Uninterruptable Power Supply (UPS) has been proposed to be installed at different locations of the electrical distribution network. The costs and payback times of these mitigation techniques have been included in the paper. Finally the paper recommends that power quality assessment has to be done continually with monitoring for longer period of time and with more number of monitoring points for sensitive projects like the one considered on the study.

Prafull A. Desale et al [4], in 2014, publish a brief review paper on the CPDs for power quality improvement. The paper gives a comprehensive survey of CPDs by presenting different application of these devices on a distribution network to compensate a number of power quality disturbances. The paper indicates that a DSTATCOM, being one of the compensating type CPDs, can be used effectively for harmonic current compensation, flicker effect compensation, power factor improvement and load current balancing in distribution systems. The paper presents sample simulation result only for voltage sag /swell compensation using DVR in a MATLAB/Simulink environment.

Shabana Urooj and Pikasha Sharma [6], in 2016, publish a paper on "Harmonic Elimination using DSTATCOM" on which the analysis and comparison of two DSTATCOM control theories are presented. The two control theories analyzed on this paper are IRP theory and SRF theory which are used for extracting reference currents to be compensated by DSTATCOM. The analysis is done by simulating the DSTATCOM with the two control theories connected to a sample network configuration with non-linear load, on a MATLAB environment using SIMULINK's Simscape Power System toolbox. Finally, the paper presents different simulation results and indicates that both the control techniques are reliable and useful for eliminating harmonic distortion.

Gokulananda Sahu et al [7], in 2014, publish a paper on performance analysis of DSTATCOM. The paper presents the design and analysis of instantaneous P-q control based DSTATCOM for composite compensation, i.e. harmonic distortion and reactive power compensation. A simulation of DSTATCOM performance is done for balanced and unbalanced non-linear load cases using MATLAB's SIMULINK.

Gunjan Varshney et al [8], in 2016, publish a paper on Photovoltaic (PV) based DSTATCOM in which the DC link voltage is regulated by the PV module. MATLAB/Simulink software is used to evaluate the performance of DSTATCOM in unity power factor and AC voltage control mode. This paper performs comparative analysis of three different control theories of DSTATCOM based on simulation results. The control theories are synchronous reference frame based control theory, instantaneous reactive power control theory and unit template based control theory.

2.2 Power Quality Definitions

Power Quality can be defined as any power problem manifested in voltage, current, or frequency deviations those results in failure or mis-operation of customer equipment [1]. Power quality disturbances are usually caused by load switching, system faults, motor starting, load variations, non-linear loads, intermittent loads and arc furnaces. These results in many electrical disturbances like surge, sag, swell, harmonic distortions, interruptions, flickers, and signaling voltages.

Categories & typical characteristics of different power quality phenomena, as defined and presented in IEEE Std 1159-2009: Recommended Practice for Monitoring Electric Power Quality, are listed in Appendix A of this document. Each of these classes of power quality problem is defined and discussed herein after as presented by [1].

2.2.1 Transients

The term Transient/Surge denotes an event that is undesirable but momentary in nature that disappears during transition from one steady state operating condition to another. Based on the wave shape of voltage or current, transients can be classified in to two categories, impulsive and oscillatory.

Impulsive transient is a sudden, non–power frequency change in the steady-state condition of voltage, current, or both that is unidirectional in polarity (primarily either positive or negative). Impulsive transients are normally characterized by their rise and decay times, which can also be revealed by their spectral content. They are commonly caused due to lightning striking on a power system, poor grounding, switching of inductive loads, switching of power factor correction capacitors, and utility fault clearing. Impulsive transients can excite the natural frequency of power system circuits and produce oscillatory transients.
Oscillatory transient is a sudden, non–power frequency change in the steady-state condition of voltage, current, or both, that includes both positive and negative polarity values. It is a brief, bidirectional variation of voltage/current and described by its spectral content, duration, and magnitude. Oscillatory transients are most commonly a result of switching, capacitor energization, and local system response to impulsive transients.

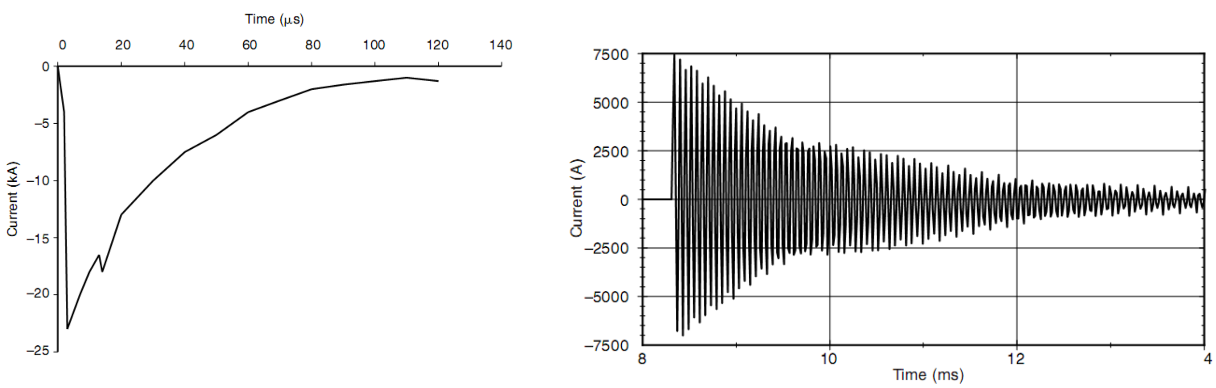

(a) (b)

Figure 2.1: (a) Lightning stroke impulsive transient and (b) Oscillatory transient. [1]

Transients lead to equipment failure, nuisance tripping of adjustable-speed Drives, system lock-up, data corruption and data loss. Different techniques and devices can be utilized to minimize and/or avoid transient problems:

- Surge arresters and transient voltage surge suppressors
- Synchronous closing breakers with pre-insertion resistors
- Line reactors
- Isolation transformers
- Low-pass filters
- Shielding on overhead utility line

2.2.2 Short Duration Voltage Variation

Short-duration voltage variations are caused by fault conditions, switching actions to isolate the faulted sections, the energization of large loads which require high starting currents, or intermittent loose connections in power wiring. Depending on the fault location and the system conditions, the fault can cause either temporary voltage drops (sags or dips), voltage rises (swells), or a complete loss of voltage (interruptions).

Sag/dip is a decrease to between 0.1 and 0.9 pu in rms (root mean square) voltage or current at the power frequency for durations from 0.5 cycle to 1 min and commonly caused by faults on the power system and starting of large loads such as motors. Voltage sag reduces the energy being delivered to the load and causes sensitive equipment to trip, computer systems to fail and lose their memory, adjustable-speed drive to shut down, motors to stall and over heat. Solutions to voltage sag problems include equipment such as ferroresonant transformer (Constant Voltage Transformer, CVT), Motor-generator set, flywheel energy storage devices, Super conducting Magnetic Energy Storage (SMES) devices, automatic transfer switches, uninterruptible power supply (UPS) and DVR. A typical voltage wave form during sag caused by an SLG (Single Line to Ground) fault.

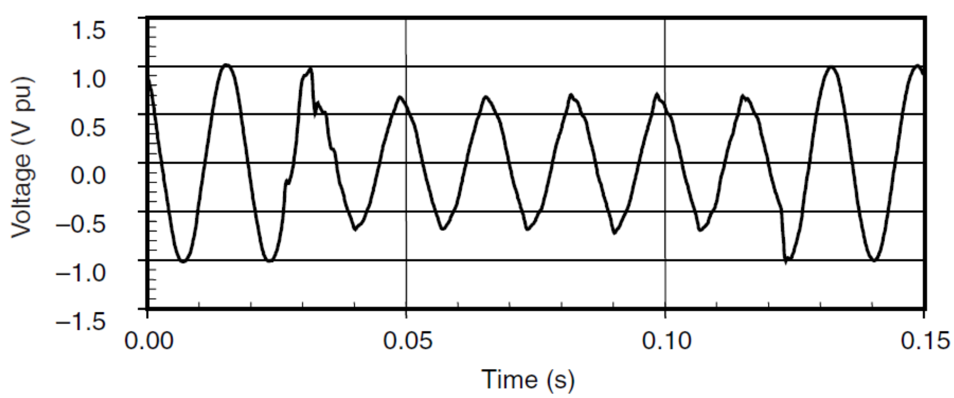

Figure 2.2: Typical voltage wave form during sag caused by an SLG fault. [1]

Swell is defined as an increase to between 1.1 and 1.8 pu in rms voltage or current at the power frequency for durations from 0.5 cycle to 1 min. As with sags, swells are usually associated with system fault conditions like the temporary voltage rise on the unfaulty phases during a Single Line to Ground (SLG) fault, but they are not as common as voltage sags. Swells can also be caused by switching off a large load or energizing a large capacitor bank.

The increased energy from a voltage swell often overheats equipment and reduces its life. Solutions to voltage swell problems include equipment such as voltage regulator, motor-generator set and uninterruptible power supply (UPS), automatic transfer switches. A typical voltage wave form during swell caused by an SLG fault.

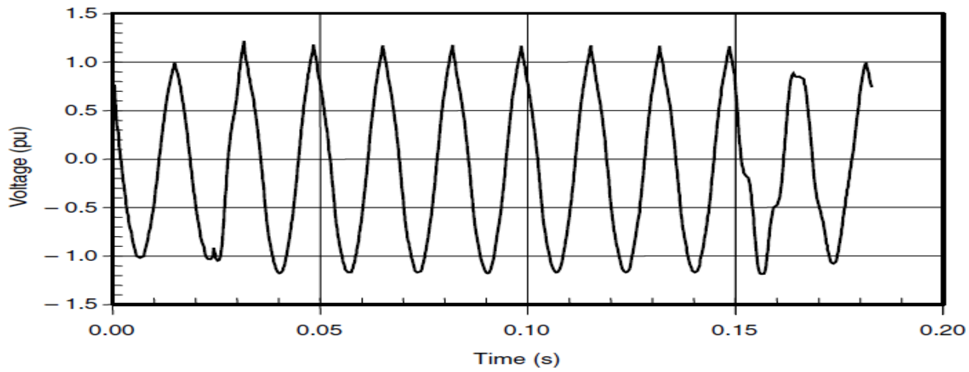

Figure 2.3: Typical voltage wave form during swell caused by an SLG fault. [1]

Interruption is an occurrence of the supply voltage or load current reduced to less than 0.1 pu for a period of time not exceeding 1 min. Interruptions can be a result of power system faults, the actions taken by utilities to clear transient faults, equipment failures, and control malfunctions.

2.2.3 Long Duration Voltage Variation

Long-duration variations encompass root-mean-square (rms) deviations at power frequencies for longer than 1 min. Long duration variations can be under-voltages, over-voltages and sustained interruptions. Long duration voltage variation power quality problems can be mitigated by different voltage regulating devices like motor-generator set, tap changing regulators, ferroresonant transformer, online Uninterruptable Power Supplies (UPS) and static VAR compensator.

Over-voltage is an increase in the rms ac voltage greater than 110 percent at the power frequency for duration longer than 1 min. Over-voltages are usually the result of load switching (e.g., switching off a large load or energizing a capacitor bank).

Under-voltage is a decrease in the rms ac voltage to less than 90 per- cent at the power frequency for duration longer than 1 min. A load switching on or a capacitor bank switching off may result in an under-voltage until voltage regulation equipment on the system can bring the voltage back to within tolerances. Overloaded circuits and the loss of major transmission support can also result in under voltages.

Sustained interruption is a long duration voltage variation when disappearance of the supply voltage for a period of time in excess of one minute occurs.

2.2.4 Voltage Imbalance

Voltage imbalance (also called voltage unbalance) is sometimes defined as the maximum deviation from the average of the three-phase voltages or currents, divided by the average of the three-phase voltages or currents, expressed in percent.

$$\%\,Voltage\;\; Unbalance\, ratio = \frac{Maximum\, Voltage\, deviation}{Average\, Voltage} \times 100 \quad \text{………..} \; (2.1)$$

Imbalance is more rigorously defined in the standards using symmetrical components. The ratio of either the negative- or zero-sequence component to the positive-sequence component can be used to specify the percent unbalance. Voltage unbalance can be the result of single-phase loads on a three-phase system, blown fuses in one phase of a three-phase capacitor bank, different line impedances on long run lines, open circuit on the distribution system primary. Voltage unbalance can create a current unbalance 6 to 10 times the magnitude of voltage unbalance. Consequently, this current unbalance causes motors and transformer windings to overheat which may result in insulation failure.

2.2.5 Voltage Fluctuation (Flicker)

Voltage fluctuations are cyclical variations in the voltage rms values or a series of random voltage changes, whose magnitude does not normally exceed voltage ranges of 0.9 p.u. to 1.1 p.u. Loads which can exhibit continuous, rapid variations in the load current magnitude can cause voltage fluctuations that are often referred to as flicker. The term flicker is derived from the impact of the voltage fluctuation on lamps such that they are perceived by the human eye to flicker. Arc furnace and welders are the most common causes of voltage fluctuations in utility transmission and distribution systems. Flickers can be mitigated by increasing the system capacity or by implementing static capacitors and power electronic-based switching devices. Typical voltage fluctuation on a wave form caused by an arc furnace is shown in Figure 2.4.

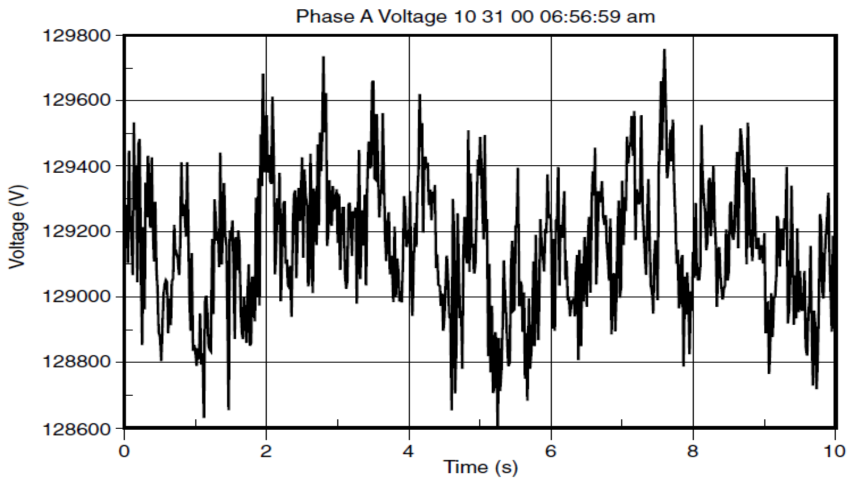

Figure 2.4: Voltage Fluctuation Caused by an Arc Furnace. [1]

2.2.6 Power Frequency Variation

Power frequency variations are defined as the deviation of the power system fundamental frequency from it specified nominal value (50 or 60 Hz). Frequency variations can be caused by faults on the bulk power transmission system, a large block of load being disconnected, or a large source of generation going off-line. Frequency variation is rare in an interconnected utility system. In isolated generation system, the dynamic response of the control system (Governor of the generating system) to an abrupt and huge load changes may not be adequate to regulate within the narrow bandwidth required by frequency-sensitive equipment.

2.2.7 Waveform Distortion

Waveform distortion is defined as a steady-state deviation from an ideal sine wave of power frequency characterized by the spectral content of the deviation. There are five primary types of waveform distortion: Harmonics, Inter-harmonics, DC offset, Notching and Noise.

Harmonics are sinusoidal voltages or currents having frequencies that are integer multiples of the frequency at which the supply system is designed to operate (termed the fundamental frequency; usually 50 or 60 Hz). Periodically distorted waveforms can be decomposed into a sum of the fundamental frequency and the harmonics, using the Fourier series representation as shown in Figure 2.5 below. The equation for such waveform is given below.

$$V(t) = a_0 + \sum_{h=1}^{\infty} V_h \, Sin(h.2\pi f.t + \theta_h) \quad \text{…………..………….} \quad (2.2)$$

Where, a_0 is a dc component, V_h is peak voltage level; f is fundamental frequency and θ_h is Phase angle.

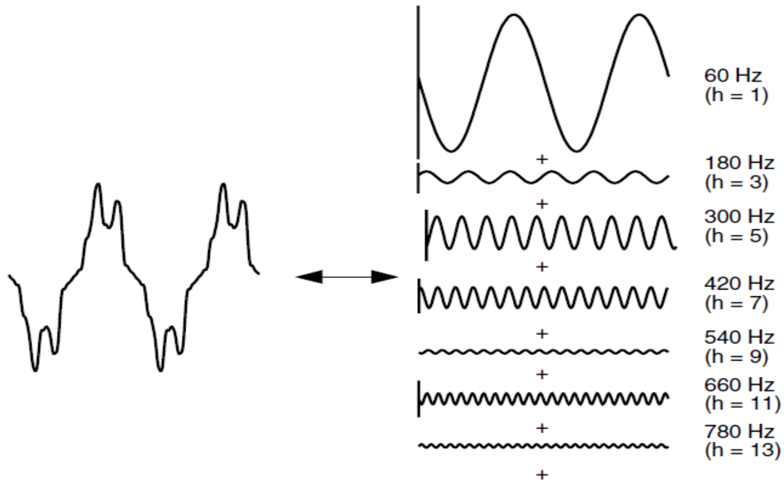

Figure 2.5: Fourier series representation of a distorted waveform. [1]

Harmonic current distortion originates from the nonlinear characteristics of devices and loads on the power system. Voltage distortion is the result of harmonic distorted currents passing through the linear, series impedance of the power delivery system. One of the major problems related to harmonic disturbances is harmonic resonance. The resonance can magnify harmonic distortions to a level that can damage the equipment or cause equipment malfunction. Power factor correction capacitors in distribution system are the main cause of harmonic resonance. Electric power system disturbances caused by harmonic effect include

- Overload on distribution system (transformers, cables & capacitors) due to increase in rms value
- Overload of neutral conductor due to 3^{rd} (triplen) harmonic current
- Overload and torsional oscillation of motors and generators due to 5^{th} harmonics
- Distortion of supply voltage capable of distorting sensitive loads like computer and control systems
- Premature failure or operation of protective devices (such as fuses)
- Disturbance of communication networks and telephone lines
- flickering fluorescent lighting
- inaccuracy of demand and watthour meter

Nonlinear loads in industrial and commercial facilities which are responsible for creating harmonic currents include Single-phase switch mode power supplies, AC/DC Adjustable speed drives, Discharge type lightings with magnetic and electronic ballasts, three phase power converters, saturated reactors, static VAR systems, inverters for distributed generation, Arc furnaces and arc welders. Harmonics in electric system can be controlled by adding different types of passive and active filters (to take out the harmonic current from the system, block the harmonic current from entering the system, or supply harmonic currents locally), reducing the harmonic currents produced by loads, modifying the frequency response of the system by filters, inductors, or capacitors.

The two most commonly used indices for measuring the harmonic content of a waveform are the Total Harmonic Distortion (THD) and the Total Demand Distortion (TDD). The THD is a measure of the effective value of the harmonic components of a distorted waveform relative to the fundamental. This index can be calculated for either voltage or current:

$$THD_V = \frac{\sqrt{\sum_{V_2}^{\infty} V_h^2}}{V_1} \times 100\% \qquad THD_I = \frac{\sqrt{\sum_{I_2}^{\infty} I_h^2}}{I_1} \times 100\% \quad \text{……….. (2.3)}$$

Where, V_h and I_h represent the rms voltage and current values at harmonic orders of h, respectively. V_1 and I_1 represent the fundamental rms voltage and current, respectively.

Current distortion levels can be characterized more effectively by TDD factor, which is calculated relative to maximum demand load current rather than the fundamental of the present sample. This is due the fact that a small current may have a high THD but not be a significant threat to the system.

$$TDD = \frac{\sqrt{\sum_{I_2}^{\infty} I_h^2}}{I_L} \times 100\% \quad \text{…………………………….. (2.4)}$$

Where I_L is the maximum demand load current at the fundamental frequency component.

Inter-harmonics are voltages or currents having frequency components that are not integer multiples of the frequency at which the supply system is designed to operate (e.g., 50 or 60 Hz). Inter-harmonics can be found in networks of all voltage classes. The main sources of inter-harmonic waveform distortion are static frequency converters, cycloconverters, induction furnaces, and arcing devices.

DC offset occurs when there is the presence of a dc voltage or current in an AC power system. DC injection into the low-voltage and medium-voltage AC grids comes mostly from grid connected static power converters (caused by the delay mismatch in gating circuits and imperfections of power switches), HVDC transmission, and railway signaling equipment. Direct current in AC networks can have a detrimental effect by biasing transformer cores so they saturate in normal operation. This causes additional heating and loss of transformer life. Direct current may also cause the electrolytic erosion of grounding electrodes and other connectors. Active compensation methods can be advantageously used in suppressing the DC bias at grid connection points.

Notching is a periodic voltage disturbance caused by the normal operation of power electronic devices when current is commutated from one phase to another. During commutation, there is a momentary short circuit between two phases, pulling the voltage as close to zero as permitted by system impedances. A typical voltage notching caused by a three-phase converter is shown in Figure 2.6. Since notching occurs continuously, it can be characterized through the harmonic spectrum of the affected voltage.

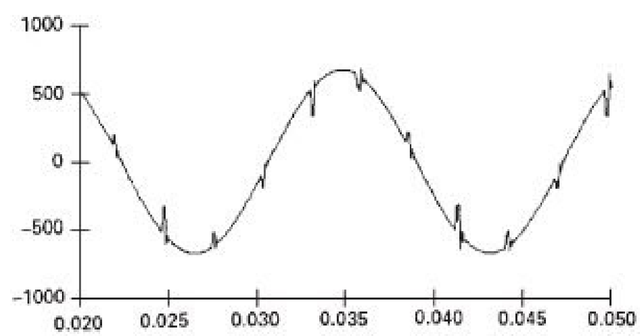

Figure 2.6: Voltage notching caused by a three-phase converter. [1]

Noise is defined as unwanted electrical signals with broadband spectral content lower than 200 kHz superimposed upon the power system voltage or current in phase conductors, or found on neutral conductors or signal lines. Noise in power systems can be caused by power electronic devices, control circuits, arcing equipment, loads with solid-state rectifiers, and switching power supplies. The problem can be mitigated by using filters, isolation transformers, and line conditioners.

2.3 Power Quality Standards

The increasing concern on power quality issues resulted in a lot of power quality monitoring and case studies to be done by different utilities and consumers around different parts of the world. This increasing need for power quality monitoring has driven the requirement for standards that describe measuring methods and how the different power quality parameters are calculated and interpreted. As a result a lot of international standards related to power quality have been formulated by different standard organizations and put into work. Such organization includes Institute of Electrical and Electronics Engineers (IEEE), European Union Standards organization (CENELEC), International Electro-technical Commission (IEC), American National Standard Institute (ANSI), National Electrical Manufactures Association (NEMA), and so on.

The purpose of power quality standards is to protect utility and end-user equipment from failing or misoperation when the voltage, current or frequency deviates from normal values. These standards provide protection by setting measurable limits as to how far the voltage, current or frequency can deviate from normal values. Moreover, power quality standards help utilities and customers to gain agreement on what are acceptable and unacceptable levels of service.

In this study, mostly the IEC and IEEE standards and definitions will be used for their widely usage in academic and research areas, and their high-level of completeness to characterize all the major electrical phenomena comprising power quality. Moreover, the position of Ethiopia's national standard on power quality issues will be addressed.

2.3.1 IEC Standards

Founded in 1906, the IEC is the world's leading organization for the preparation and publication of international standards for all electrical, electronic and related technologies. [12] The IEC family, with 84 member countries and 87 affiliate member countries (developing countries), spread across more than 97% of the world's population. IEC standards have been adopted by the European Committee for Electrotechnical Standardization (CENELEC) and many other countries all over the world.

The IEC has defined a category of standards called Electromagnetic Compatibility (EMC) Standards that deal with power quality issues. These standards are broken down into six parts: General (IEC 61000-1-x), Environment (IEC 61000-2-x), Limits (IEC 61000-3-x), Testing and Measurement Techniques (IEC 61000-4-x), Installation and Mitigation Guidelines (IEC 61000-5-x), Generic and Product Standards (IEC 61000-6-x). IEC standards for each power quality parameters are not given on a single publication; rather they are separated into several publications which fall into different parts of the standard and also for different levels of current and voltage. For example the IEC standard relating to harmonics generally fall in parts 2 and 3, which includes:

- IEC 61000-2-2 (1993): Compatibility Levels for Low-Frequency Conducted Disturbances and Signaling in Public Low-Voltage Power Supply Systems,
- IEC 61000-3-2 (2000): Limits for Harmonic Current Emissions (Equipment Input Current Up to and Including 16 A per Phase),
- IEC 61000-3-4 (1998): Limitation of Emission of Harmonic Currents in Low-Voltage Power Supply Systems for Equipment with Rated Current Greater Than 16 A,
- IEC 61000-3-6 (1996): Assessment of Emission Limits for Distorting Loads in MV and HV Power Systems. Basic EMC publication.

2.3.2 IEEE Standards

The IEEE is a professional association formed in 1963 from the amalgamation of the American Institute of Electrical Engineers and the Institute of Radio Engineers. The institute is the world's largest association of technical professionals with more than 420,000 members in over 160 countries around the world [13]. The IEEE Standards Association (IEEE-SA) is an organization within IEEE that develops global standards in a broad range of industries. Some of the standards developed by IEEE which are related to power quality phenomena are:

- IEEE Standard 1159-2009: Recommended Practice for Monitoring Electric Power Quality.
- IEEE Standard 1159.3-2003: Recommended practice for the transfer of power quality data.

- IEEE Standard 519-2014: Recommended Practices and Requirements for Harmonic Control in Electrical Power Systems.

2.3.3 Ethiopian Standards Agency (ESA)

ESA is a governmental non-profitable organization and the sole national standards body which represents Ethiopian interest in economic, social and environmental aspects with regard to standard benefits across international and regional arena. ESA has three core business areas which mainly focus on the standard formulation, training and technical support and organizing and disseminating standards, conformity assessment procedures and technical regulation for the customers. [11]

National Electro-technical Committee of Ethiopia (NECE) was established in November 2012 under ESA with an expert group from five different organizations: ESA, Addis Ababa University, Ethiopian Electric Utility, Ministry of Energy, and Ethiopian Conformity Assessment Enterprise. NECE, together with the Technical Committees on different fields, is the responsible body within the ESA, for the approval and adoption of IEC standards for national use. Ethiopia, as one of the affiliate plus member country of IEC, has adopted 251 IEC standards through NECE, out of the free 400 standards allowed for national adoption by such member countries. Unfortunately, NECE has not adopted the IEC 61000: EMC standards related to power quality phenomena as a national standard still now (when this research work is prepared).

Ethiopian Energy Authority (EEA) is another organization possibly concerned with standards associated with electrical power quality. As per the information gathered from the authority staffs, the EEA is on the process of preparing a national "Grid Code" which may contain some electrical power quality standards.

CHAPTER THREE

DESCRIPTION OF CASE STUDY AND METHODS

3.1 Background of Adama Spinning Factory [15]

Adama Spinning Factory, a subsidiary of ADAMA DEVELOPMENT PLC, is a privately owned 100% Cotton yarn manufacturer with a state of the art spinning facility. The Factory is situated at Adama, the seat of Oromiya regional state, which is 110 km away from Addis Ababa the capital of Ethiopia. Adama Spinning Factory started its operation in mid of the year 2008 with the state of the art machinery supplied by Rieter AG Switzerland with a production capacity of 10 tons/day. The Factory was expanded in 2012 by increasing the capacity to produce up to 12.5 ton/day of 100 % cotton yarn. As a part of forward integration, the factory has also established Twisting, Reeling and Socks knitting plants in 2013 G.C. The virtue of its location has the advantage of getting enough electric power supply, proximity to cotton growing areas, availability of abundant labor, basic infrastructure of water supply, easy access to Addis Ababa-Djibouti road and rail way, Schools, hospitals and other infrastructural facilities.

Figure 3.1: Adama Spinning Factory top view.

The Factory has a facility to deliver 100 % cotton yarn in cone & reeled hank form for export market and local market by using locally cultivated lint cotton which originates mainly from Awash valley and Gonder Area. The complete range of spinning machines right from Blowroom to Ring frame & Open End Spinning are supplied by Rieter AG Switzerland. The winding machines are from Muratec Japan, equipped with Uster Quantum 2 & 3 yarn clearers. The Factory has also 1,088 spindles of two for one twister machines from M/s Savio Italy. Adama Spinning Factory is a one stop solution for the customers by providing 100 % cotton yarn according to their variety of requirements for weaving & Knitting like carded & combed single yarn, carded open end yarn and ply yarns.

The company has implemented and awarded a certificate in IS0 9001 QMS and WRAP principle. So far, it has created a direct job opportunity for about 450 employees. The company has planned to undertake a vertical integration projects, ginnery and knit to garment plants, to be realized in the near future.

Figure 3.2: Adama Spinning Factory: partial interior view of the spinning plant.

3.2 Electric Power Supply System to Adama Spinning Factory

The electrical system of Adama Spinning Factory is fed from Adama substation which is located 3.9km from the factory. The substation is connected to the national grid network of Ethiopia. Adama substation has two 132KV incoming lines, one from Koka power generating station and the other from Adama Wind power generation station. Currently, the substation has two 132±10x1.25%/15KV, 25000kVA, %Z=18, Wye-Delta stationary step-down transformers and one 132±10x1.25%/15KV, 50000kVA, %Z=10.75, Wye-Delta portable stepdown transformer. A total number of eleven feeder lines, six feeders from the stationary and five feeders from the portable step-down transformers, are supplying electric power to a number of industrial, commercial and industrial customers mainly in Adama city through two different common bus bars. In addition, a number of customers located on the way to and inside neighboring cities like wolenchiti, Modjo, Wonji, Koka, etc are fed from this substation.

Out of the seven 15KV primary distribution feeder lines on the stationary step-down transformers, one feeder is allocated only to Adama spinning Factory (including the factory's socks/Reeling plant) and ELSE Addis Textile Factory. Additional two small distribution transformers are tapped to this feeder line, which gives power to one micro-industry and one warehouse located around the factory.

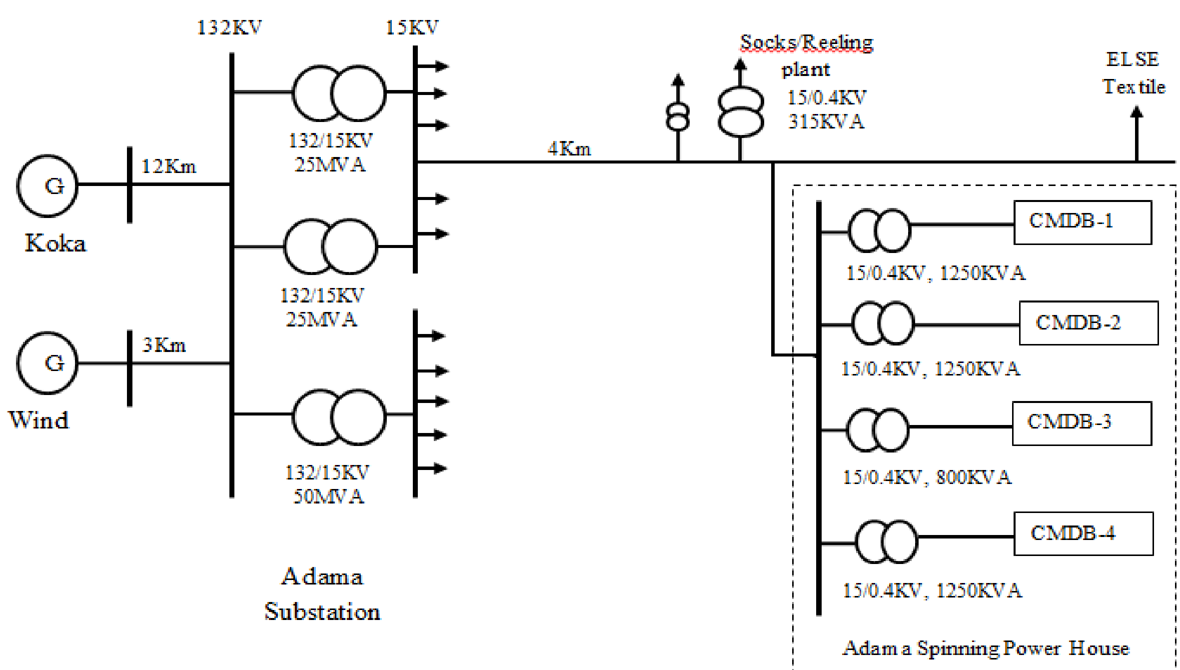

Figure 3.3: Single line diagram of Adama substation-Adama Spinning Factory power network.

Figure 3.4: Partial view of Adama Spinning Factory power house.

3.3 Electrical Power Distribution Network of Adama Spinning Factory

The 15KV primary distribution feeder line from Adama substation to Adama Spinning Factory is an overhead distribution system. The spinning plant is fed from a power house which is constructed within the plant. Partial view of the power house is shown in Figure 3.4. The distribution feeder line enters the power house by underground system. As shown in Figure 3.3, the 15kV feeder line is connected to three 15/0.4Kv, 1250kVA, %Z=5.05, Delta-Wye and one 15/0.4Kv, 800kVA, %Z=5.03, Delta-Wye step down net distribution transformers, through a common bus bar, to supply a maximum load of 4.55MVA. In addition to the power house supplying the spinning plant, there is one pole mounted 15/0.4KV, 315KVA distribution transformer supplying the Socks Knitting/Reeling plant.

The electrical power in the spinning plant is distributed through four Central Main Distribution Boards (CMDBs), as shown in Figure 3.5. These four CMDBs supply a number of different and scattered loads through Main Distribution Boards (MDBs) and Sub Distribution Boards (SDBs), placed at different locations in the plant near to the loads they fed. Partial view of the CMDB boards is shown in Figure 3.6.

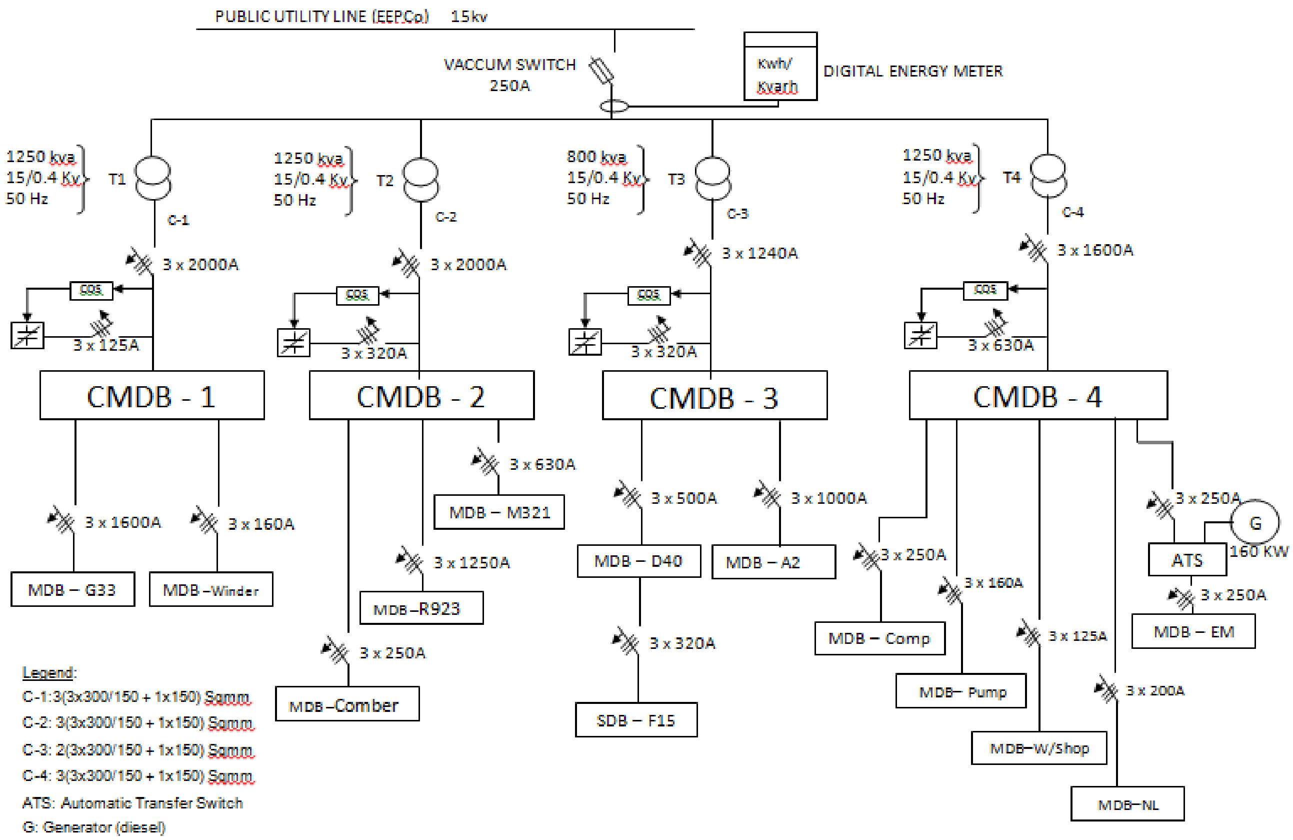

Figure 3.5: Single line diagram of the Spinning plant electrical distribution.

Figure 3.6: CMDB boards of Adama Spinning Factory distribution system.

CMDB-1, -2 and -3 supply power to the majority of the production machineries in the plant. On the other hand, the connected loads to CMDB-4 are mainly utility loads like huge Air Conditioning (AC) units, lighting loads, office and kitchen equipments, and welding machines. The factory has one 200KVA Stand-by Diesel generator connected to the emergency main distribution board (MDB-EM) via an ATS (Automatic Transfer Switch) as shown in Figure 3.5. This generator supplies power to administrative office, canteen, stores, physical laboratory, compound lighting, and factory emergency lighting in the case of power interruption. The complete Adama Spinning Factory electrical installation layout is presented in Appendix B of this document.

As a modern manufacturing facility, the factory uses technologically advanced and energy efficient machineries, which are sensitive to small deviation in the supplied power quality and at the same time, have a tendency to distort the supplied pure sine wave. The loads in the factory can be categorized as follows.

- AC and DC motors
- ASD (Inverters)
- Resistive heaters
- Single and three phase Power Supplies
- Microprocessor based controllers
- Fluorescent lamps
- Gas discharge lamps
- Welding machines
- Office equipments (computers , printers, …)

Of these load categories, the ASD and the AC induction motors are the most dominant loads in the factory. A total number of 155 ASD (frequency converters) with power ratings staring from 0.55 Kw up to 75 Kw are connected to the distribution network. The distribution of these ASDs on each distribution transformer is presented on Table 3.1. More harmonic distortion levels are likely to present on transformers T1 and T3 for the fact that higher total number and installed capacity of ASDs are connected to these two transformers.

In addition to the induction motors controlled by these ASD, there are a lot of AC induction motors installed in the factory which controlled by Direct on line (DOL) and Star-Delta starting methods.

Table 3.1: Number and capacity of ASD on each transformer.

Transformer	Total number of ASDs (frequency inverters)	Total estimated power capacity of ASDs
T1	64	942 Kw
T2	21	202 Kw
T3	66	370 Kw
T4	4	56 Kw

All the CMDB boards have Automatic Power Factor Controller (PFC) units, which monitors the instantaneous power factor (cos φ) and correct when it falls below 0.95 by connecting different size capacitors to the network step by step. The capacitor steps are pre-designed based on the types and patterns of the loads connected to each CMDB. In series to each power factor correcting capacitor, anti-resonance harmonic filters (reactors) are connected to avoid resonance phenomena by detuning the system. As stated on the PFC manufacturer product profile [17], experience shows that the self-resonant frequency of the resonant circuit, formed by the power factor correction capacitors in conjunction with the feeding transformer, is typically between 250 and 500 Hz, i.e. in the region of the 5^{th} and 7^{th} harmonics. Such detuned systems are scaled so that the self-resonant frequency is below the lowest line harmonic. The installed anti-resonant reactors in series with the capacitors are aimed to bring down the self-resonance frequency to f_r=189Hz, so that the detuned PFC system is purely inductive seen by harmonics above this frequency. For the 50 Hz line frequency, the detuned system acts purely capacitively, thus correcting the reactive power. The different capacitor steps (KVAr) and inductance values of the series ant resonant reactors available on each CMDB boards are presented in Section 3.7.2 on Table 3.3.

3.4 Power Quality Related Problems in the Factory

The weekly/monthly maintenance performance reports [18] of the factory are reviewed in search of electrical problems happened in the factory as a result of power quality disturbances. Additionally, detail discussion with the factory engineers has been conducted to investigate additional problems related to power quality disturbance, which may not be recorded on reports due to different reasons. While conducting measurements for this study, a fire accident happens in CMDB-1 PFC board and all fuse boxes and connecting cables of the capacitors have been damaged. The weekly/monthly maintenance performance reports indicate that this problem happens for the second time on the same CMDB board. Figure 3.7 shows the damaged part in CMDB-1 board due to this problem. Following are some of the problems, related to power quality and reliability, happened in the factory during the last couple of years.

- A lot of problems happened in the PFC unit including failure of power factor correcting capacitor, contactors and HRC fuses which connect the capacitors to the bus bar. Moreover, such problems have led to fire accidents three times in the PFC boards.
- A lot of fluorescent lamps and ballasts failing at abnormal rate.
- Repeated burn out of some specific electric motors which are operating at their maximum rated capacity.
- Failure of some electrical parts including ASD (frequency invers), control printed circuit boards and Panels, different type of fuses
- Overheating and burn out of conductors and terminal connectors.
- Freezing and unresponsiveness of control systems.
- Data loss and corruption on control boards and flash memory cards.
- As the monthly energy consumption report presented on Appendix C shows, the overall power factor of the spinning plant has become lower than 0.9 starting from September, 2016. As a result, in the last 18 months (starting from September, 2016 up to February, 2018) the factory has payed 26,381.88 Birr as a penalty charge for having a power factor lower than 0.9.

Figure 3.7: Damaged part due a sudden fire inside CMDB-1 board.

3.5 Harmonic Distortion Assessment Procedure

Every industrial and commercial consumers of electric power in Ethiopia is facing a lot of power interruption and problem related to power quality and reliability. Due to lack of awareness, in the past years, such problems have been considered as a normal phenomenon and related to the quality or operation of the consumers' equipment. As a result, most consumers focus on replacing defective parts instead of questioning and assessing the level of power quality they are using. However, in recent years, due to the growth in technologically advanced, sophisticated and sensitive industrial facilities in Ethiopia, problems related to power quality and reliability becomes more sensitive and customers start to focus on performing power quality assessment.

Power quality assessment procedure provides a general framework that contains all the possible elements that may be needed for power quality study. As one type of power quality phenomena, similar procedure can be used for the evaluation and assessment of harmonic distortion on a given electrical power system. A general procedure that can be followed in performing such assessment on existing system is discussed below [1].

1. Perform harmonic distortion level measurements for existing installation to characterize the harmonic sources on the system. These measurements should be performed at the PCC (Point of Common Coupling) for at least 1 week so that all the cyclical load variations can be captured.
2. Evaluate the measured distortion levels with respect to selected standard limit/s. In addition of the measurement data, different standards may require some additional parameters of the system under consideration. For instance, the short circuit ratio (I_{sc}/I_L) of the system needs to be calculated, in order to use the current distortion limits on IEEE std 519-2014.
3. If the system measurement does not meet the limits recommended by the selected standards, mitigation measures are necessary. Possible mitigation techniques for the problems will be identified; and the optimum one which fits the system under consideration best will be selected.
4. Evaluate the system again with the selected mitigation technique added to the system. Here different computer software can be utilized to model the system together with the selected mitigation technique and observe the overall response of the system.

The above general procedure is followed for the assessment of harmonic distortion level in Adama Spinning Factory distribution network. The detail of each steps for this specific study are presented on the next sub topics and chapters.

3.6 Measuring Process

Harmonic measurements are performed to characterize the level of harmonic generation for the existing nonlinear loads in the factory. The measurements are performed using DELAB NV8s Power Factor Controller (PFC). The technical specification and the points at which the monitoring has been carried out are discussed in the following sub topics.

3.6.1 Measuring Equipment

Monitoring was carried out using DELAB NV8s PFC. DELAB NV8s is a microprocessor based PFC which complies with IEC 6100-4-2/4-4/4-5/255-5:1 standards. [14] The front view of the controller is shown in Figure 3.8. The controller, in addition to controlling and correcting power factor, it has a capability to measure some electrical parameters like:

- Secondary current
- Voltage and Frequency
- Total Harmonic Distortion voltage and current (%THD_V and %THD_I)
- Voltage and current odd harmonic spectrum level up to 11^{th} order

On the contrary, these monitoring devices have some drawbacks:

- It monitors current and voltage of only one phase. Thus, they are not suitable for unbalanced three-phase systems.
- They don't show wave form of measured value.
- They don't have any data storage (logging) capability. As a result, the instantaneous measured values have to be recorded manually at different times.
- Since, these devices are mainly intended for power factor correction, they are prepared to be installed on a fixed location on a specific panel. They are not suitable to easily change the measurement locations.

There are four DELAB NV8s PFC devices in the factory installed on each CMDB boards for controlling and correcting the power factor on the respective transformers. Due to software version difference on these devices, only the device installed on CMDB-1 is capable of measuring both voltage and current harmonic levels. The other three devices installed on CMDB-2, -3 and -4 are capable of measuring only the current harmonic distortion level. Therefore, the DELAB NV8s PFC device installed on CMDB-1 is used in this study, for monitoring both voltage and current harmonic distortion level on all the four CMDB boards. The measured secondary current values (I_{sec}) and the individual n^{th} odd harmonic current amplitude values (I_h) using these devices are actual values of the CT (Current Transformer) secondary. Therefore, all these values have to be multiplied by the respective CT ratios, in order to get the actual current values. The primary/secondary CT ratios installed on each CMDB board are: 2500/5A on CMDB-1 and -2; 1250/5A on CMDB-3 and 1600/5A on CMDB-4.

Figure 3.8: Front view of *DELAB NV8s Power Factor Controller.*

3.6.2 Measuring Locations

IEEE Std 1159-2009 recommends that if the monitoring objective is to investigate the overall quality of a facility, then the monitor should be placed on the secondary of the main service entrance transformer, which is usually 600 V class service equipment. The monitor will record the quality of power supplied to the facility as well as the effect of major loads within the facility [19]. Therefore, measurements were carried out on the secondary low voltage side of each transformer for this study. Four CTs have already been installed on the secondary side of each transformer after the main circuit breaker (CB) of the respective CMDB boards. Measurements were taken on one CMDB board at a time, because only one device, which is capable measuring both voltage and current harmonic level, is available as stated earlier. Measurements were taken on each transformer, one at a time, for an average of four days. Figure 3.9 shows the monitoring points for each transformer on a single line diagram. This figure also displays the total installed load on each transformer in Kilo Watt (KW).

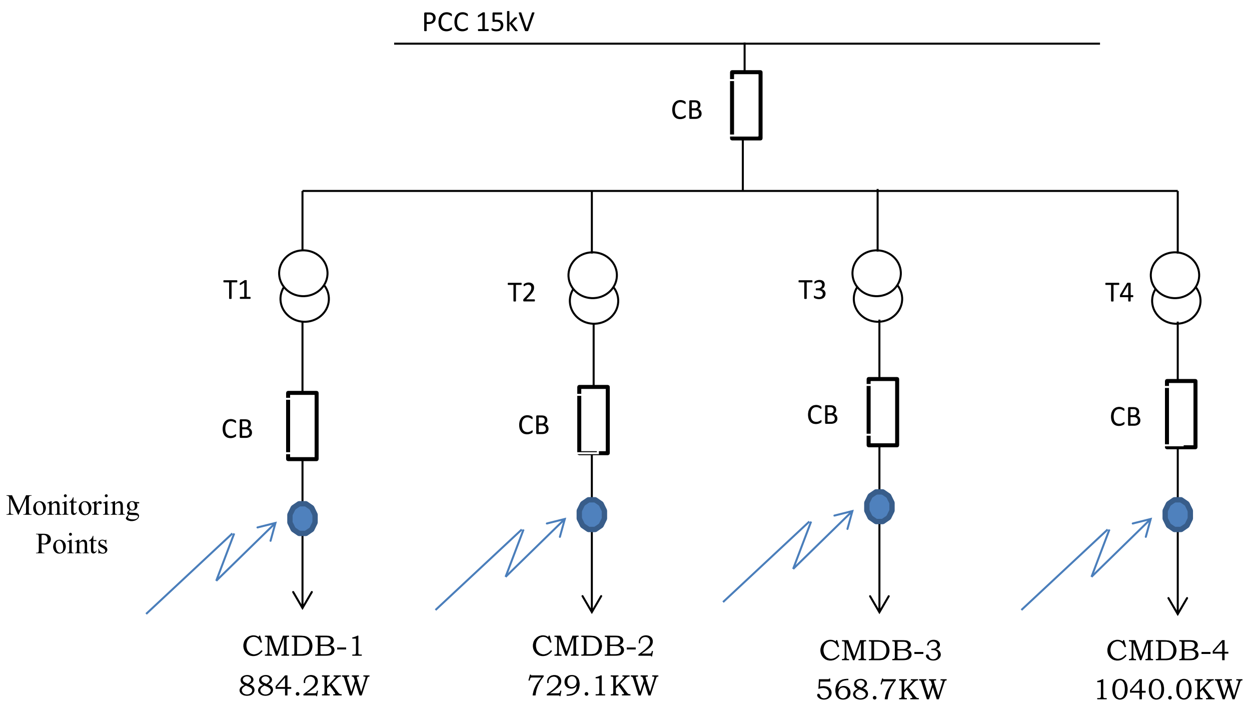

Figure 3.9: Single line diagram showing monitoring points on each transformer.

3.7 Modelling the Distribution Network

MATLAB/SMULINK is a graphical programing environment for modeling, simulating and analyzing multi-domain dynamical system. This simulation software environment is used for simulating and analyzing the power quality performance of Adama Spinning Factory distribution network. The distribution system is modeled by its equivalent circuit (impedance diagram). Calculations and assumptions taken in modeling different components of the distribution network are presented in the next sub-topics.

3.7.1 Distribution Transformers

Transformers are specified by their output voltage, kVA rating, percent impedance (%Z), and X/R ratio. The transformers are modeled by their series resistances and leakage reactances. The magnetizing current, Shunt admittances and core losses are neglected, as is the case in most power system analysis. The impedance of the transformer, Z_{tr} can be calculated from the percentage impedance by using equation 4.1.

$$Z_{tr} = \frac{\%Z\times(KV)^2\times 10}{KVA} \quad \text{......} (3.1)$$

$$\%Z_{at\ new\ KVA} = (\frac{base\ KVA_{new}}{KVA_{given}}) * \%Z_{at\ given\ KVA} \quad \text{......} (3.2)$$

The base KVA is selected to be 1250KVA. Normally, the X/R ratio of the transformers is not given on the name plate. It can be requested from the manufacturer or can be calculated from transformer full load and no load loss values. Moreover, standard value of X/R ratio for different Transformer ratings is given on IEEE standard 141-1993 (Page 184), based on IEEE C37.010-1997. Since, no load and full load losses are specified only on one transformer nameplate, for uniformity of calculation, the standard values from IEEE Std 141-1993 is used for this study. From the graph, the X/R ratios for 1250KVA and 800KVA transformers are around 6.5 and 5, respectively. Then, the resistance and reactance values referred to the secondary side of the transformer are calculated for all the transformers as follows.

i. Three transformers (T1, T2 and T4) of rating 1250 KVA, 50Hz, 15/0.4KV, %Z=5.01, I_{pri}=48.11A, I_{sec}=1804.22A, vector group: Dyn 5.

By using equation 3.1,

$$Z_{tr} = \frac{5.01 * (0.4)^2 * 10}{1250} = 6.413 * 10^{-3}\,\Omega$$

$$Z_{base} = \frac{V_{base}^2}{S_{base}} = \frac{(KV)_{base}^2}{MVA_{base}} = \frac{(0.4)^2}{1.25} = 0.128\Omega$$

By using the relation $Z^2=R^2+X^2$ and the X/R ratio of 6.5, the values of R_{tr} and X_{tr} of T1/T2/T4 become: $R_{tr}=0.975*10^{-3}\Omega$, $X_{tr}=6.34*10^{-3}\Omega$.

ii. One transformers (T3) of rating 800 KVA, 50Hz, 15/0.4KV, %Z=5.03, I_{pri}=30.8A, I_{sec}=1154.7A, vector group: Dyn 5, No load loss=1508w, Load loss=7236w

Since the name plate %Z value is given on the transformer's rating as a base KVA, it has to be converted to the selected base KVA, 1250KVA. The %Z on the base KVA of 1250 is:

$$\%Z_{at\ new\ KVA} = \left(\frac{1250KVA}{800KVA}\right) * 5.03 = 7.859$$

Similarly, by using equation 3.1,

$$Z_{tr} = \frac{7.859 * (0.4)^2 * 10}{1250} = 10.06 * 10^{-3}\ \Omega$$

Again, by using the relation $Z^2=R^2+X^2$ and the X/R ratio of 5, the values of R_{tr} and X_{tr} of T3 become: $R_{tr}=1.97*10^{-3}\Omega$, $X_{tr}=9.87*10^{-3}\Omega$.

Table 3.2 presents the calculated values of resistances and reactances for the four distribution transformer.

Table 3.2: Calculated values of R_{tr} and X_{tr} for T1-T4.

Transformer	Transf. Rating	R_{tr}	X_{tr}	L_{tr}
T1, T2 & T4	1250KVA	$0.975*10^{-3}\Omega$	$j6.34*10^{-3}\Omega$	0.0202mH
T3	800KVA	$1.97*10^{-3}\Omega$	$j9.87*10^{-3}\Omega$	0.0314mH

3.7.2 Power Factor Correcting 3φ Capacitors and Series Reactors

The 3φ capacitors shunt connected to the distribution network on each CMDB boards are specified by KVAr values. In addition to the KVAr values, the name plate data also indicates the capacitance values of each step capacitors for 50 and 60Hz systems. The KVAR values of all the step capacitors and the series connected inductance values of the anti-resonant reactors on each CMDB board are given on Table 3.3. These values are used to model the shunt detuned power factor correcting system (series LC branch) installed in the distribution system. The PFC capacitors are detuned by inserting a series anti resonant reactor to scale down the parallel self-resonant frequency (f_r) of the system seen from the load side from around 250-500Hz to specifically 189Hz, i.e from around 5th and 7th to around the 4th harmonic order.

Table 3.3: Detail of the capacitors and reactors installed in each CMDB board.

Dist. Boards	**PFC Capacitors**			**Anti-resonant Reactor**	
	KVAr	**Steps**	**Detail**	**Inductance**	**Quantity**
CMDB-1	40	3	2x10KVAr, 1x20KVAr	3.876mH 1.922mH	2 1
CMDB-2	162.5	5	1x12.5KVAr, 2x25KVAr, 2x50KVar	3.07mH 1.533mH 0.768mH	1 2 2
CMDB-3	150	5	2x12.5KVAr, 1x25KVAr, 2x50KVAr	3.07mH 1.533mH 0.768mH	2 1 2
CMDB-4	262.5	7	1x12.5KVAr, 2x25KVAr, 4x50KVAr	3.07mH 1.533mH 0.768mH	1 2 4

3.7.3 Installed Loads

The electrical loads connected to the distribution boards are characterized as linear loads of active and reactive powers computed based on the actual power factor (cos φ) and the installed load data of each distribution board. The actual power factor of the loads is gathered from the factory's monthly energy consumption report of each cost centers [18]. Twelve months (March, 2017-February, 2018) power factor data of each cost center is averaged for this analysis.

For the loads connected to MDB-G33, the apparent power can be calculated as:

$$S_{installed} = \frac{P_{installed}}{cos\varphi} = \frac{652.8}{0.943} = 692.0KVA$$

Then, the reactive power becomes:

$$Q_{installed} = \sqrt{S_{installed}^2 - P_{installed}^2} = \sqrt{692.0^2 - 652.8^2} = 229.6KVAr$$

Similarly, the installed inductive reactive power of all the loads are calculated and presented on Table 3.4. The power factor data for MDB-w/shop and Bale press is not included in the energy consumption report. Therefore, it is assumed to be cos φ=0.8 for these two loads.

Table 3.4: The active and reactive power of loads connected to each transformer.

Transformer	Distribution Boards	Cos φ	$P_{installed}$ (kw)	$Q_{installed}$ (KVAr)	$P_{installed}$ (kw)	$Q_{installed}$ (KVAr)
T1	MDB-G33	0.943	652.8	229.6	884.2	442.9
	MDB-Winder	0.735	231.4	213.3		
T2	MDB-R923	0.775	392	319.2	729.1	731.7
	MDB-M321	0.923	255	106.0		
	MDB-Comber	0.259	82.1	306.4		
T3	MDB-A2	0.704	368.2	371.0	568.8	446.7
	MDB-D40	0.936	200.6	75.7		
T4	MDB-Comp.	0.861	95.6	56.4	1040.1	454.1
	MDB-W/shop	0.800	40.8	30.6		
	MDB-Pump	0.996	210.7	19.0		
	MDB-NL	0.998	67	4.2		
	MDB-EM	0.975	202.5	46.5		
	AC 1+2	0.827	261	177.6		
	AC 3+4	0.805	154	113.3		
	Bale press	0.800	8.5	6.4		

In the model, the supplied voltage to the factory's distribution network is assumed to be balanced and pure sinusoid and represented by a balanced three phase voltage source. The distribution transformers are represented by their equivalent winding resistances and leakage reactances connected in series. The magnetizing branch components are not considered in the model. All the step delta capacitor banks of the PFC unit with the respective anti-resonant reactors are included in the model to see their effect on the system. The installed electrical loads of the factory are represented by the equivalent active and reactive loads connected to each transformer. The non-linear loads on transformers T1, T2 and T3 are modeled as ideal harmonic current sources and their detail will be presented in section 5.5.1 of chapter four. The overall distribution network of the factory modeled in MATLAB SIMULINK environment is presented in Figure 3.10 below.

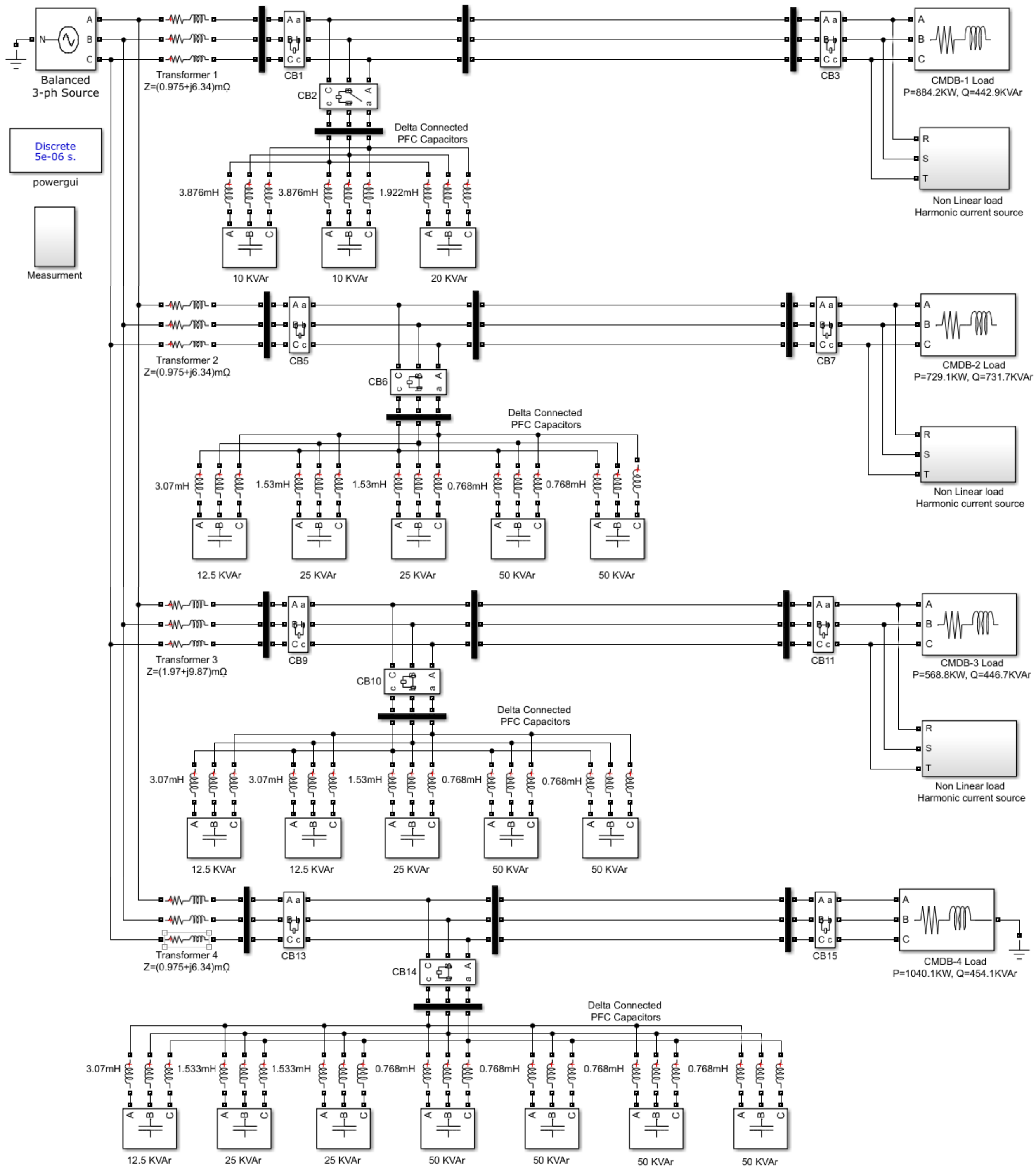

Figure 3.10: SIMULINK model of Adama Spinning Factory distribution system.

3.8 Standards on Harmonics

As discussed in chapter 2, Ethiopia has no national standard for limiting the level of harmonic distortion on electrical system. Moreover, the National Electro-technical Committee of Ethiopia (NECE) under the Ethiopia Standards Agency (ESA), which is responsible to approve and adopt international IEC standards to national standard, did not adopt the IEC 61000: EMC standards related to power quality phenomena for national use. As a result, the widely used and comprehensive international standards, IEEE and IEC harmonic distortion standards, will be used as a reference for this study.

3.8.1 IEEE Std 519-2014

IEEE Recommended Practice and Requirements for Harmonic Control in Electric Power Systems. This standard includes recommended harmonic voltage limits and recommended current distortion limits for systems nominally rated 120V - 69kV, 69kV - 161kV and above 161kV.

Recommended harmonic voltage limits: The voltage distortion limit is presented in Table 3.5. All values should be in percent of the rated power frequency voltage at the PCC [20].

*Table 3.5: IEEE voltage distortion limits***.** [20]

Bus voltage V at PCC	Individual harmonic (%)	Total harmonic distortion THD (%)
$V \leq 1.0$ kV	5.0	8.0
1 kV $< V \leq$ 69 kV	3.0	5.0
69 kV $< V \leq$ 161 kV	1.5	2.5
161 kV $< V$	1.0	1.5[a]

[a]High-voltage systems can have up to 2.0% THD where the cause is an HVDC terminal whose effects will have attenuated at points in the network where future users may be connected.

Recommended current distortion limits for systems nominally rated 120V - 69 kV: This current value is established at the PCC and should be taken as the sum of the currents corresponding to the maximum demand during each of the twelve previous months divided by 12. All values should be in percent of the maximum demand current, I_L. [20]

Table 3.6: IEEE current distortion limit for systems rated 120V through 69kV. [20]

Maximum harmonic current distortion in percent of I_L						
Individual harmonic order (odd harmonics)[a, b]						
I_{SC}/I_L	$3 \le h < 11$	$11 \le h < 17$	$17 \le h < 23$	$23 \le h < 35$	$35 \le h \le 50$	TDD
$< 20^c$	4.0	2.0	1.5	0.6	0.3	5.0
$20 < 50$	7.0	3.5	2.5	1.0	0.5	8.0
$50 < 100$	10.0	4.5	4.0	1.5	0.7	12.0
$100 < 1000$	12.0	5.5	5.0	2.0	1.0	15.0
> 1000	15.0	7.0	6.0	2.5	1.4	20.0

[a]Even harmonics are limited to 25% of the odd harmonic limits above.

[b]Current distortions that result in a dc offset, e.g., half-wave converters, are not allowed.

[c]All power generation equipment is limited to these values of current distortion, regardless of actual I_{sc}/I_L.

where

I_{sc} = maximum short-circuit current at PCC

I_L = maximum demand load current (fundamental frequency component) at the PCC under normal load operating conditions

The short circuit ratio (I_{SC}/I_L) is determined as follows:

- The three-phase short-circuit duty I_{SC} at the PCC may be obtained directly from the utility and expressed in amperes. If the short-circuit duty is given in MVA, it can be converted to an amperage value using the following expression:

$$I_{SC} = \frac{1000 \times MVA}{\sqrt{3} \times kV} \qquad (3.3)$$

Where MVA and kV represent the three-phase short-circuit capacity in mega-volt-amperes and the line-to-line voltage at the PCC in kV, respectively. Alternatively, the short circuit current in a circuit can be expressed as:

$$I_{SC} = \frac{V_{ph}}{Z_{SC}} \qquad (3.4)$$

Assume that the impedance is purely reactive. This is a reasonably good assumption for industrial power systems for buses close to the mains and for most utility systems. Moreover, at utilization voltages, such as industrial power systems, the equivalent system reactance is often dominated by the service transformer impedance. Therefore the short circuit impedance can be approximated by the service transformer reactance.

We have the expression for percentage reactance, $\%X_{tr}$

$$\%\,X_{tr} = \frac{I_{FL}\,X_{tr}}{V_{ph}} \times 100 \quad \ldots\ldots\ldots\ldots\ldots\ldots\ldots\ldots\ldots\ldots\ldots... (3.5)$$

$$X_{tr} = \frac{V_{ph}}{I_{FL}} \times \frac{\%\,X}{100} \quad \ldots\ldots\ldots\ldots\ldots\ldots\ldots\ldots\ldots\ldots\ldots\ldots (3.6)$$

Where I_{FL} is the full load current; V_{ph} is phase voltage; X_{tr} is reactance in ohms per phase of each transformer. Thus,

$$I_{SC} = \frac{I_{FL} \times 100}{\%\,X_{SC}} = \frac{I_{FL} \times 100}{\%\,X_{tr}} \quad \ldots\ldots\ldots\ldots\ldots\ldots\ldots\ldots\ldots\ldots\ldots (3.7)$$

The percentage reactance, $\%X_{tr}$, is calculated using equation 3.1 and 3.7, for T1, T2 and T4:

$$\%X_{tr} = \frac{KVA \times X_{tr}}{10(KV)^2} = \frac{1250 \times 0.00634}{10 \times (0.4)^2} = 4.95$$

$$I_{Sc} = \frac{1804.22 \times 100}{4.95} = 36448.9A$$

And, for T3:

$$\%X_{tr} = \frac{KVA \times X_{tr}}{10(KV)^2} = \frac{800 \times 0.00987}{10 \times (0.4)^2} = 4.94$$

$$I_{Sc} = \frac{1154.7A \times 100}{4.94} = 23374.5A$$

- The load average kilowatt demand P_D for the most recent 12 months is found from the factory's monthly energy consumption report, shown on Appendix C of this document. This report is prepared based on the measured value at the PCC for all four transformers and used for billing purpose by the electric power utility. The average kilowatt demand P_D for the period from March, 2017 to February, 2018 becomes:

$$P_D = \frac{Sum\ of\ max.demand\ of\ previous\ 12\ months\ (Mar\ 2017 - Feb\ 2018)}{12}$$

$$P_D = \frac{15240\ kW}{12} = 1270\ kW$$

Then, the average demand current calculated as follows:

$$I_L = \frac{kW}{PF \times \sqrt{3} \times kV} \text{ .... (3.8)}$$

Where PF is the average billed power factor, also can be found from the factory's monthly energy consumption report presented on Appendix C of this document. The power factor for the same duration (March, 2017-February, 2018) is calculated, using the total reactive energy (total KVArh) and active energy (total KWh) consumed during the same period, as:

$$PF = \cos[tan^{-1}\left(\frac{total\ KVArh}{total\ KWh}\right)] \text{ .... (3.9)}$$

$$PF = 0.8817$$

Therefore,

$$I_L = \frac{1270}{0.8815 \times \sqrt{3} \times 0.4} = 2079.5A$$

The average demand current of each transformer is calculated based on the average percentage load share of the four transformers. The average percentage load share is calculated based on the monthly energy consumption by cost center report [18] of the factory for the same duration from March, 2017 to February, 2018. The monthly percentage load share of each transformer is calculated by dividing the monthly energy consumption of each transformer to the total energy consumption of the four transformers. Then, the sum of the monthly percentage load share of the 12 months (March, 2017 to February, 2018) is divided by 12 to get the average load share of each transformer. Therefore, the average load share and corresponding average demand current becomes:

T1: 21.9% of I_L = 455.4A

T2: 24.1% of I_L = 501.2A

T3: 10.1% of I_L = 210.0A

T4: 43.9% of I_L = 912.9A

- Then, the short circuit ratio (I_{SC}/I_L) for each transformer found to be:

$$For\ T1: \quad {}^{I_{SC}}/_{I_L} = \frac{36448.9A}{455.4\text{A}} = 80 \qquad For\ T2: \quad {}^{I_{SC}}/_{I_L} = \frac{36448.9A}{501.2\text{A}} = 72.7$$

$For\ T3$: ${}^{I_{SC}}/_{I_L} = \dfrac{23374.5A}{210\text{A}} = 111.3$ $For\ T4$: ${}^{I_{SC}}/_{I_L} = \dfrac{36448.9A}{912.9\text{A}} = 39.9$

Therefore, as per the IEEE Std 519-2014, for the electrical system under consideration:

- Maximum acceptable voltage THD level of 8%, with a maximum percentage of 5% for individual harmonic components will be used for all the CMDB boards.
- Maximum acceptable current TDD level of 12%, 15%, and 8% with maximum percentage of 10%, 12%, and 7% for the individual harmonic components (3^{rd} to 9^{th}) will be used for CMDB-1/-2, CMDB-3, CMDB-4, respectively.

3.8.2 IEC Standards [1]

As mentioned in chapter 2, IEC standards for each power quality parameters are not given on a single publication. The IEC standard relating to harmonic distortions are discussed below.

IEC 61000-2-2 (1993): Compatibility Levels for Low-Frequency Conducted Disturbances and Signaling in Public Low-Voltage Power Supply Systems. These levels are given in percentage of the fundamental voltage and are given in Table 3.7.

Table 3.7: Compatibility Levels for Individual Harmonic Voltages in the Low-Voltage Public Network According to IEC 61000-2-2. [1]

Not multiple of 3		Multiple of 3			
Odd order h	Harmonic voltage (%)	Odd order h	Harmonic voltage (%)	Even order h	Harmonic voltage (%)
5	6	3	5	2	2
7	5	9	1.5	4	1
11	3.5	15	0.3	6	0.5
13	3	21	0.2	8	0.5
17	2	>21	0.2	10	0.2
19	1.5			12	0.2
23	1.5			>12	0.2
25	1.5				
>25	$0.2 + 1.3 \times 25/h$				

*The THD of the supply voltage including all harmonics up to the 40^{th} order shall be less than 8 %.

IEC 61000-3-4 (1998): Limits for Harmonic Current Emissions from equipment drawing input current of larger than 16A per phase. These limits are in percent of the fundamental input current and are shown in Table 3.8.

Table 3.8: Harmonic Current Limits According to IEC 61000-3-4. [1]

Harmonic order h	Max. permissible harmonic current* (%)	Harmonic order h	Max. permissible harmonic current* (%)
3	21.6	19	1.1
5	10.7	21	0.6
7	7.2	23	0.9
9	3.8	25	0.8
11	3.1	27	0.6
13	2	29	0.7
15	0.7	31	0.7
17	1.2	33	0.6

IEC 61000-3-6 (1996): limits of harmonic current emission for equipment connected to medium-voltage (MV) and high-voltage (HV) supply systems. This standard provides compatibility levels and planning levels for harmonic voltages in the LV and MV systems. The IEC 61000-3-6 compatibility levels for harmonic voltages as a percentage of the fundamental voltage in both LV and MV system are similar to the levels presented in Table 3.8.

These IEC 61000 EMC standards, presented in Tables 3.7 and 3.8, are used to check the compatibility levels of the voltage and current distortion in all CMDB boards in Adama Spinning Factory.

CHAPTER FOUR

RESULTS AND DISCUSSION

4.1 Measurement Results

This section illustrates the analysis and discussions of the results collected during measurement and check the compatibility of the voltage and current harmonic distortion levels in accordance with IEEE Std 519-2014, IEC 61000-3-6(1996) and IEC 61000-3-4(1998) harmonic distortion standards. The monitoring has been carried out using DELAB NV8s PFC devices and the four measuring points on each distribution transformer are shown on Figure 3.9 in the previous chapter.

One drawback of the monitoring devices used in this study is that they don't have any data storage (logging) capability. As a result, the instantaneous measured values at different times have been recorded manually by the factory electricians. This way of manual recording is error prone and highly dependent on the accuracy of the person recording the data. Due to this fact, some recorded values, which have huge variation from the mean of all the recorded data, have been suspected as a recording error and are not considered on the analysis.

4.2.1 Measurement Results of CMDB-1

As mentioned on the previous chapter, the monitoring device which is capable of measuring the voltage and current distortion levels has been installed on CMDB-1 on the secondary side of transformer T1 (1250 KVA, 15/0.4KV, %Z=5.01, I_{pri}=48.11A, I_{sec}=1804.22A) and measurements has been taken for three days. The measurement data are presented on Appendix D: Measured data on CMDB-1 of this document. In order to get the actual current values, the measured secondary current values (I_{sec}) and the individual n^{th} odd harmonic current values on this table have to be multiplied by 2500/5=500, which is transformation ratio of the CT installed on CMDB-1. The THD_V, THD_I and cos φ values from the measured data for CMDB-1 are plotted as shown on Figure 4.1.

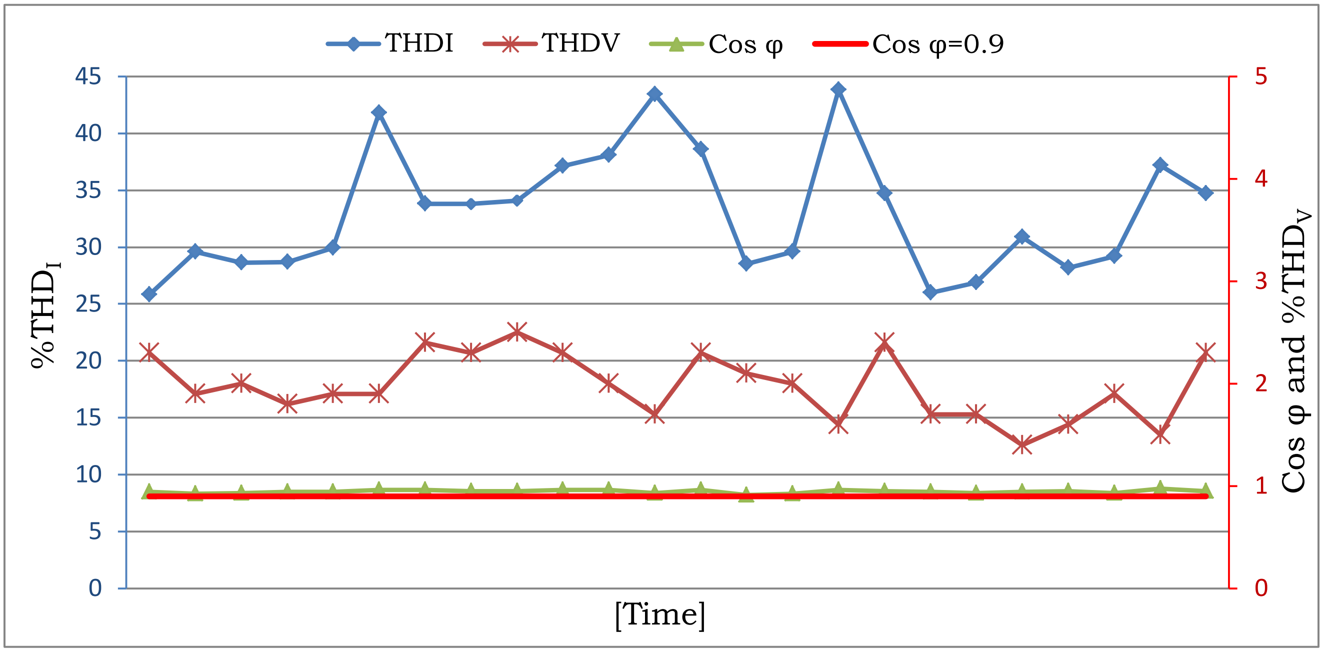

Note: the vertical scale on the left is for THD_I and on the right is for THD_V and cos φ.

Figure 4.1: Plot of THD_V, THD_I and cos φ values of CMDB-1

The IEC voltage and current distortion limits are given in percent of the fundamental voltage and current values, respectively. Therefore, the individual current and voltage harmonic values in percent of the respective fundamental values can be calculated using the following expressions.

$$\%I_h = \frac{I_h}{I_1} \times 100 \qquad\qquad \%V_h = \frac{V_h}{V_1} \times 100 \quad \ldots\ldots\ldots\ldots\ldots\ldots (4.1)$$

Where, $\%I_h$ is the current harmonic level in percent of the fundamental current value, I_1 and $\%V_h$ is the voltage harmonic level in percent of the fundamental voltage value, V_1 for each harmonic orders, h=3, 5, 7, 9 and 11.

The current harmonic level in percent of the fundamental current value ($\%I_h$) is calculated using the measured data recorded on March 22, 2018 at 10:50 PM on which the THD_I is the maximum.

$$\%I_1 = \frac{I_1}{I_1} \times 100 = \frac{0.43}{0.43} \times 100 = 100 \qquad\qquad \%I_3 = \frac{I_3}{I_1} \times 100 = \frac{0.02}{0.43} \times 100 = 4.7$$

Similarly, $\%I_5$=37.2, $\%I_7$=20.9, $\%I_9$=0 and $\%I_{11}$=4.7. The THD_I can also be calculated as:

$$\%THD_I = \sqrt{I_3^2 + I_5^2 + I_7^2 + I_9^2 + I_{11}^2} = 43.18$$

The maximum measured THD_I value is 43.8 % and the calculated one from the individual harmonics up to 11th order is 43.2%. This shows that there are some values of harmonic currents above the 11th order, though they cannot be recorded with this measuring device. The percentage values of each harmonic current are plotted as a function of the harmonic order (frequency) as shown on Figure 4.2.

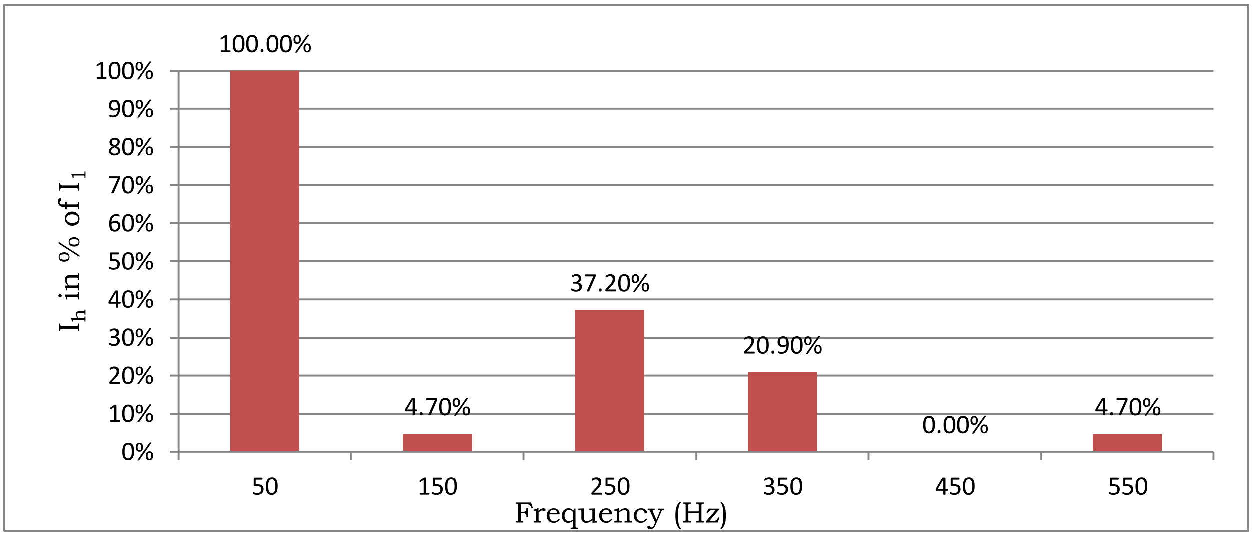

Figure 4.2: Individual current harmonics in % of the fundamental current for CMDB-1.

Similarly, the voltage harmonic level in percent of the fundamental voltage value ($\%V_h$) is calculated using the measured values recorded on March 20, 2018 at 2:00 PM, on which the THD_V is the maximum.

$$\%V_1 = \frac{V_1}{V_1} \times 100 = \frac{227}{227} \times 100 = 100 \qquad \%V_3 = \frac{V_3}{V_1} \times 100 = \frac{0}{227} \times 100 = 0$$

Similarly, $\%V_5$=1.3, $\%V_7$=1.3, $\%V_9$=0 and $\%V_{11}$=0.44. The THD_V can also be calculated as:

$$\%THD_V = \sqrt{V_3^2 + V_5^2 + V_7^2 + V_9^2 + V_{11}^2} = 1.89$$

The maximum measured THD_I value is 2.5 % and the calculated one from the individual harmonics up to 11th order is 1.9%. This shows that there are some values of harmonic voltages above the 11th order, though they cannot be recorded with this measuring device. The percentage values of each harmonic voltage are plotted as a function of the harmonic order (frequency) as shown on Figure 4.3.

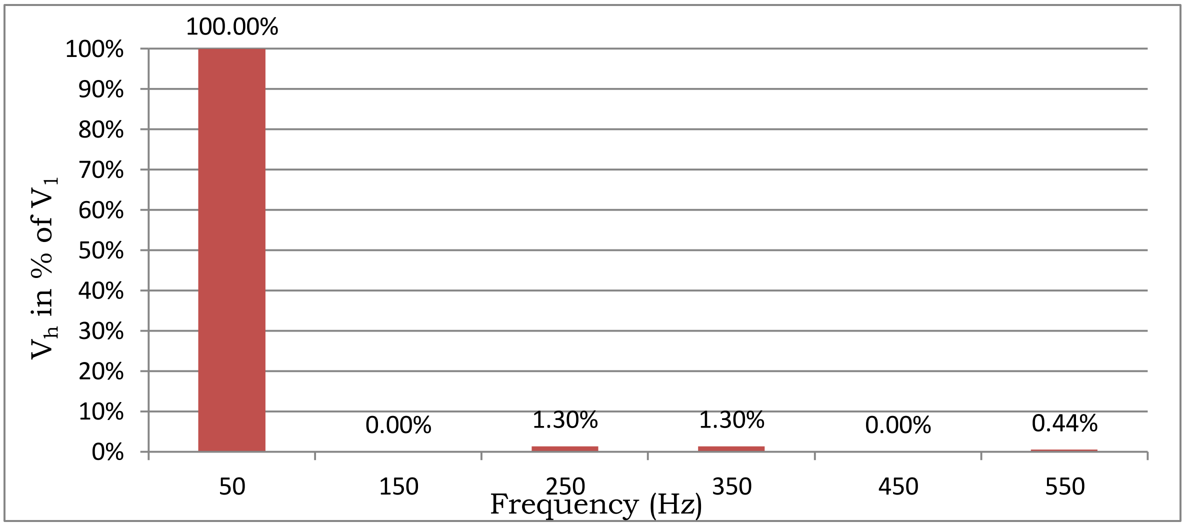

Figure 4.3: Individual voltage harmonics in % of the fundamental voltage for CMDB-1.

The IEEE recommended voltage and current distortion limits presented in Table 3.5 and 3.6 are specified in percent of the rated power frequency voltage, V_r and the maximum demand current, I_L, respectively. The average demand current of the previous 12 months for transformer T1 is calculated in the previous chapter. This value has to be transferred to the primary side of the CT, in order to make calculations with the measured values. i.e. I_L at the CT secondary is 455.4A and with CT ratio of 500, I_L at the primary is 0.91A. The rated power frequency voltage is the nominal fundamental phase voltage supplied by the utility, which is 400V/√3=230.9V.

Then, the individual current value in percent of maximum demand current, I_L and the individual voltage harmonic values in percent of the rated power frequency voltage, V_r can be calculated using the following expressions.

$$\%I_h = \frac{I_h}{I_L} \times 100 \qquad \%V_h = \frac{V_h}{V_r} \times 100 \quad \ldots\ldots\ldots\ldots\ldots\ldots\ldots (4.2)$$

Where, $\%I_h$ is the current harmonic level in percent of the maximum demand current value, I_L and $\%V_h$ is the voltage harmonic level in percent of the rated power frequency voltage, V_r for each harmonic order.

Using the expression in 4.2, $\%I_h$ is calculated for h=3, 5, 7, 9 and 11 and become $\%I_3$=3.3, $\%I_5$=24.2, $\%I_7$=11, $\%I_9$=0 and $\%I_{11}$=4.4.

Similarly, the values of $\%V_h$ become $\%V_3$=0, $\%V_5$=2.2, $\%V_7$=1.7, $\%V_9$=0 and $\%V_{11}$=0.4.

The TDD factor and the Total Harmonic Distortion, THD_V of voltage in percent of the rated power frequency voltage can also be calculated as:

$$\%TDD = \sqrt{I_3^2 + I_5^2 + I_7^2 + I_9^2 + I_{11}^2} = 27.1 \qquad \%THD_V = \sqrt{V_3^2 + V_5^2 + V_7^2 + V_9^2 + V_{11}^2} = 2.8$$

The maximum measured THD_V, THD_I/TDD and the individual current and voltage harmonic values up to 11^{th} order are compared with the corresponding IEC and IEEE standard limits on Tables 4.1 and 4.2.

Table 4.1: Comparison of the maximum measured harmonic values with corresponding IEC standards for CMDB-1.

Harmonic order/THD	Actual %V	IEC Std 61000-2-2	Actual %I	IEC Std 61000-3-4
3^{rd}	0	5	4.5	21.6
5^{th}	2.2	6	30.1	10.7
7^{th}	1.7	5	16.4	7.2
9^{th}	0	1.5	0	3.8
11^{th}	0.4	3.5	5.9	3.1
THD	2.5	8	43.8	-

Table 4.2: Comparison of calculated harmonic values with the corresponding IEEE standards for CMDB-1.

Harmonic order/ THD_V/ TDD	Actual %V	IEEE Std 519	Actual %I	IEEE Std 519
3^{rd}	0	5	3.3	10
5^{th}	2.2	5	24.2	10
7^{th}	1.7	5	11	10
9^{th}	0	5	0	10
11^{th}	0.4	5	4.4	4.5
THD/TDD	2.8	8	27.1	12

The analysis of all the data collected during the monitoring period of CMDB-1 shows that the harmonic current distortion level on this distribution transformer is the worst one in relation to the other three distribution transformers. As indicated on chapter 2, the total capacity of ASDs installed on this transformer is the highest and more harmonic distortion is expected on this transformer. The measurement also revealed that the highest THD_I of 43.8% is recorder on this transformer. As shown on Tables 4.1 and 4.2, the individual 5^{th}, 7^{th} and 11^{th} order harmonic currents are also outside the IEC and/or IEEE standard limits, with the 5th and 7th orders being the most dominant ones. On the other hand, all the individual voltage harmonic levels as well as the THD_V are within the IEC and IEEE voltage harmonic distortion limits.

Moreover, as indicated in the previous chapter, there were two incidents of fire accident on the contactors controlling the power factor correcting capacitors of this distribution board. Of these incidents, one was happened while carrying out monitoring of the other distribution boards for this study.

During the measurement period the power factor level of this distribution transformer was above the minimum allowable limit set by the utility not to be penalized, which is 0.9. Currently, all the three capacitor banks and the measuring device are disconnected from the system due to the fire accident. As a result, the power factor may become below 0.9.

4.1.2 Measurement Results of CMDB-2

The same measuring device has been installed and configured on CMDB-2, on the secondary side of transformer T2 (1250 KVA, 15/0.4KV, %Z=5.01, I_{pri}=48.11A, I_{sec}=1804.22A) and measurements has been taken for eight days. The measurement data are presented on Appendix D: Measured data on CMDB-2 of this document. The transformation ratio of the CT installed on CMDB-2 is 2500/5=500. By taking similar assumptions and calculations, the graphs on Figure 4.4 to 4.6 have been plotted.

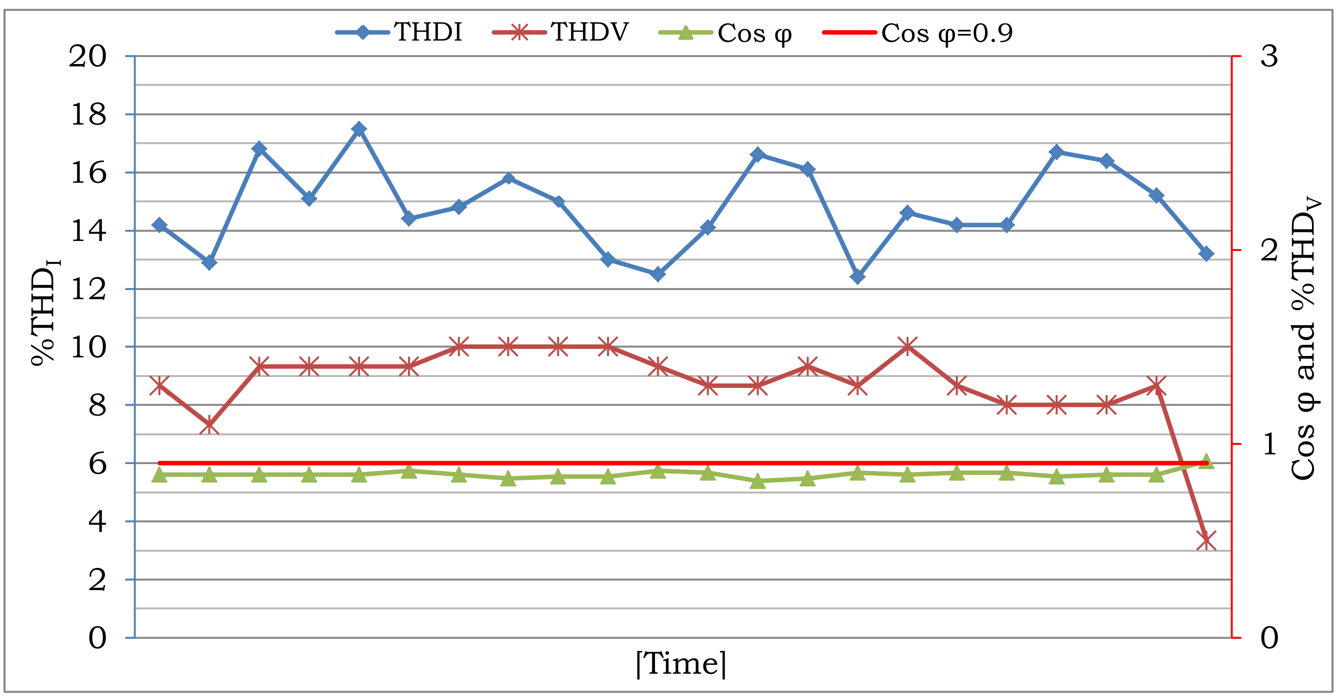

Note: the vertical scale on the left is for THD_I and on the right is for THD_V and cos φ.

Figure 4.4: Plot of THD_V, THD_I and cos φ values of CMDB-2.

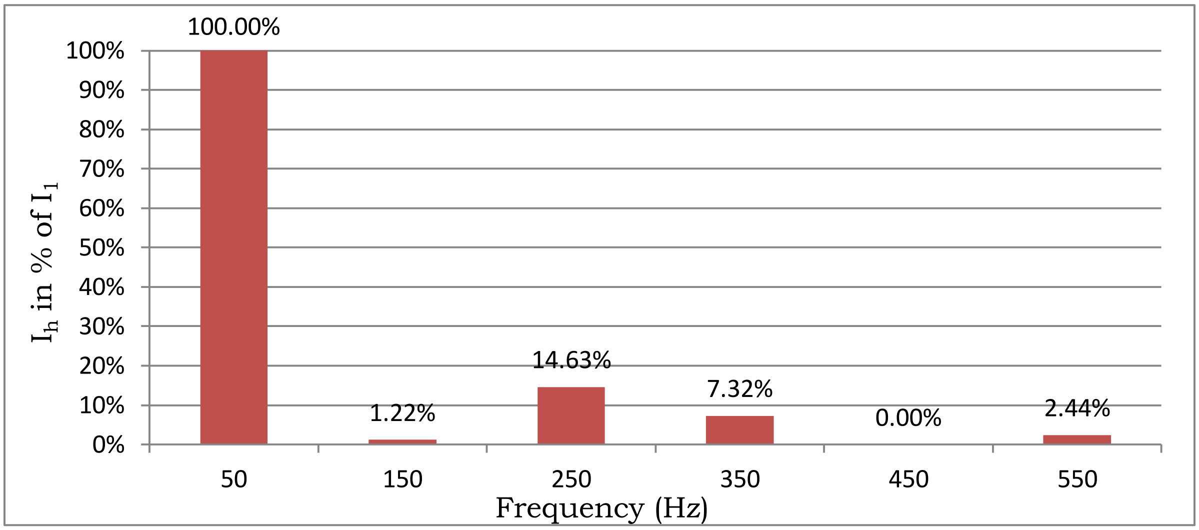

Figure 4.5: Individual current harmonics in % of the fundamental current for CMDB-2.

The maximum measured THD_I value is 17.5% and the calculated one from the individual harmonics up to 11^{th} order is 16.6%. Similarly, the maximum measured THD_V value is 1.5% and the calculated one from the individual harmonics up to 11^{th} order is 1.3%. This shows that there are some values of harmonic currents and voltages above the 11^{th} order, though they cannot be recorded with this measuring device.

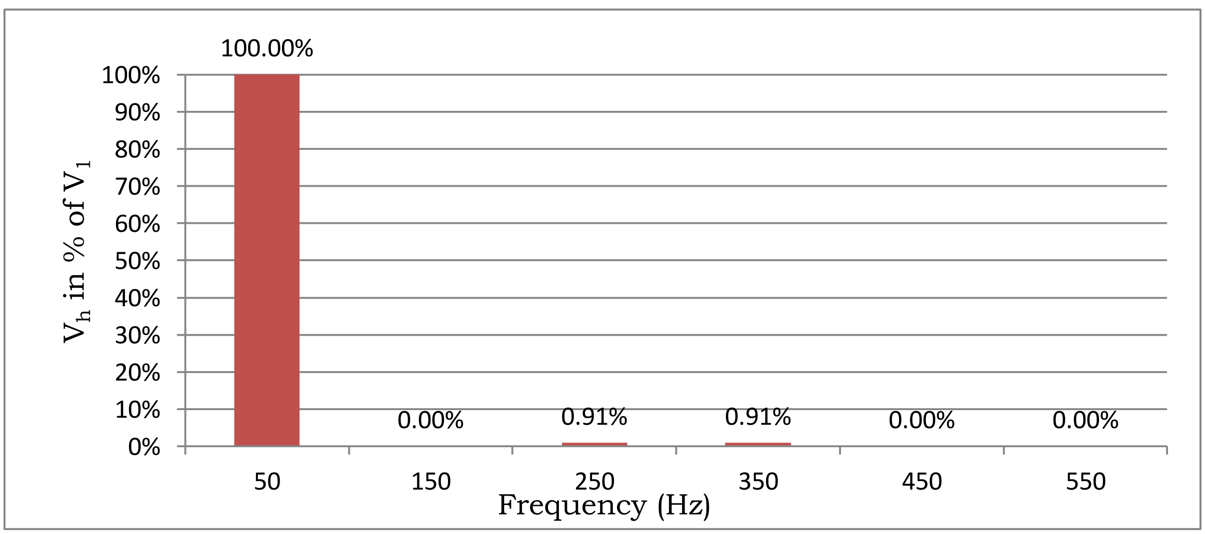

Figure 4.6: Individual voltage harmonics in % of the fundamental voltage for CMDB-2.

The maximum measured THD_V, THD_I and the individual current and voltage harmonic values up to 11^{th} order are compared with the corresponding IEC standard limits on Table 4.3. For CMDB-2, I_L at the CT secondary is 501.2A and with CT ratio of 500, I_L at the primary is 1.0A and the rated power frequency voltage is 380V/√3=219.4V (As per the information from the factory Engineers, the tap changer setting of this transformer is at 380V while for the other three transformers are at 400V). Using this values of I_L and V_r, the corresponding THD_V and TDD values with their respective individual harmonic levels as per the IEEE standard are calculated and compared with the limits on Table 4.4.

Table 4.3: Comparison of the maximum measured harmonic values with corresponding IEC standards for CMDB-2.

Harmonic order/THD	Actual %V	IEC Std 61000-2-2	Actual %I	IEC Std 61000-3-4
3^{rd}	0	5	2.2	21.6
5^{th}	0.9	6	14.1	10.7
7^{th}	0.9	5	7.6	7.2
9^{th}	0	1.5	0	3.8
11^{th}	0.5	3.5	2.5	3.1
THD	1.5	8	17.5	-

Table 4.4: Comparison of calculated harmonic values with the corresponding IEEE standards for CMDB-2.

Harmonic order/ THD_V/ TDD	Actual %V	IEEE Std 519	Actual %I	IEEE Std 519
3^{rd}	0	5	2.0	10
5^{th}	0.9	5	13.0	10
7^{th}	0.9	5	6.0	10
9^{th}	0	5	0	10
11^{th}	0.5	5	2.0	4.5
THD/TDD	1.4	8	14.6	12

The analysis of all the data collected during the monitoring period of CMDB-2 shows that the TDD and the 5^{th} order harmonic current distortion level on this distribution transformer is outside the IEEE standard limits. As shown on Tables 4.3 and 4.4, the 5^{th} and 7^{th} order current harmonics are the most dominant ones by exceeding the IEC and/or IEEE standards. On the other hand, all the individual voltage harmonic levels as well as the THD_V are within the IEC and IEEE voltage harmonic distortion limits. During the measurement period the power factor level of this distribution transformer was below 0.9, the minimum allowable limit set by the utility not to be penalized.

4.1.3 Measurement Results of CMDB-3

The same measuring device has been installed and configured on CMDB-3, on the secondary side of transformer T3 (800 KVA, 15/0.4KV, %Z=5.03, I_{pri}=30.8A, I_{sec}=1154.7A) and measurements has been taken for three days. The measurement data are presented on Appendix D: Measured data on CMDB-3 of this document. The transformation ratio of the CT installed on CMDB-3 is 1250/5=250. By taking similar assumptions and calculations, the graphs on Figure 4.7 to 4.9 have been plotted.

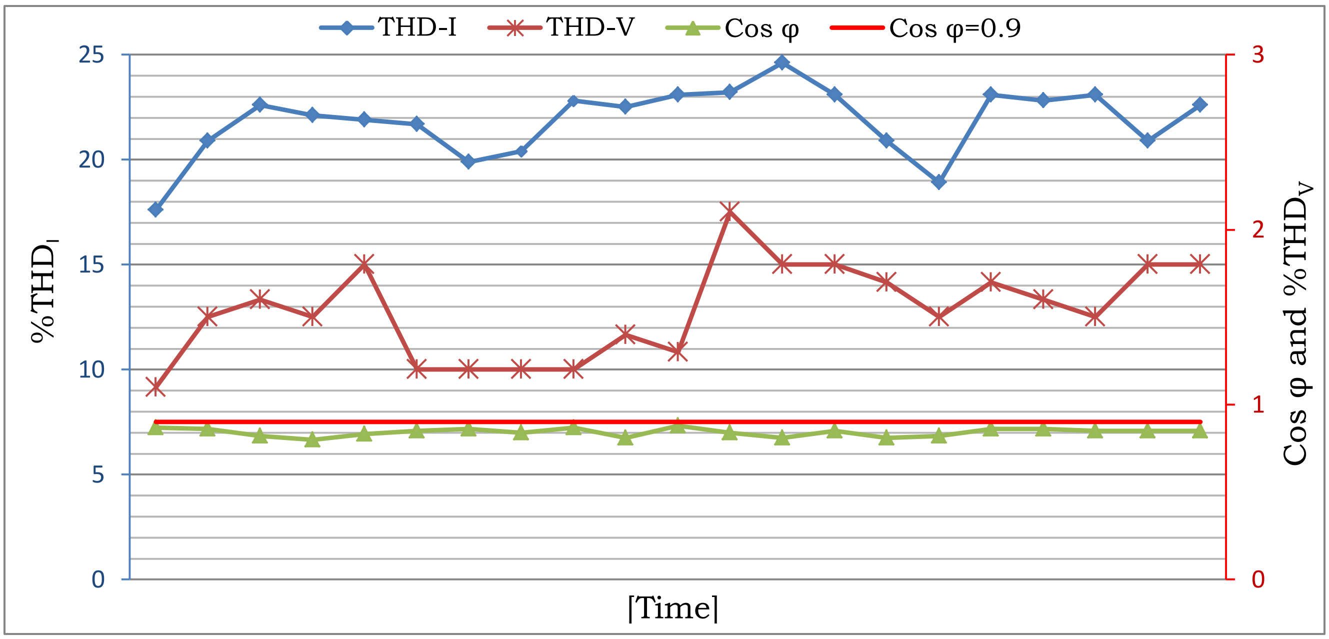

Note: the vertical scale on the left is for THD_I and on the right is for THD_V and cos φ.

Figure 4.7: Plot of THD_V, THD_I and cos φ values of CMDB-3.

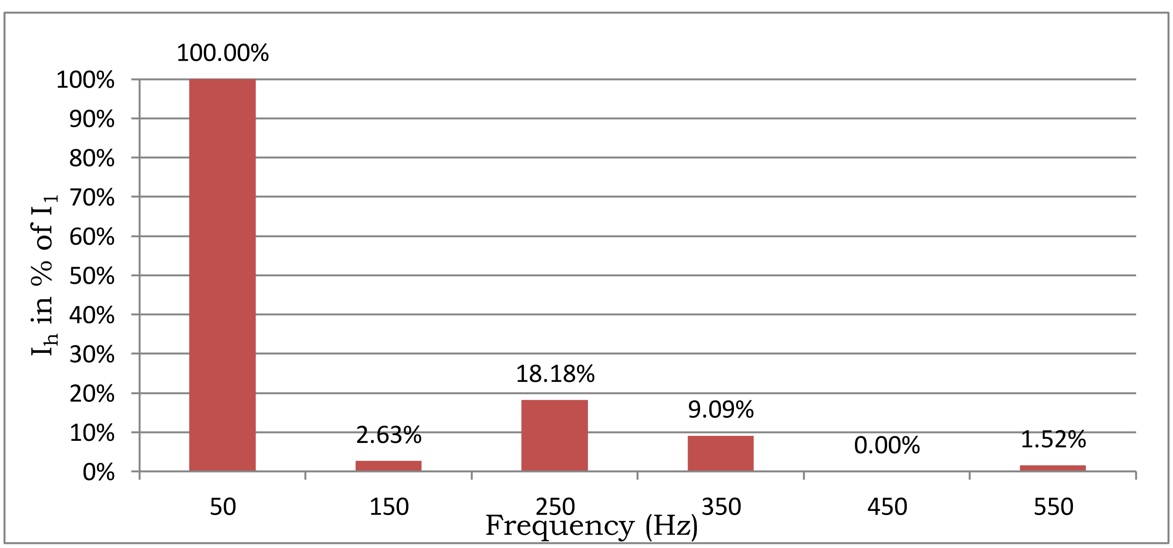

Figure 4.8: Individual current harmonics in % of the fundamental current for CMDB-3.

The maximum measured THD_I value is 24.6% and the calculated one from the individual harmonics up to 11^{th} order is 20.6%. Similarly, the maximum measured THD_V value is 2.1% and the calculated one from the individual harmonics up to 11^{th} order is 2.1%. This shows that there are some values of harmonic currents above the 11^{th} order, though they cannot be recorded with this measuring device.

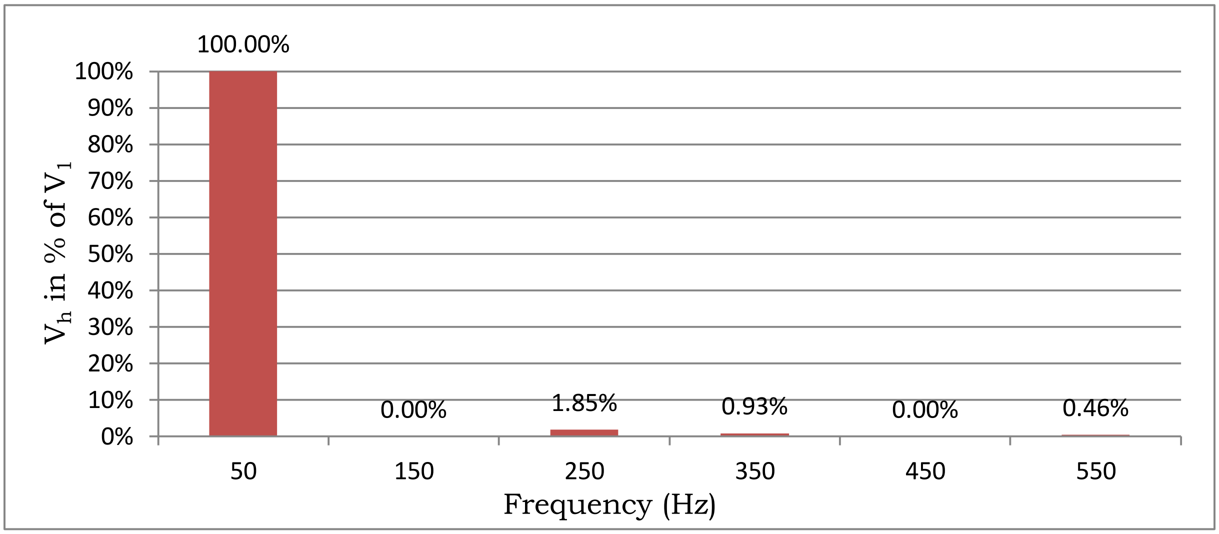

Figure 4.9: Individual voltage harmonics in % of the fundamental voltage for CMDB-3.

The maximum measured THD_V, THD_I and the individual current and voltage harmonic values up to 11^{th} order are compared with the corresponding IEC standard limits on Table 4.5. For CMDB-3, I_L at the CT secondary is 210A and with CT ratio of 250, I_L at the primary is 0.84A and the rated power frequency voltage is 400V/√3=230.9V. Using this values of I_L and V_r, the corresponding THD_V and TDD values with their respective individual harmonic levels as per the IEEE standard are calculated and compared with the limits on Table 4.6.

Table 4.5: Comparison of the maximum measured harmonic values with corresponding IEC standards for CMDB-3.

Harmonic order/THD	Actual %V	IEC Std 61000-2-2	Actual %I	IEC Std 61000-3-4
3^{rd}	0.5	5	3.6	21.6
5^{th}	1.9	6	23.2	10.7
7^{th}	1.4	5	10.1	7.2
9^{th}	0	1.5	0	3.8
11^{th}	0.5	3.5	3.1	3.1
THD	2.1	8	24.6	-

Table 4.6: Comparison of calculated harmonic values with the corresponding IEEE standards for CMDB-3.

Harmonic order/ THD_V/ TDD	Actual %V	IEEE Std 519	Actual %I	IEEE Std 519
3^{rd}	0.4	5	2.4	12
5^{th}	1.7	5	22.6	12
7^{th}	1.3	5	11.9	12
9^{th}	0	5	0	12
11^{th}	0.4	5	2.4	5.5
THD/TDD	2.3	8	25.8	15

The analysis of all the data collected during the monitoring period of CMDB-3 shows that the TDD and the 5^{th} order harmonic current distortion level on this distribution transformer is outside the IEEE standard limits. As shown on Tables 4.5 and 4.6, the 5^{th} and 7^{th} order current harmonics are the most dominant ones by exceeding the IEC and/or IEEE standards. On the other hand, all the individual voltage harmonic levels as well as the THD_V are within the IEC and IEEE voltage harmonic distortion limits. During the measurement period the power factor level of this distribution transformer was below 0.9, the minimum allowable limit set by the utility not to be penalized.

4.1.4 Measurement Results of CMDB-4

The same measuring device has been installed and configured on CMDB-4, on the secondary side of transformer T4 (1250 KVA, 15/0.4KV, %Z=5.01, I_{pri}=48.11A, I_{sec}=1804.22A) and measurements has been taken for four days. The measurement data are presented on Appendix D: Measured data on CMDB-4 of this document. The transformation ratio of the CT installed on CMDB-4 is 1600/5=320. By taking similar assumptions and calculations, the graphs on Figure 4.10 to 4.12 have been plotted.

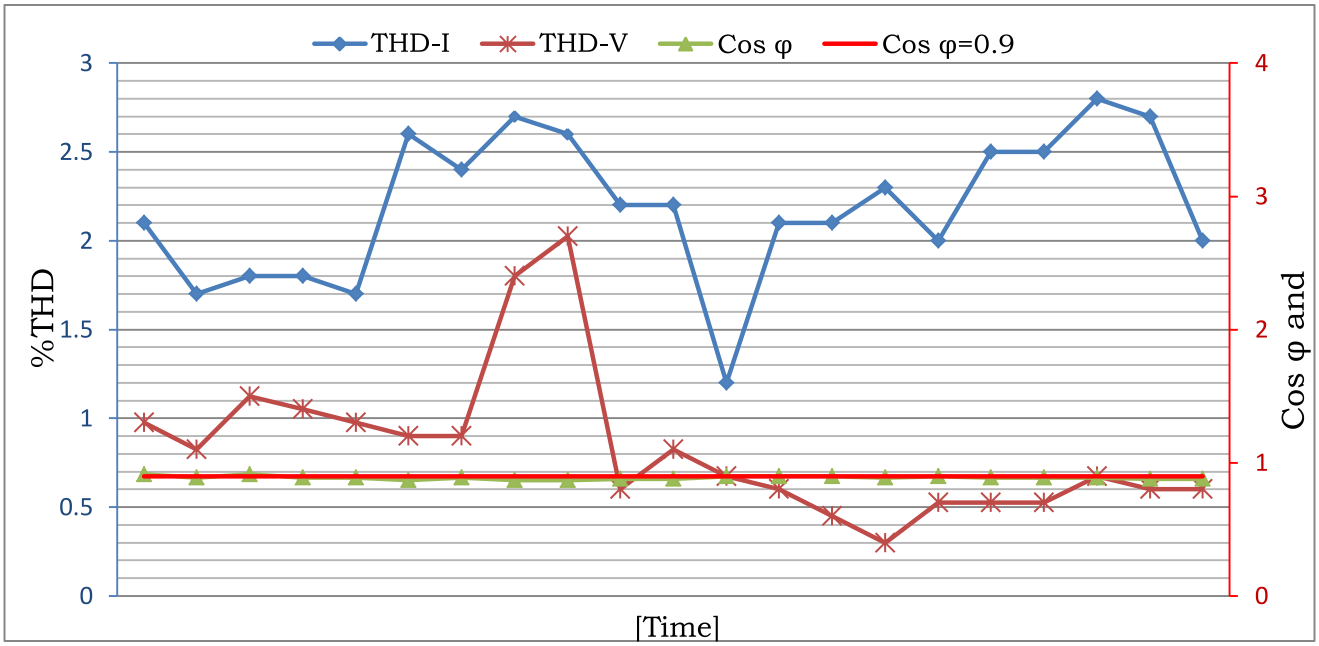

Note: the vertical scale on the left is for THD_I and on the right is for THD_V and cos φ.

Figure 4.10: Plot of THD_V, THD_I and cos φ values of CMDB-4.

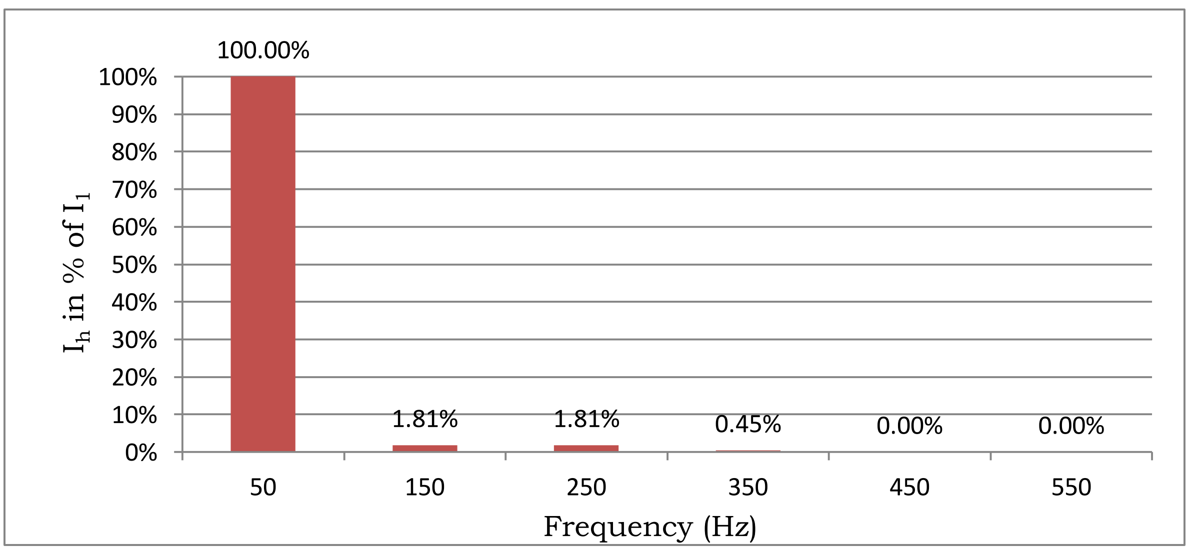

Figure 4.11: Individual current harmonics in % of the fundamental current for CMDB-4

The maximum measured THD_I value is 2.9% and the calculated one from the individual harmonics up to 11^{th} order is 2.6%. Similarly, the maximum measured THD_V value is 2.7% and the calculated one from the individual harmonics up to 11^{th} order is 0.9%. This shows that there are some values of harmonic currents and voltages above the 11^{th} order, though they cannot be recorded with this measuring device.

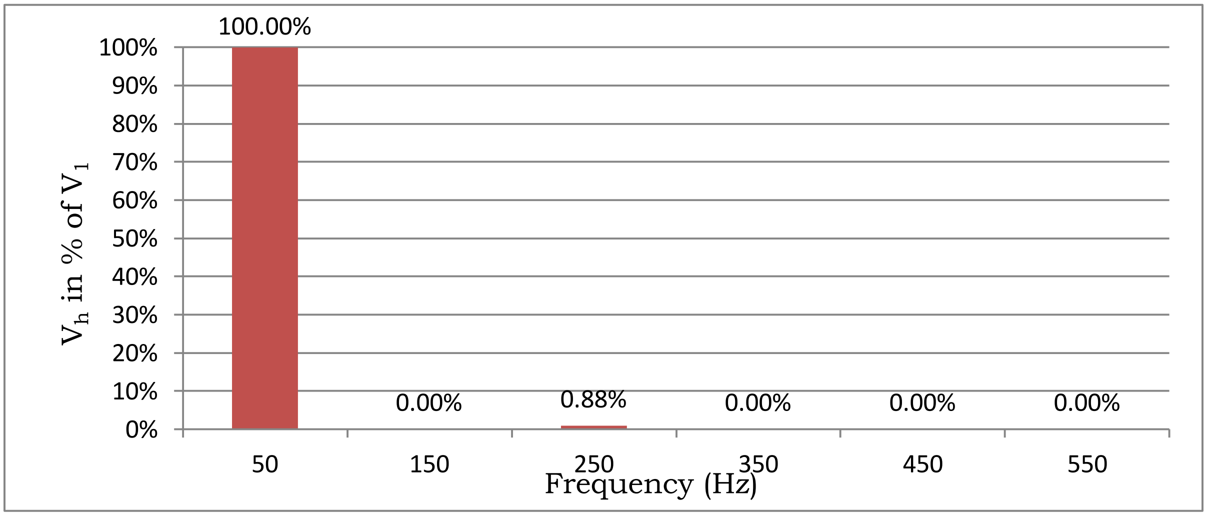

Figure 4.12: Individual voltage harmonics in % of the fundamental voltage for CMDB-4

The maximum measured THD_V, THD_I and the individual current and voltage harmonic values up to 11th order are compared with the corresponding IEC standard limits on Table 4.7. For CMDB-4, I_L at the CT secondary is 912.9A and with CT ratio of 320, I_L at the primary is 2.85A and the rated power frequency voltage is 400V/√3=230.9V. Using this values of I_L and V_r, the corresponding THD_V and TDD values with their respective individual harmonic levels as per the IEEE standard are calculated and compared with the limits on Table 4.8.

Table 4.7: Comparison of the maximum measured harmonic values with corresponding IEC standards for CMDB-4.

Harmonic order/THD	Actual %V	IEC Std 61000-2-2	Actual %I	IEC Std 61000-3-4
3rd	0	5	1.9	21.6
5th	1.3	6	1.8	10.7
7th	0.9	5	1.1	7.2
9th	0	1.5	0.4	3.8
11th	0.4	3.5	0.9	3.1
THD	2.7	8	2.9	-

Table 4.8: Comparison of calculated harmonic values with the corresponding IEEE standards for CMDB-4.

Harmonic order/ THD_V/ TDD	Actual %V	IEEE Std 519	Actual %I	IEEE Std 519
3rd	0	5	1.4	7
5th	1.3	5	1.4	7
7th	0.9	5	1.1	7
9th	0	5	0.4	7
11th	0.4	5	0.7	3.5
THD/TDD	1.6	8	2.4	8

The analysis of all the data collected during the monitoring period of CMDB-4 shows that all the individual current and voltage harmonic levels as well as the THD_I/TDD and THD_V are within the IEC and IEEE harmonic distortion limits. During the measurement period the power factor level of this distribution transformer was slightly below 0.9, the minimum allowable limit set by the utility not to be penalized.

4.2 Evaluation of Measurement Results

The measurement results, gathered during the monitoring period from the four secondary distribution transformers located in Adama Spinning Factory, have been investigated to identify the level of harmonic distortion in the system. The level of individual harmonic levels up to the 11^{th} order and the harmonic indices THD_I/TDD and THD_V of the distribution system have been analyzed. The following points summarize the analysis results.

- The current distortion levels on transformers T1, T2 and T3 exceed the IEC and IEEE limits with the highest distortion on T1.
- The 5^{th} and 7^{th} current harmonic distortions are the most dominant ones in the system due a lot of ASDs installed in the system.
- The voltage harmonic distortion levels on all the transformers are well below the standard limits
- The current harmonic distortion levels on transformer T4, which is supplying the utility loads in the factory, is well below the IEC and IEEE standards
- The analysis also indicate that there are individual harmonic distortions above the 11^{th} order
- The overall power factor levels on the system is below 0.9, the minimum allowable limit set by the utility, due to low levels of power factor on three of the transformers. Transformer T1 has a power factor above 0.9.

Therefore, a mitigation technique has to be proposed to tackle the problems associated with the current harmonic distortions on the three transformers and bring down the distortion levels below the limits set by IEC and IEEE standards. The following chapter describes the mitigation techniques used to minimize the harmonic current distortion levels on transformers T1, T2 and T3.

CHAPTER FIVE

MITIGATION TECHNIQUES

5.1 Introduction

The power quality problems in power distributions systems are not new, but the awareness of the customers, utilities and equipment manufacturers has increased in recent years. Starting from the time of awareness and identification of power quality problems a lot of conventional solutions, which typically use passive elements, have been proposed and implemented in different parts of the world. Even though these solutions have existed for a long period of time in the field of electrical power engineering, they do not always respond correctly and perform as expected on the modern power system.

Passive filters consisting of tuned L-C component have been widely used to suppress harmonic distortions. Even though these passive filters have low initial cost and high efficiency, they also have various drawbacks like instability, fixed compensation, resonance with supply as well as loads and utility impedance.

On the research paper done on Adama Spinning Factory in 2010 [2], such a tuned passive filter had been proposed and designed to filter out the current harmonic distortion in the distribution network. The factory has carried out an expansion project in 2011, to increase its production capacity by 35%. This expansion project includes installation of additional machineries with total additional installed capacity of about 1107.04 KVA. To accommodate the new installed loads, one distribution transformer has been installed and some of the new loads have been distributed on the already existing three distribution transformers. As a result the whole electrical characteristics of the distribution network have been changed and the designed tuned passive filters on this research paper may not suitably serve their intended task.

As presented in chapter two, the distribution network of Adama Spinning Factory has an Automatic Power Correcting unit, in which different step 3-phase capacitors are switched in to and out from the system dynamically based on the power factor level of the loads. Tuned L-C passive filters like the one proposed for Adama Spinning Factory on [2] are not effective due to the dynamically changing nature of the system impedance.

The evolution of power electronics controller devices has given to the birth of custom power applications, in which a wide range of flexible controllers using power electronics components are utilized to improve the power quality at distribution level.

5.2 Custom Power Devices (CPD)

The term custom power refers to the use of power electronic controllers for distribution systems to enhance the quality and reliability of power that is delivered to customers. These power electronics controller devices are called CPD. They have good performance at medium distribution levels and most are available as commercial products. [4] The CPDs are basically of two types – network reconfiguring type and compensating type. The complete classification of CPDs is shown in the Figure 5.1.

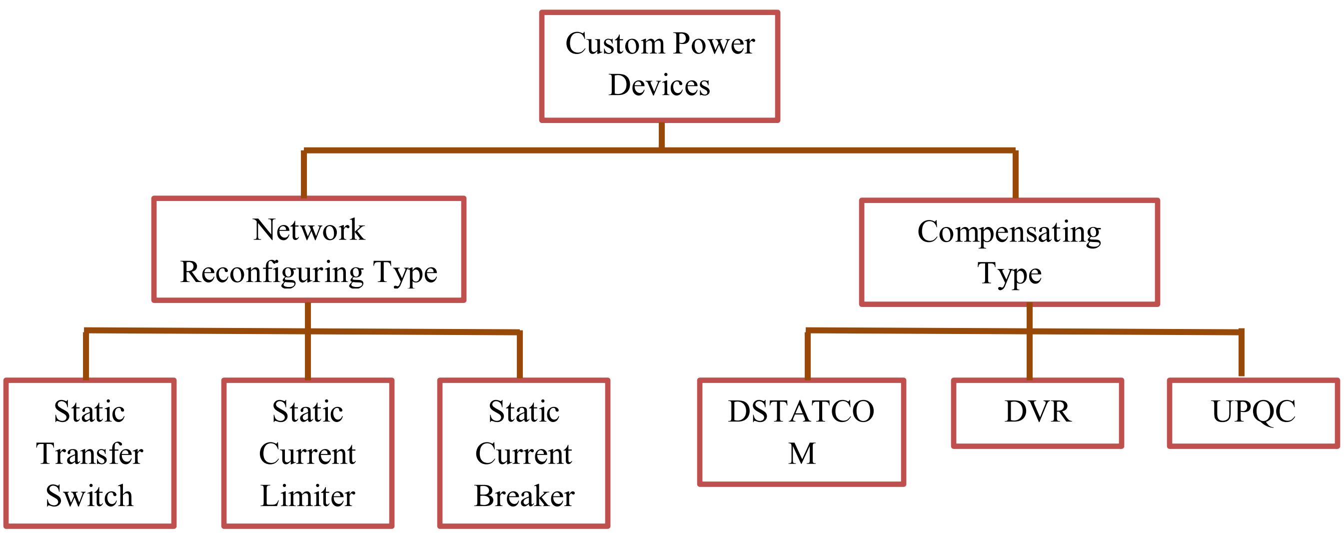

Figure 5.1: General Classification of Custom Power Devices.

5.2.1 Network Reconfiguring Type CPDs

The network reconfiguring equipment can be normal thyristor or gate turn-off thyristor base. The Static Current Limiter/ Static Circuit Breaker are usually used for fast current limiting and current breaking during faults. On the other hand, the Static Transfer Switches (STS) are used to promptly transfer load to an alternate feeder to protect a load from voltage sag/swell or fault in the supplying feeder. Uninterruptable Power Supply (UPS) is also categorized as a network reconfiguring type CPD, which is used to mitigate voltage dip and short duration interruption.

5.2.2 Compensating Type CPDs

The compensating CPDs are used for active filtering, load balancing, power factor improvement and voltage regulating (sag/swell). These devices are mainly three types: Distribution STATCOM, Dynamic Voltage Restorer and Unified Power Quality Conditioner.

Distribution Static Compensator (DSTATCOM) is a shunt connected device, designed to inject unbalanced and harmonically distorted current to distribution line via coupling inductor to eliminate unbalance or distortions in the load current or the supply voltage. It can also perform voltage regulation when connected to a distribution bus. In this mode it can hold the bus voltage constant against any unbalance or distortion in the distribution system. Generally, DSTATCOMs can be used in distribution networks for load current balancing, flicker effect compensation, current harmonic distortion compensation and power factor improvement. The single line diagram of DSTATCOM is shown in Figure 5.2.

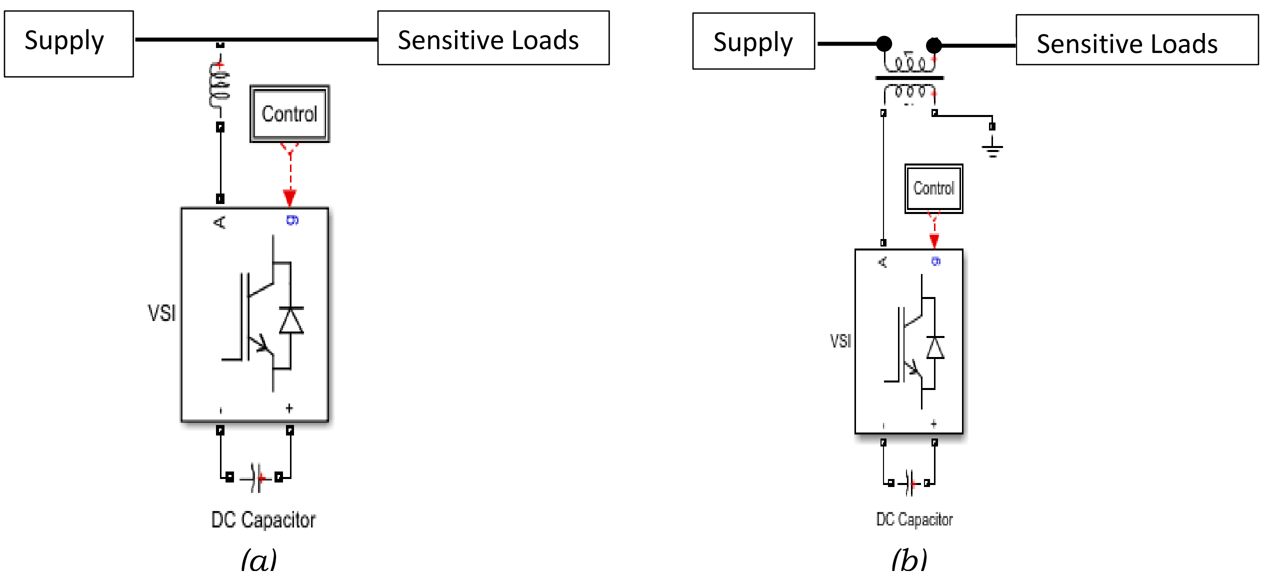

Figure 5.2: Single line diagram of (a) DSTATCOM and (b) DVR.

Dynamic Voltage Restorer (DVR) is a series connected CPD, designed to inject a dynamically controlled voltage in magnitude and phase in to distribution line via coupling transformer to correct load voltage. The main purpose of this device is to protect sensitive loads from sag/swell, interruptions in the supply side. Since this is a series device, it can also be used as a series active filter.

Generally, DVRs can be used in distribution networks for voltage regulation, flicker attenuation, voltage sag/swell protection and voltage balancing. The single line diagram of DVR is shown in Figure 5.2.

Unified Power Quality Conditioner (UPQC) is a very versatile device that can inject unbalanced and distorted current in shunt and voltage in series simultaneously in a dual control mode. Therefore it can perform both the functions of load compensation and voltage control at the same time. Applications of UPQC include VAR compensation, harmonic suppression, current balancing, active/ reactive power control, voltage balancing and voltage regulation.

5.3 Current Harmonic Distortion Mitigation with DSTATCOM

Harmonic distortion is present to some degree on all power systems. Mitigating techniques has to be implemented on a system when the distortion levels exceed the limits set by different standard organizations in order to avoid failure of equipments both in the utility and customer premises. The analysis of measurements carried out in Adama Spinning Factory distribution network in the previous chapter shows that current harmonic distortion levels which exceeds the limits set by IEC and IEE standards, are present on transformers T1, T2 and T3. Moreover, the power factor correcting system installed in the distribution network is not efficient and reliable resulting in an overall power factor level below 0.9. The power factor correcting unit, in addition to its incapability to maintain the power factor level above 0.9, it has high rate of failure of components like capacitors, fuses and contactors.

There are a number of devices and techniques available to control harmonic distortion in an electrical system. As presented in the previous sub-topics, CPD has a great advantage over the traditional passive and active harmonic filtering techniques in mitigating harmonic distortions and other power quality disturbances. As a result, DSTATCOM is proposed for compensating the current harmonics and improving the power factor in Adama Spinning Factory distribution network, as it is capable of mitigating both these disturbances as presented in the previous sub topic.

There are two modes of DSTATCOM operation namely load compensation in current-control mode and voltage regulation in voltage-control mode. Since the main concern of this study is harmonic distortion, the DSTATCOM in current control mode is used in this study for load compensation, i.e. current harmonic compensation, power factor improvement and load balancing.

Figure 5.3 shows a schematic diagram of the distribution network of Adama Spinning Factory with three independent DSTATCOM in Current Control Mode (CCM) are connected to transformers T1, T2 and T3.

The desired performance from the compensator is that it generates a current I_{comp} such that it cancels the reactive component, harmonic component and unbalance of the load current. Assuming the load current vector has real, reactive and harmonic components, for unity power factor operation, the source supplies only the real component. The remaining part will be injected by the compensator. The performance of the proposed DSTATCOM for compensating the harmonic current distortion in Adama Spinning Factor distribution network is analyzed by simulating the network with and without the DISTATCOM in MATLAB's SIMULINK environment. The following subtopic explains the working principles, simulation and results of the proposed DSTATCOM for Adama Spinning Factory.

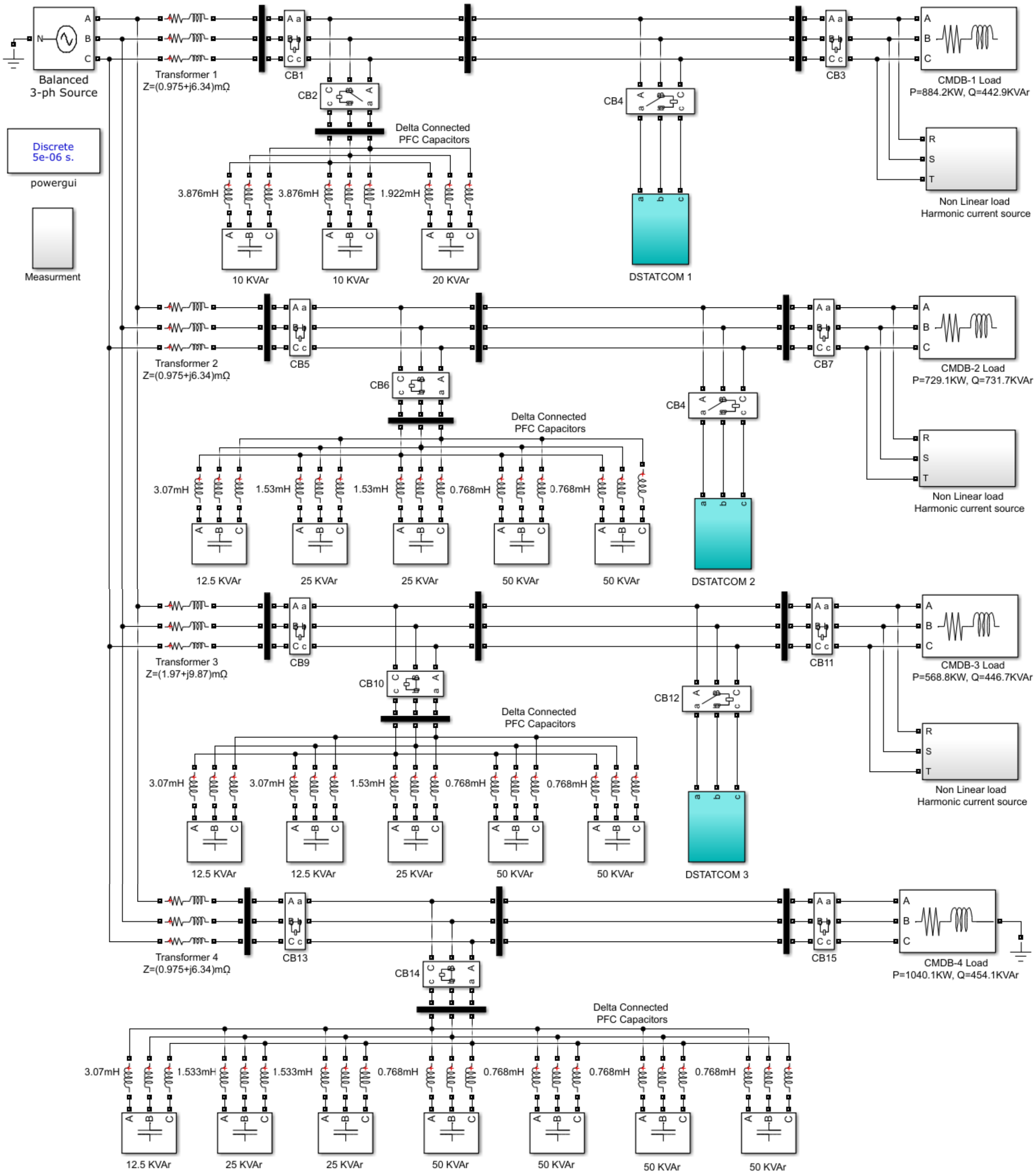

Figure 5.3: Schematic diagram of Adama Spinning Factory network with DSTSTCOM.

5.4 Simulation of Adama Spinning Distribution Network with DSTATCOM

The main building blocks of the DSTATCOM used in the simulation are VSI (Voltage Source Inverter) with DC link capacitor, control unit for generating the reference current and control technique for generating the pulses for driving the VSI. The detail schematic diagram of a DSTATCOM used for this study is shown in Figure 5.4.

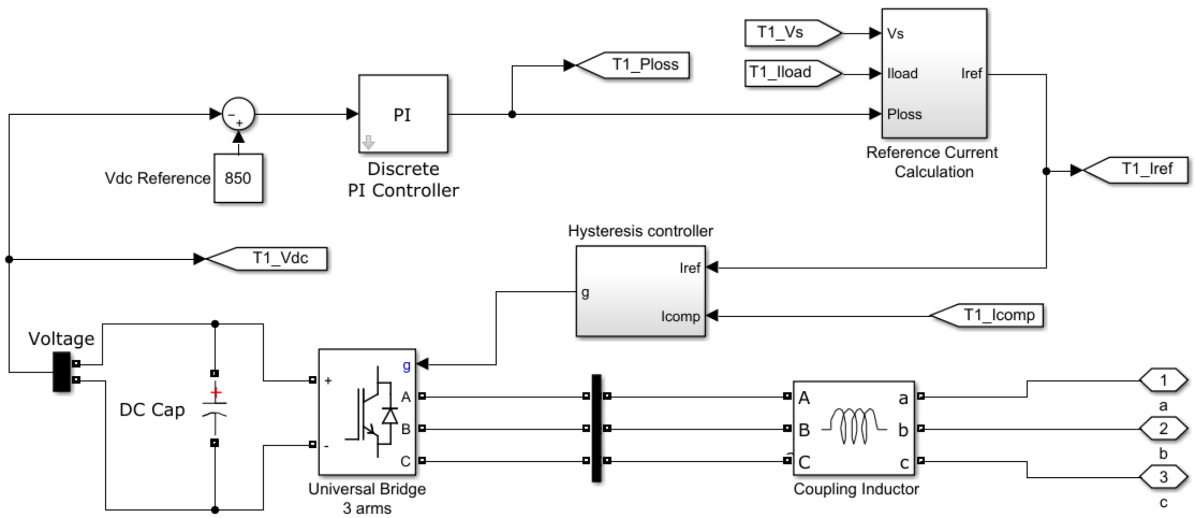

Figure 5.4: Detail schematic diagram of IRP based DSTATCOM.

5.4.1 Generating a Reference Current

There are various theories and techniques available for generating the three phase reference currents which have to be generated by the DSTATCOM in order to accomplish load compensation. Some of these theories are Synchronous Reference Frame (SRF) based control theory, Instantaneous Reactive Power (IRP) control theory, Unit Template based control theory and Synchronous Detection Mode (SDM) based theory.

SRF and IRP based controls are the most commonly used control theories with DSTATCOMs and also different researches show that they have a better compensating performance than other theories. The analysis done by [6] and [8] shows that, even though the source current THD level with the SRF theory is slightly lower than with the IRP theory, both control theories are equally reliable and applicable to reduce the THD levels to the acceptable range set by IEEE and IEC standards. A DSTATCOM with IRP based control theory is used in this study, for its simplicity in simulation of the control technique.

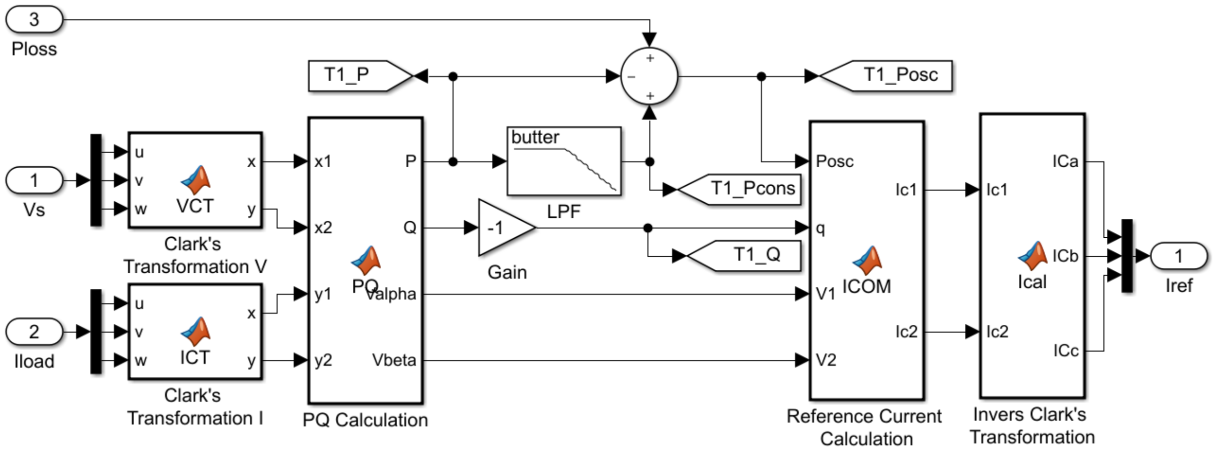

Figure 5.5: MATLAB/SIMULINK model of IRP control.

In this technique, the reference current for the control of DSTATCOM are obtained from the instantaneous active and reactive power components in the α−β coordinate. The Simulink model of IRP based controller for generating the reference current is shown in Figure 5.5. In the model different MATLAB function block are shown. These function blocks are used for transforming the voltages and currents in to the α−β coordinate, calculating the instantaneous active and reactive powers, calculate the reference currents and transferring back it to the a-b-c coordinate. The snapshot of the codes used by each of the function blocks are shown in Figure 5.6 below. As shown in Figure 5.5, initially, the source voltage and load current waveforms in the a-b-c coordinate are transformed to the stationary orthogonal α−β coordinates using Clark's Transformation according to the given matrix in equation 5.1.

$$\begin{bmatrix} I_\alpha \\ I_\beta \end{bmatrix} = \sqrt{\frac{2}{3}} \begin{bmatrix} 1 & -\frac{1}{2} & -\frac{1}{2} \\ 0 & \frac{\sqrt{3}}{2} & -\frac{\sqrt{3}}{2} \end{bmatrix} \begin{bmatrix} I_a \\ I_b \\ I_c \end{bmatrix} \qquad \begin{bmatrix} V_\alpha \\ V_\beta \end{bmatrix} = \sqrt{\frac{2}{3}} \begin{bmatrix} 1 & -\frac{1}{2} & -\frac{1}{2} \\ 0 & \frac{\sqrt{3}}{2} & -\frac{\sqrt{3}}{2} \end{bmatrix} \begin{bmatrix} V_a \\ V_b \\ V_c \end{bmatrix} \ldots\ldots (5.1)$$

Then, the instantaneous active and reactive power is obtained by the product of the voltage and current waveforms in the α−β coordinate according to the given matrix in equation 5.2.

$$\begin{bmatrix} p \\ q \end{bmatrix} = \begin{bmatrix} V_\alpha & V_\beta \\ V_\beta & -V_\alpha \end{bmatrix} \begin{bmatrix} I_\alpha \\ I_\beta \end{bmatrix} \ldots\ldots (5.2)$$

Instantaneous active and reactive powers p and q can be decomposed into an average (dc) and oscillatory components as:

$$p = \bar{p} + \tilde{p} \ldots\ldots (5.3)$$

$$q = \bar{q} + \tilde{q} \ldots\ldots (5.4)$$

Clark's Transformation of Voltage

```
function [x,y] = VCT(u,v,w)

x = sqrt(2/3)*(u-(0.5*v)-(0.5*w));
y = sqrt(2)*(0+(0.5*v)-(0.5*w));
```

Clark's Transformation of Current

```
function [x,y] = ICT(u,v,w)

x = sqrt(2/3)*(u-(0.5*v)-(0.5*w));
y = sqrt(2)*(0+(0.5*v)-(0.5*w));
```

Instantaneous P and Q Calculation

```
function [P,Q,Valpha,Vbeta] = PQ(x1,x2,y1,y2)

P = (x1*y1)+(x2*y2);
Q = (x2*y1)-(x1*y2);
Valpha = x1;
Vbeta = x2;
```

Reference Current Calculation

```
function [Ic1,Ic2] = ICOM(Posc,q,V1,V2)

Ic1 = (-1/(V1^2 + V2^2))*((Posc*V1)+(q*V2));
Ic2 = (-1/(V1^2 + V2^2))*((Posc*V2)-(q*V1));
```

Inverse Clark's Transformation

```
function [ICa,ICb,ICc] = Ical(Ic1,Ic2)

ICa = sqrt(2/3)*(Ic1);
ICb = sqrt(2/3)*((-0.5*Ic1)+((sqrt(3)/2)*Ic2));
ICc = sqrt(2/3)*((-0.5*Ic1)-((sqrt(3)/2)*Ic2));
```

Figure 5.6: Snapshot of the codes in the function blocks of IRP control.

As shown in Figure 5.5, the constant (dc) term of the instantaneous active power is extracted using 5^{th} order LPF (Low Pass Filter). The source has to supply the constant term ($\bar{p}$) and the power loss (P_{loss}) due to switching losses and coupling inductor loss. These losses force the DC capacitor to discharge. In order to maintain a constant stored DC voltage in the capacitor, additional power has to be drawn from the source to compensate the losses. Thus, the oscillating component of the instantaneous active power ($\tilde{P}$, presented as P_{osc} in Figure 5.5) is obtained by extracting the constant term ($\bar{p}$) and the power loss (P_{loss}) from the instantaneous active power (p). On the other hand, both the constant and oscillatory instantaneous reactive powers have to be supplied by the DSTATCOM compensator in order to maintain unity power factor at the source. Therefore, the total instantaneous active and reactive power which has to be supplied by the DSTATCOM is:

$$\tilde{p} = p - (\bar{p} + p_{loss}) \quad (5.5)$$

$$q = \bar{q} + \tilde{q} \quad (5.6)$$

Then the instantaneous reference currents in the α−β coordinate can be calculated as:

$$\begin{bmatrix} I_\alpha \\ I_\beta \end{bmatrix} = \frac{1}{{V_\alpha}^2 + {V_\beta}^2} \begin{bmatrix} V_\alpha & V_\beta \\ V_\beta & -V_\alpha \end{bmatrix} \begin{bmatrix} \tilde{p} \\ q \end{bmatrix} \quad (5.7)$$

Finally, these reference currents are transformed to the a-b-c coordinate using the inverse Clark's transformation according to equation 5.8.

$$\begin{bmatrix} {I_a}^* \\ {I_b}^* \\ {I_c}^* \end{bmatrix} = \begin{bmatrix} 1 & 0 \\ -\frac{1}{2} & \frac{\sqrt{3}}{2} \\ -\frac{1}{2} & -\frac{\sqrt{3}}{2} \end{bmatrix} \begin{bmatrix} I_\alpha \\ I_\beta \end{bmatrix} \quad (5.8)$$

These reference currents have to be generated by the DSTATCOM and actually correspond to the oscillating component of the instantaneous active power and both the oscillating and constant components of the instantaneous reactive power. The reference currents are then used by the HCC (Hysteresis Current Control) to generate the firing pulses for the power semiconductor switches.

5.4.2 Hysteresis Current Control

Hysteresis Current Control (HCC) is a stable, fast and accurate method of generating switching pulses for producing the compensating current in shunt CPDs. To generate the compensator current (I_{comp}) a hysteresis band $\pm h$ is used so that,

If $I_{comp} \geq I_{ref} + h$, then the compensator current has to be lowered by applying a negative voltage across the output. This is accomplished by turning on the switches on the negative dc line of the inverter.

If $I_{comp} \leq I_{ref} - h$, then the compensator current has to be raised by applying a positive voltage across the output. This is accomplished by turning on the switches on the positive dc line of the inverter.

The tracking performance of the hysteresis current control method is inversely proportional to the load inductor and the size of the hysteresis band and directly proportional to the magnitude of dc voltage. As the number of switching increased to get a better tracking, the inverter losses will become higher. The MATLAB/SIMULINK model of the hysteresis current control technique is shown in Figure 5.7 below. A hysteresis band of [-h, h] = [-0.1, 0.1] is used for the simulation in the study.

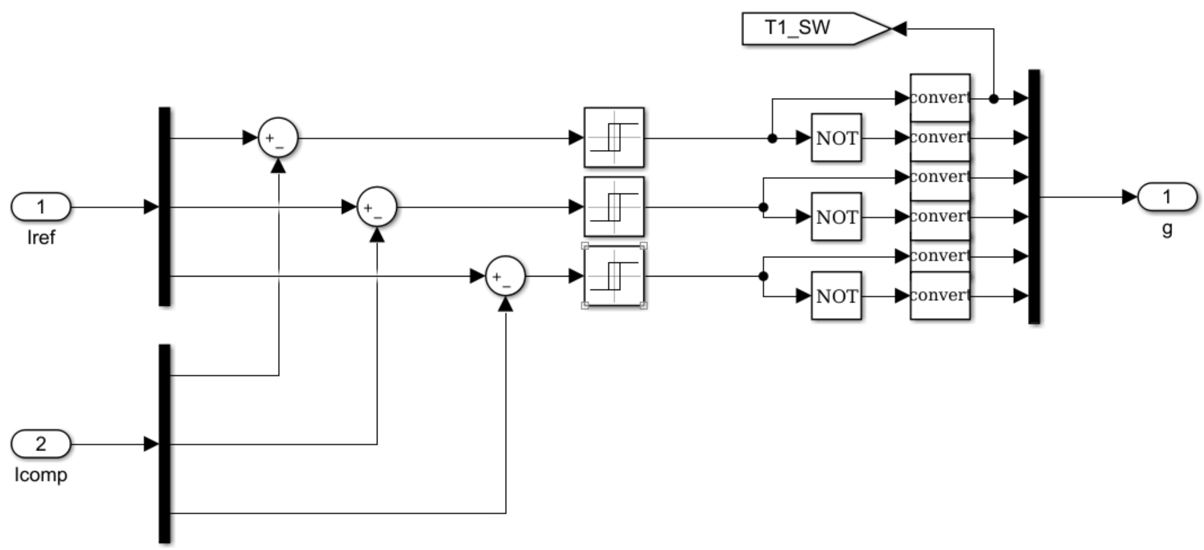

Figure 5.7: MATLAB/SIMULINK model of Hysteresis Current Control.

5.4.3 Voltage Source Inverter (VSI)

VSI in a DSTATCOM is used to generate the compensating three phase AC currents at any required magnitude, phase and frequency. It consists of power semiconductor switches and DC link capacitor. The power semiconductor device can be a Metal Oxide Field Effect Transistor (MOSFET) or Gate Turn-Off (GTO) thyristor or Insulated Gate Bipolar Transistor (IGBT) or Field Controlled Thyristor (FCT) based on the specific application requirements. Gate turn-off thyristors are recommended for high voltage application with lower switching speeds. On the other hand, MOSFETs have very low switching losses but are not suitable for very high voltage applications. IGBTs and MOSFETs are the preferred devices for distribution system applications as they can carry fairly large current and has fast switching characteristics and low losses. These two power semiconductor devices are also selected for realizing the VSI of the DSTATCOM proposed for this study.

The capacitor at the DC side of the DSTATCOM is responsible for supplying the current harmonics and the fluctuations caused by the compensation of the reactive power. The switching losses and the coupling inductor losses force the DC capacitor to discharge. On the other hand the average value of the voltage across the capacitor terminals must be kept at a constant value in order to the capacitor perform its duty. The voltage across the capacitor is regulated by absorbing or releasing active power into the electrical network. The Discrete PI (Proportional and Integral) controller from SIMULINK's Simscape power system toolbox, with proportional gain K_P=0.5 and integral gain K_I=1, is used to regulate this dc voltage across the capacitor as shown on the DSTATCOM block diagram in Figure 5.4.

The DC bus voltage, V_{DC} is calculated using the following expression: [6]

$$V_{DC} = \frac{\sqrt{2} * V_{LL}}{m_a} \quad \text{.. (5.9)}$$

Where, V_{LL} is the line to line output voltage at the DSTATCOM terminal and m_a is the modulation index. By considering a system voltage of 400V, 10% voltage drop at the coupling inductor and maximum variation of 10% in the system voltage, the line voltage required at the VSI becomes 480V and the DC bus voltage becomes 678.8V. However, in the practical case, the attainable voltage at the DSTATCOM output terminal will be less than the estimated one due to the dead-band and the transition times of the switching device. Therefore, taking these factors in to account, a DC link voltage of 850V is selected for the simulation.

5.5 Simulation Results with and without DSTATCOM

The previous subtopics in this chapter mainly focus on the operating principle and design of the DSTATCOM which is proposed to compensate the current harmonic distortion in Adama Spinning Factory distribution network. The performance of the DSTATCOM is examined by simulating the factory's distribution network with the effect of the non-linear loads and the proposed DSTATCOM included in to the system.

5.5.1 Non-linear Loads

For simulation purpose the non-linear loads are modeled by ideal harmonic current sources which are connected to each distribution transformer in parallel with the linear loads. The ideal current sources are configured to generate a balanced and 120^0 spaced three phase currents, which have different peak amplitudes for each of the 3rd (150Hz) to 11th (550Hz) harmonic orders. The peak amplitudes are calculated based on the maximum measured harmonic rms current values of each harmonic order. All the measured data of the four CMDB boards during the monitoring period are presented on Appendix D of this document. The schematic diagram of the ideal harmonic current sources, for simulating the effect of non-linear loads on each transformer, is modeled in Simulink environment as shown in Figure 5.8 below.

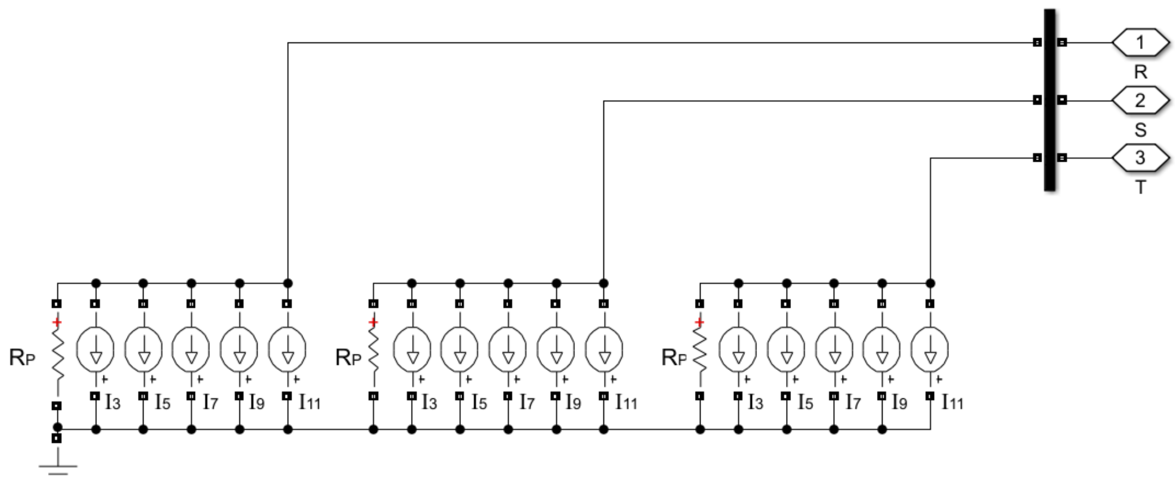

Figure 5.8: Balanced 3 phase ideal harmonic current source model.

The non-linear loads are modeled for the four transformers in the distribution network. From the measurement data on Appendix D, the maximum rms (root mean square) current values of each harmonic order are selected and converted to the actual current value by multiplying it with the respective CT ratio used for measurement. These rms current values are multiplied by √2 to obtain the peak amplitude of the current harmonics. Table 5.1 presents the peak amplitudes of each current harmonics (3rd up to 11th), in amperes, for the four transformers.

Table 5.1: Peak amplitudes of 3rd to 11th current harmonics in Amperes.

Transformer	Harmonic order				
	3rd	5th	7th	9th	11th
T1	21.2	155.6	120.2	56.6	28.3
T2	14.1	91.9	42.4	0	14.1
T3	7.1	67.2	35.4	0	7.1
T4	18.1	18.1	13.6	4.5	9.1

5.5.2 Simulation Results

Different simulation results are obtained for different cases of the modeled distribution network. Voltage/current waveforms and harmonic spectrum of source current signal, which are helpful for the assessment of the proposed mitigation technique, are captured from two different simulation cases for each of the four transformers.

Case 1: The distribution network is simulated by excluding both the PFC and the DSTATCOM unit from the system for the first 0.06 seconds of the simulation (three full cycles). Then at 0.06 second of the simulation, the PFC units of all the four transformers are switched-in to the system and the simulation runs for additional five full cycles (up to 0.16 seconds). The simulation results gathered during the simulation period of [0, 0.06] seconds are useful to see the response of the distribution system without any compensation. On the other hand, the simulation results gathered during the simulation period of [0.06, 0.16] seconds will be helpful to see the capability of the installed PFC unit to compensate the reactive power demand of the loads and maintain the power factor above 0.9. Moreover, by comparing the harmonic spectrum of the simulation results for the two simulation periods, i.e. [0, 0.06] and [0.06, 0.16], it is possible to see whether the addition of the shunt PFC capacitors in to the system increases the harmonic distortion level of the system. This in turn indicates whether or not the PFC capacitors are creating parallel harmonic resonance with the network impedance. This also proves the effectiveness of the anti-resonant reactors inserted in series to the PFC capacitors, to scale down the parallel self-resonant frequency (f_r) of the system seen from the load side from around 250-500Hz to specifically 189Hz.

Case 2: The distribution network is simulated by excluding both the PFC and the DSTATCOM units from the system for the first 0.06 seconds of the simulation (three full cycles). Then at 0.06 second of the simulation, the proposed DSTATCOMs for transformers T1, T2 and T3 are switched-in to the system and the simulation runs for additional five full cycles (up to 0.16 seconds). The results from this simulation will verifies that the performance of the proposed DSTATCOM for compensating the current harmonic distortion and maintaining unity power factor at the source.

Simulation Results of Transformer T1

Case 1: Distribution nework of T1 with PFC unit included in the system at 0.06 second, but without DSTATCOM.

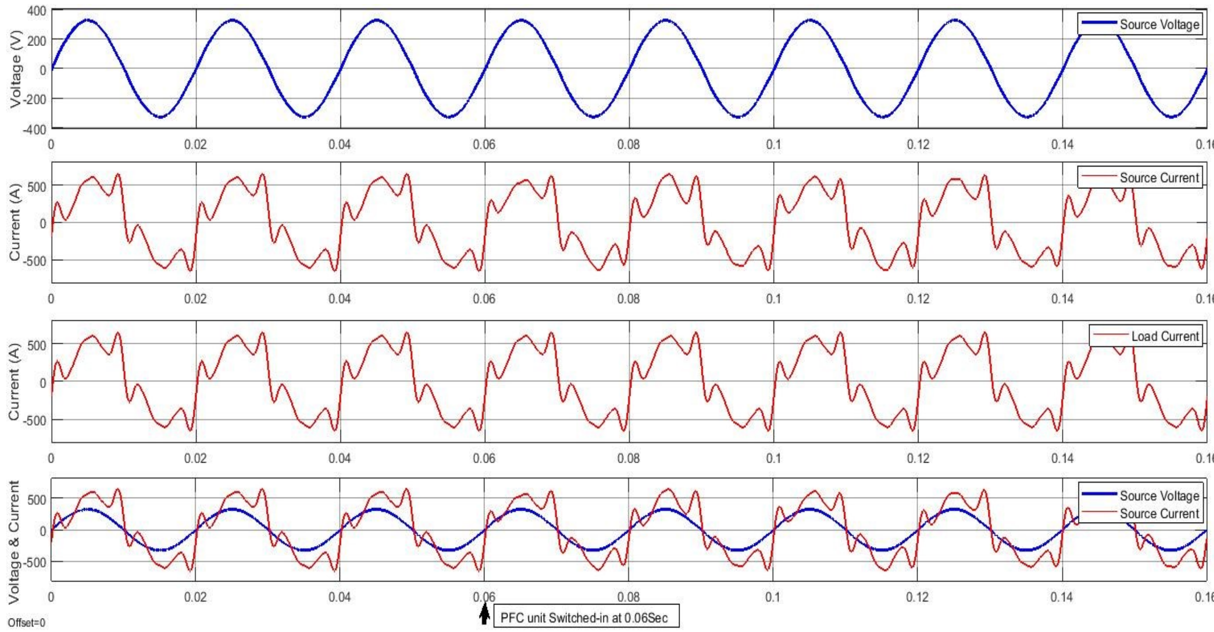

Case 2: Distribution network of T1 with DSTATCOM included in the system at 0.06 second, but without PFC unit.

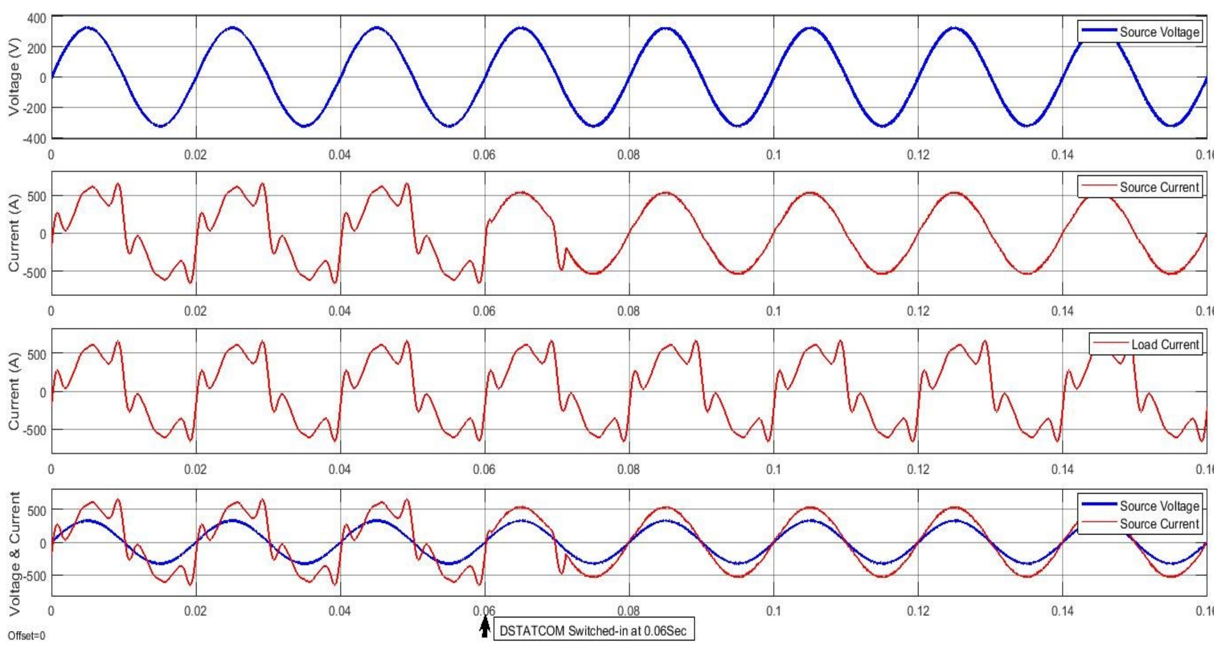

Figure 5.9: Single phase source voltage, source current, load current and source voltage/current waveforms (from top to bottom) of transformer T1.

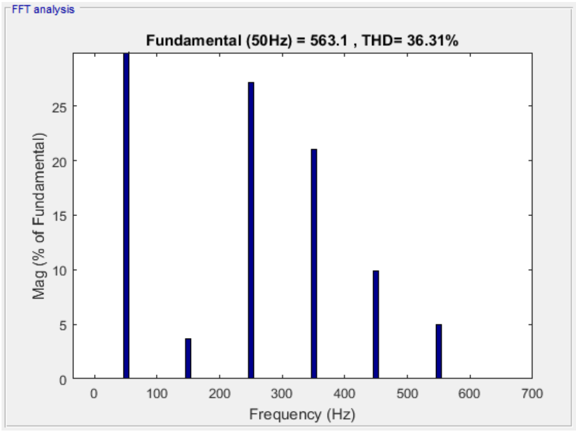

Network without PFC and DSTATCOM before 0.06 sec of case-1 & -2.

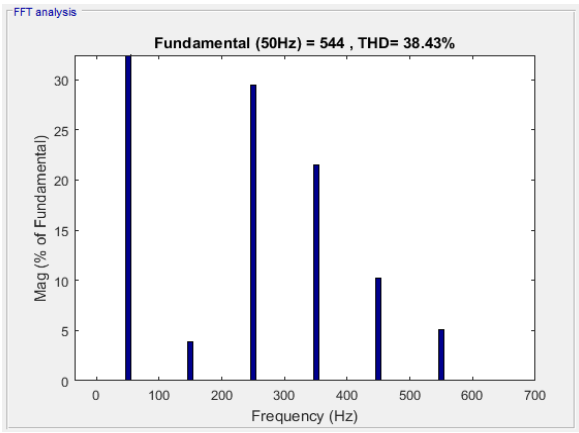

Case 1: Network with PFC unit after 0.06 sec.

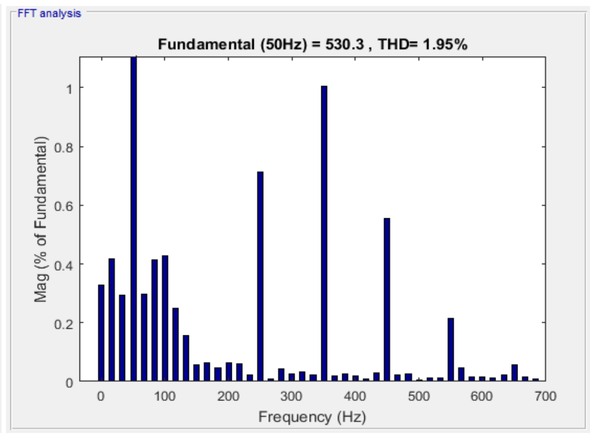

Case 2: Network with DSTATCOM after 0.06 sec.

Figure 5.10: Harmonic Spectrum of the source current on transformer T1.

The simulation results of transformer T1 show that the source current waveform of becomes pure sinusoid and in-phase with the voltage within 0.02 seconds (one cycle) after the DSTATCOM is switched-in to the system. The harmonic spectrum also shows that, when the DSTATCOM is in operation, the THD_I level becomes below 1.95%, which is well below the recommended limits set by IEEE and IEC standards. The simulation results also show that, if the PFC unit installed on this transformer is fully operational, it is capable of bringing the source voltage and current waveforms in-phase.

Simulation Results of Transformer T2

Case 1: Distribution nework of T2 with PFC unit included in the system at 0.06 second, but without DSTATCOM.

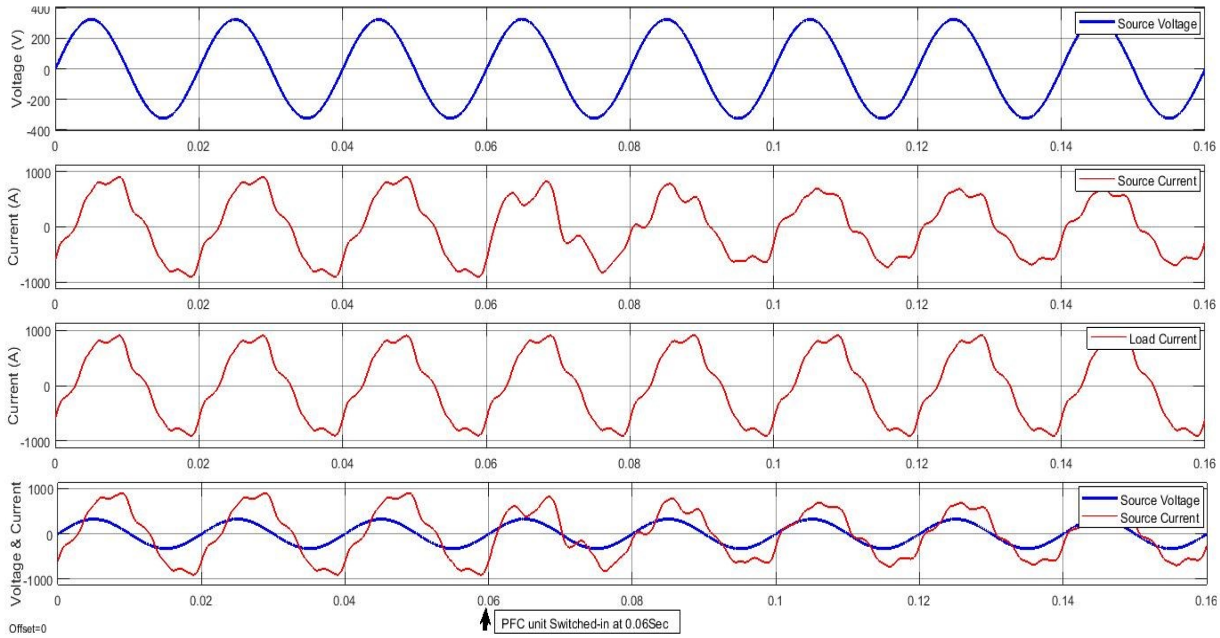

Case 2: Distribution network of T2 with DSTATCOM included in the system at 0.06 second, but without PFC unit.

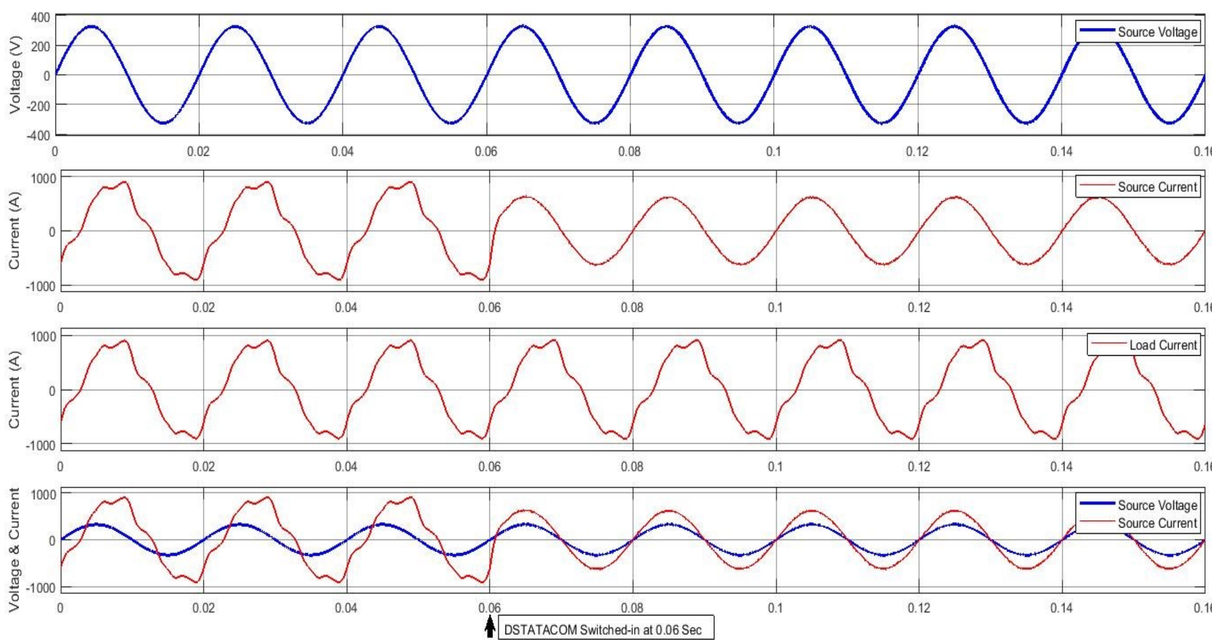

Figure 5.11: Single phase source voltage, source current, load current and source voltage/current waveforms (from top to bottom) of transformer T2.

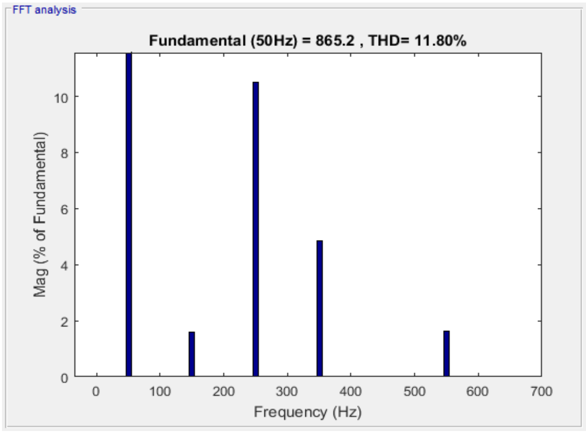

Network without PFC and DSTATCOM before 0.06 sec of case-1 & -2.

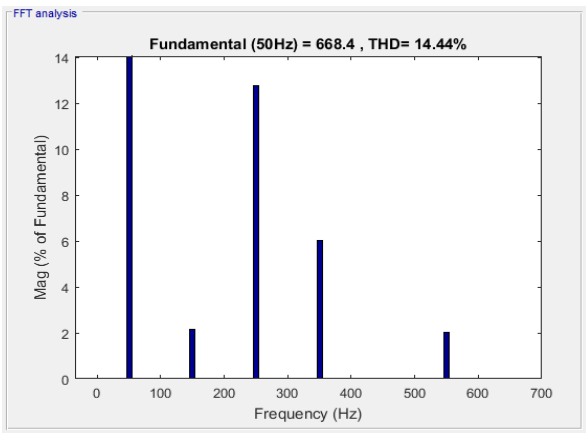

Case 1: Network with PFC unit after 0.06 sec.

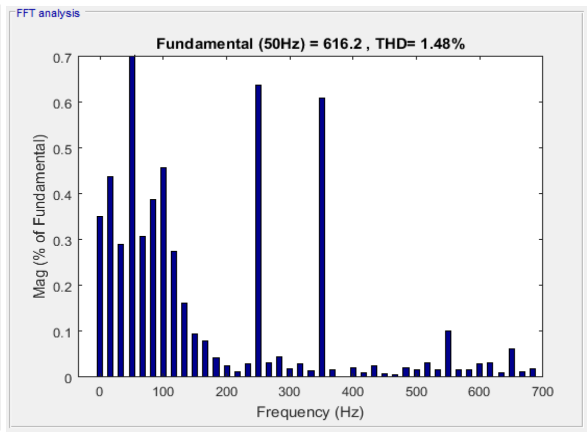

Case 2: Network with DSTATCOM after 0.06 sec.

Figure 5.12: Harmonic Spectrum of the source current on transformer T2.

The simulation results of transformer T2 show that the source current waveform of becomes pure sinusoid and in-phase with the voltage within 0.02 seconds (one cycle) after the DSTATCOM is switched-in to the system. The harmonic spectrum also shows that, when the DSTATCOM is in operation, the THD_I level becomes below 1.48%, which is well below the recommended limits set by IEEE and IEC standards. The simulation results also show that the PFC unit is not able to bring the source voltage and current waveforms in-phase. There exist a small phase shit between the source voltage and current even after the PFC unit is connected to the system.

Simulation Results of Transformer T3

Case 1: Distribution nework of T3 with PFC unit included in the system at 0.06 second, but without DSTATCOM.

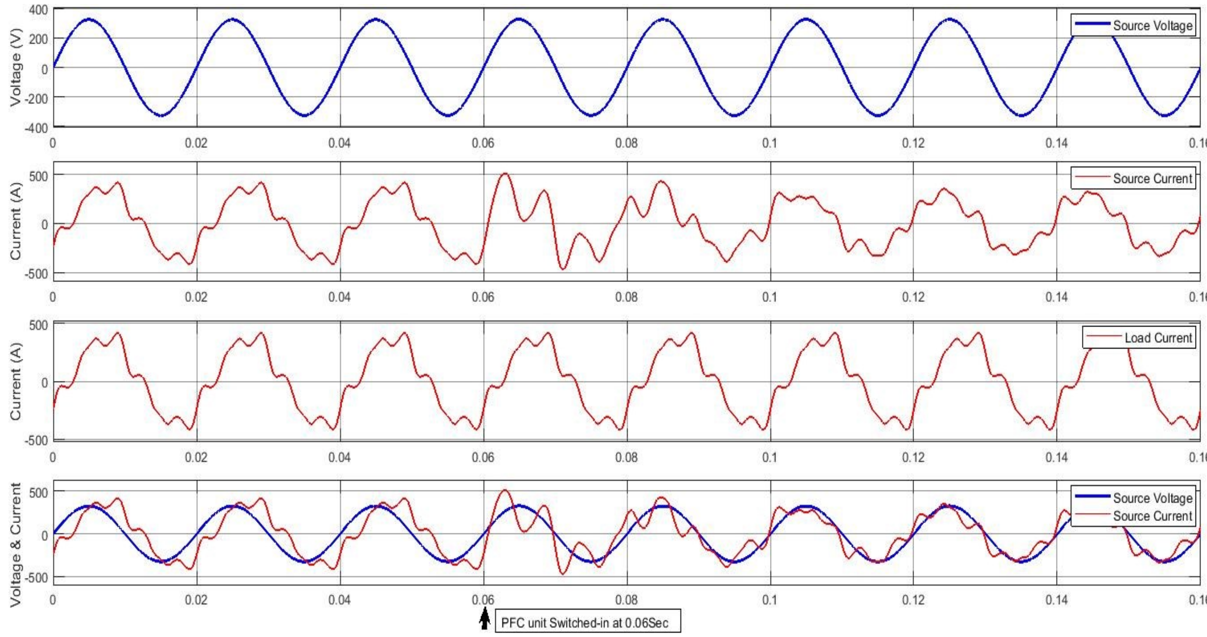

Case 2: Distribution network of T3 with DSTATCOM included in the system at 0.06 second, but without PFC unit.

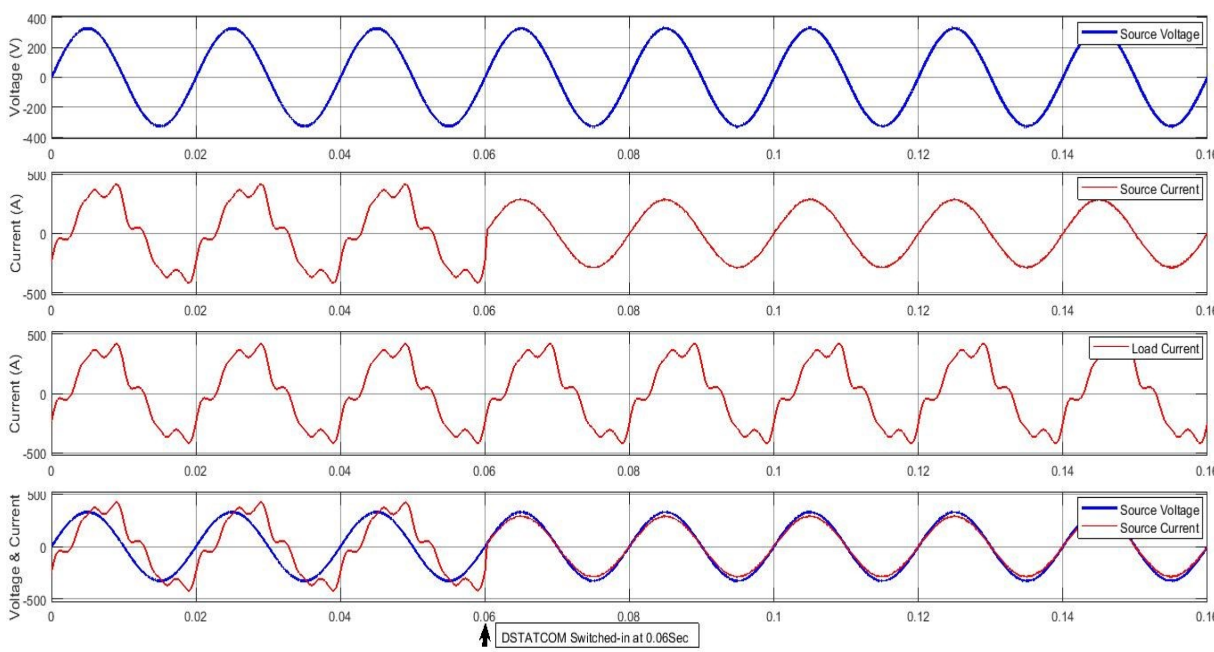

Figure 5.13: Single phase source voltage, source current, load current and source voltage/current waveforms (from top to bottom) of transformer T3.

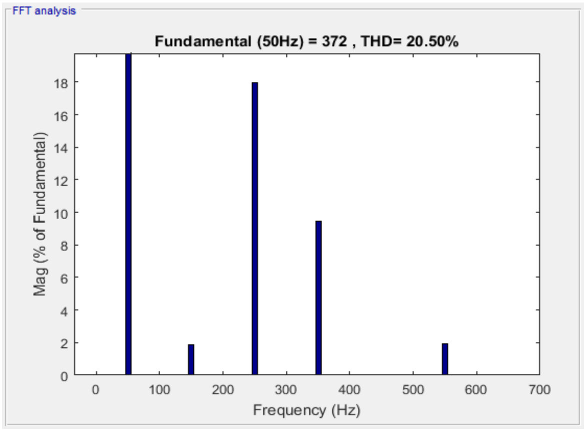

Network without PFC and DSTATCOM before 0.06 sec of case-1 & -2.

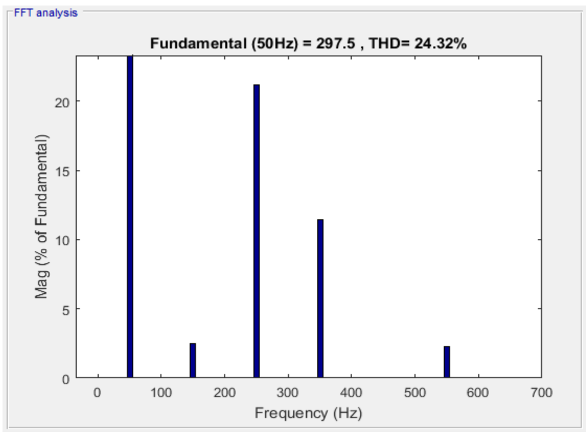

Case 1: Network with PFC unit after 0.06 sec.

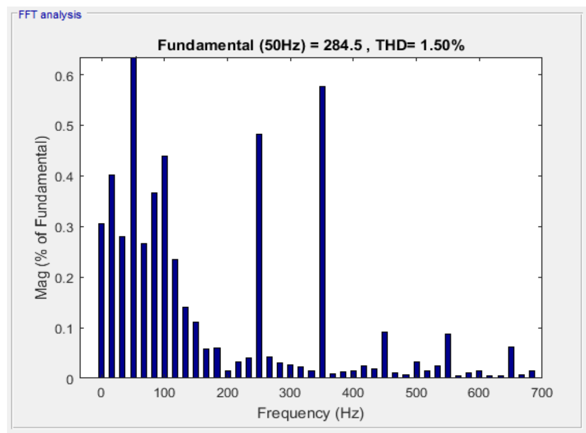

Case 2: Network with DSTATCOM after 0.06 sec.

Figure 5.14: Harmonic Spectrum of the source current on transformer T3.

The simulation results of transformer T3 show that the source current waveform of becomes pure sinusoid and in-phase with the voltage within 0.02 seconds (one cycle) after the DSTATCOM is switched-in to the system. The harmonic spectrum also shows that, when the DSTATCOM is in operation, the THD_I level becomes below 1.50%, which is well below the recommended limits set by IEEE and IEC standards. The simulation results also show that, if the PFC unit installed on this transformer is fully operational, it is capable of bringing the source voltage and current waveforms in-phase.

Simulation Results of Transformer T4

Case 1: Distribution nework of T4 with PFC unit included in the system at 0.06 second, but without DSTATCOM.

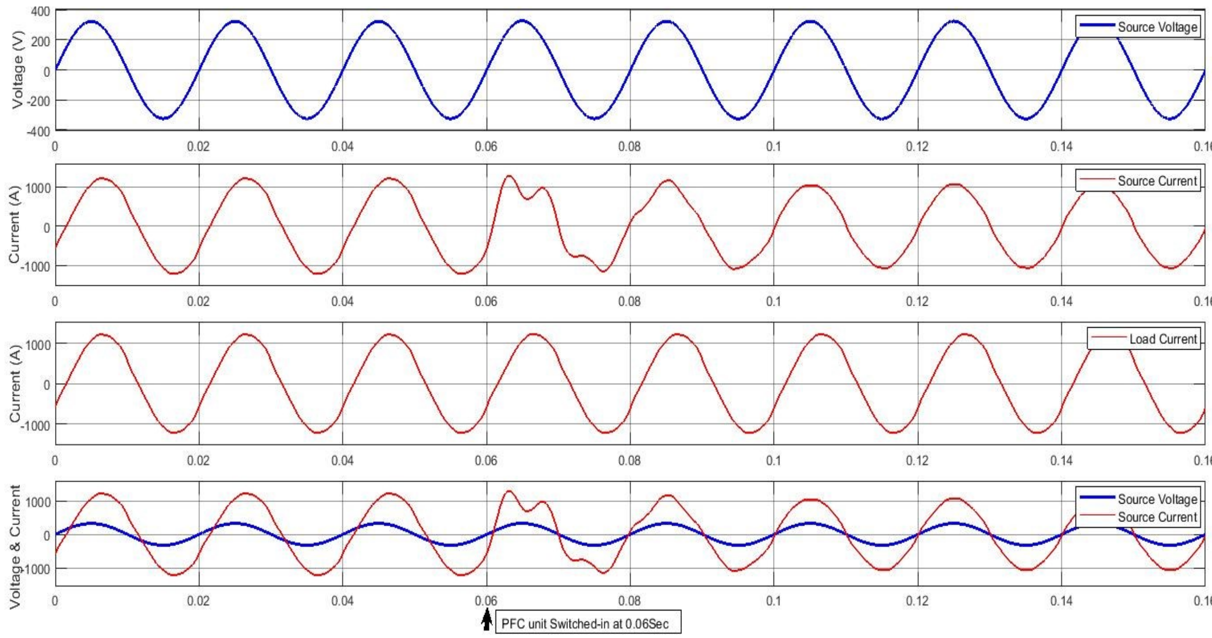

Figure 5.15: Single phase source voltage, source current, load current and source voltage/current waveforms (from top to bottom) of transformer T4.

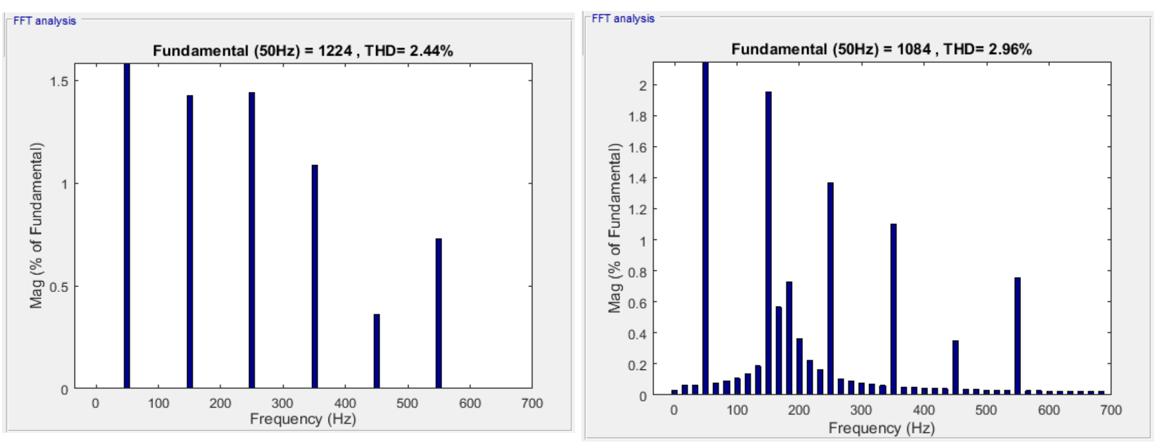

Network without PFC before 0.06 sec of case-1. **Case 1:** Network with PFC unit after 0.06 sec.

Figure 5.16: Harmonic Spectrum of the source current on transformer T4.

The simulation of transformer T4 is done only for Case-1, because a DSTATCOM is not proposed for this transformer since the voltage and current harmonic distortion levels are well below the recommended maximum limits set by IEEE and IEC standards. The simulation results show that, if the PFC unit installed on this transformer is fully operational, it is capable of bringing the source voltage and current waveforms in-phase.

5.6 Discussion and Summary

The distribution network of Adama Spinning Factory is simulated with MATLAB SIMULINK environment. The distribution network of the factory is modeled as a linear and non-linear loads connected to a balance 3-phase pure sinusoid voltage source. The linear loads are characterized by active and reactive power of a series RL load by considering the actual power factor of the loads. The non-linear loads are modeled as an ideal harmonic current source of 3^{rd} to 11^{th} order odd harmonics. The modeled distribution network is simulated for two different cases: the distribution network with PFC unit only and with DSTATCOM only. The results of the simulation have been presented on the previous subtopic.

The simulation results show that the source current waveform of transformers 1, 2 and 3 becomes pure sinusoid and in-phase with the voltage within 0.02 seconds (one cycle) after the respective DSTATCOMs are switched-in to the system. The harmonic spectrum also shows that the THD_I level becomes below 2% when the DSTATCOM is in operation. Therefore, it can be concluded that the proposed DSTATCOM is able to compensate the current harmonic distortion in the system at the same time maintain unity power factor at the source, thereby avoiding harmonic distortion related problems like overload and failure of distribution transformers and cables. It can also avoid unnecessary penalty payments of low power factor in the factory.

The simulation results of transformer T1 show that, even without connecting the PFC unit to the system, there is a very small phase shift between the source voltage and current waveforms. Connecting the total available capacitor banks (a total of 40 KVAr) to the system avoids the phase shift. As stated earlier, currently, the PFC unit on this transformer is out of service due to a recent fire incident inside the CMDB-1 board.

The simulation results of transformer T2 show that the loads connected to this transformer have the lowest power factor in system. Moreover, even after connecting the available capacitor banks (a total of 162.5 KVAr) to the system, there is a small phase shift between the source voltage and current waveforms. When some of the capacitor banks becomes out of operation, due to failure of components like fuses, contactors or the capacitor itself, the phase shift between the source voltage and current waveforms becomes more and resulted in low power factor. The measurement data on this transformer, presented on Appendix D, shows such case in which the actual average power factor is around 0.84, which is below the minimum level set by the utility not to be penalized. The simulation results of transformer T3 and 4, show that connecting the respective PFC unit to the system avoids the phase shifts between the source voltage and current waveforms. But as the measurement data on Appendix D shows that the actual power factor of these transformers is between 0.8 and 0.9. This is most probably a result of capacitors which are out operation due to failure of PFC unit components like fuses, contactors or capacitors. Therefore, transformers 2, 3 and 4 are the ones which brings the overall power factor of the factory below 0.9 and lets the factory to pay a power factor penalty starting from September, 2016 as stated in section 3.4 of chapter three.

Table 5.2: Comparison of %THD_I values for three different cases.

Transformer	THD_I without PFC and DSTATCOM	THD_I with PFC	THD_I with DSTATCOM
T1	36.31%	38.43%	1.95%
T2	11.8%	14.44%	1.48%
T3	20.5%	24.32%	1.5%
T4	2.44%	2.96%	-

Table 5.2 summarizes the comparison of the THD_I values of the distribution system for the cases without PFC & DSTATCOM, with the PFC and with DSTATCOM units in the system. The THD_I values of all the four transformers, when the PFC unit is included in the system, show an increment of 2% up to 4%. This is mainly due to the fact that the resonant frequency of the system is detuned to f_r=189Hz by the addition of the anti-resonant reactors in series to the PFC capacitor banks. Due to the parallel resonant harmonic on f_r=189Hz, the system has a tendency to magnify the harmonic components near to this resonant frequency, i.e. fr=189. This fact can be seen on the harmonic spectrum of transformer T4 with the PFC unit included in the system, on Figure 5.16. This fact cannot be seen on the harmonic spectrum figures of the other transformers due to larger Y-axis scales. Moreover, the simulation results proves that the anti-resonant reactors are effective in bringing down the resonant frequency of the system to f_r=189Hz. As a result the PFC capacitor banks are not creating a parallel resonance with the distribution transformer impedances around the 5^{th} and 7^{th} order harmonics, which are the dominant harmonic orders in the system.

CHAPTER SIX

CONCLUSIONS AND RECOMMENDATIONS

6.1 Conclusions

The distribution network of Adama Spinning Factory is assessed for voltage and current harmonic distortion levels through direct measurements on the available four distribution transformers. Then a DSTATCOM is proposed to compensate the current harmonic distortions on three of the transformers. Finally, the performance of the proposed DSTATCOM is evaluated by simulating the distribution network with and without the DSTATCOM in a MATLAB SIMULINK environment.

The analysis of the measurement data shows that the voltage harmonic distortion level on all the four transformers are well below the limits set by IEEE Std 519-2014 and IEC 61000-2-2 standards. The maximum $\%THD_V$ value obtained during measurement is around 2.5% on transformer T1 and T4. Therefore, it can be concluded that the harmonic distortion level of supplied electric power by the utility is in an acceptable condition for the proper operation of the factory.

As a modern manufacturing facility, majority of the electrical motors in Adama Spinning Factory are driven by ASD. The number and installed capacity of these ASDs are more on transformers 1, 2 and 3. The measurement analysis of the current harmonic distortion levels also reveals that the distortion levels are high at these transformers. Maximum THD_I levels of 43.8%, 17.5% and 24.6% have been found on transformers 1, 2 and 3, respectively, during measurement. Therefore, the non-linear loads installed on these transformers are injecting high level of harmonic current in to the system with the 5^{th} and 7^{th} harmonic orders are being the dominant ones. These harmonic currents are increasing the total rms current level of the system, which in turn overload and affect different equipments in the distribution system. The repeated failure of power factor correcting capacitor banks, blown out of fuses, fire accidents in the CMDB boards, burn out of cables and connection terminals in the factory's electrical system are results of such high level of harmonic current distortion.

The current harmonic distortion level on transformer T4 is well below the limits set by IEEE Std 519-2014 and IEC 61000-3-4 standards. This is due to the fact that most of the loads on this transformer are utility equipments like lightings, air conditioning units, kitchen equipments, etc…, which are mostly inductive and resistive linear loads.

During the analysis of the measured data, it is found that the power factor level of three transformers were below 0.9. The factory's electric bill also shows that they are paying a penalty for having a total power factor level below 0.9. This is mainly due to repeated failure of the components in the PFC unit as a result of high level of harmonic current distortion in the system.

The simulation of the distribution network on transformers 1, 2 and 3 with and without the proposed DSTATCOM shows that the current harmonic distortions injected into the system by the modeled non-linear loads can be compensated by the DSTATCOM. The simulation results shows that the source current becomes pure sinusoidal and also in-phase with the source voltage within 0.02 seconds (one cycle) after the introduction of the DSTATCOM in the system. Therefore, it can be concluded that the proposed DSTATCOM is capable of compensating the current harmonics and at the same time maintain a unity power factor at the service entrance.

As mentioned earlier, currently the PFC unit is not able to maintain the power factor level at 0.9 due to failure of some components like capacitor banks. As a result, in the last 18 months (starting from September, 2016 up to February, 2018) the factory has payed 26,381.88 Birr as a penalty charge for having a power factor lower than 0.9, as shown on Appendix C. Moreover the PFC unit on transformer one is not in operation due to the recent fire incident in it. Therefore, it is recommended that instead of simply budgeting for the repair and maintenance of the available PFC unit, it better to look for other options like the DSTATCOM proposed in this study after performing a detail cost analysis.

6.2 Recommendations

The scope of this thesis work was limited to voltage and current harmonic distortion assessment and mitigation due to the limitation of the instrument used for monitoring. The measuring device used in this study, DELAB NV8s, can only measure harmonic distortions and it is not capable of storing data and showing waveforms. Therefore, it is highly recommended that a complete power quality assessment has to be done using more advanced monitoring equipments like power quality analyzer in the factory. These devices are capable of measuring different power quality occurrences in a system with additional advantages of data logging, statistical analysis and waveforms outputs. Power quality assessment using such power quality analyzer gives more detailed and complete information; thus, a more precise analysis can be done to select a proper solution.

In this study the monitoring has been carried out at the CMDB boards and also the system is simulated by connecting the proposed DSTATCOMs at these boards. As shown in the simulation in the previous chapter, the harmonic current components from the nonlinear loads will propagate in the distribution system up to the CMDB boards. In order to avoid this harmonic distortion propagation in the system, the harmonic current sources have to be identified. Therefore, it is highly recommended to perform similar harmonic distortion assessments by selecting monitoring points close to the loads, in order to identify the harmonic sources and compensate them locally.

Most of the distribution systems in Ethiopia are changing from time to time due to the rapid growth of electric demand from industrial and commercial consumers. Due to this a lot of consumers are transferred from one feeder line to another and also sometimes from one substation to another. Adama Spinning Factory is one of such consumers, which has transferred from a feeder supplying a lot of small industrial and commercial consumers to a feeder dedicated to only two big textile factories, in 2016. This fact puts the characteristics of the feeder line and the supplied electric power under constant changes. Therefore, it is highly recommended to conduct power quality assessments regularly and continuously in electrical sites, to ensure proper planning, application and operation of power quality mitigation techniques.

Adama Spinning Factory has planned to undertake different vertical integration projects and have reached to machinery selection phase for one forward integration project. This project is planned to be located in the existing spinning factory premises. Therefore, it is recommended to consider power quality aspects in the planning, design and installation phases of the electrical installation of the new project.

REFERENCE

[1] Roger C. Dugan, Mark F. McGranaghan, Surya Santoso and H Wayne Beaty (2004) "Electrical Power Systems Quality", Second Edition, the McGraw-Hill Companies. 525 pp.

[2] Milkias Berhanu, (2010) "An Investigation of Power Quality Problems in Distribution Network: Case Study of Adama Spinning Factory, Unpublished" MSc thesis submitted to Adama University, 117 pp.

[3] Hussein Mohamed El-Eissawi Fathi (2012) "Power Quality Assessment", PhD thesis submitted to Al-Azhar University, Cairo, Egypt, 163 pp.

[4] Prafull A. Desale, Vishvadeep J. Dhawale and Ranjeet M. Bandgar (2014) "Brief Review Paper on the Custom Power Devices for Power Quality Improvement" International Journal of Electronic and Electrical Engineering. ISSN 0974-2174 Volume 7, Number 7, pp 723-733.

[5] Getenet Tesega (2011) "Power Quality Assessment at Selected Industrial Plants in Addis Ababa City, Unpulished" MSc thesis submitted to Addis Ababa University, 90 pp.

[6] Shabana Urooj and Pikasha Sharma (2016) "Harmonic Elimination Using DSTATCOM", Springer India, Proceedings of the Second International Conference on Computer and Communication Technologies, Advances in Intelligent Systems and Computing, pp. 577-591.

[7] Gokulananda Sahu, Kamalakanta Mahapatra, and Subrat Kumar Sahu (2014) "Design and Performance Analysis of DSTATCOM for Non-linear Load Composite Compensation", Springer International Publishing Switzerland, pp. 337-344.

[8] Gunjan Varshney, D. S. Chauhan, M. P. Dave (2016) "Modeling, Simulation and Control of Photovoltaic Based DSTATCOM", Jordan Journal of Electrical Engineering, Volume 2, Number 2, Pages 108-124

[9] Arindam Ghosh and Gerard Ledwich (2002) "Power Quality Enhancement Using Custom Power Devices" Kluwer Academic Publishers, 473 pp.

[10] P.S.R Mutry (2007) "Power System Analysis", BS Publications, 337 pp.

[11] http://www.ethiostandards.org (visited on March 23, 2018, 10:20AM)

[12] http://www.iec.ch (visited on March 23, 2018, 10:20AM)

[13] https://en.wikipedia.org/wiki/Institute_of_Electrical_and_Electronics_Engineers (visited on March 23, 2018, 10:20AM)

[14] DELAB NV8s Power Factor controller Use Guide for model NV-6s, NV-8s and NV-14s

[15] http://www.adamaspinning.com/ (visited on March 23, 2018, 10:20AM)

[16] ITI (CBEMA) Curve Application Note, (2005) Published by Information Technology Industry Council (ITI), 3 pp.

[17] EPCOS Power Factor correction, Power Quality Solutions, Product profile, (2017), 80 pp.

[18] Different Weekly/Monthly reports of Adama Spinning Factory (Maintenance performance report, Power failure report, Energy consumption report for each cost center)

[19] IEEE Std 1159-2009, IEEE Recommended Practice for Monitoring Electric Power Quality. Revision of IEEE Std 1159-1995, 26 June 2009, pp. 91

[20] IEEE Recommended Practice and Requirements for Harmonic Control in Electric Power Systems, IEEE Std 519-2014 (Revision of IEEE Std 519-1992), pp. 29

[21] Pradeep Kumar et al (2013)" Modeling and Simulation of Different System Topologies for DSTATCOM", Published by Elsevier B.V., pp. 249-261

[22] Prasad Miska and Ashok Kumar Akella (2016) "Modeling and Simulation of SRF and PI Controlled DSTATCOM for power quality enhancement" International Journal of TechnoChem Research, Vol.02, No.02, pp 141-150

APPENDICES

Appendix A: Categories & characteristics of power system electromagnetic phenomena as presented on IEEE std 1159-2009: IEEE Recommended Practice for Monitoring Electric Power Quality.

Categories	Typical spectral content	Typical duration	Typical voltage magnitude
1.0 Transients			
1.1 Impulsive			
1.1.1 Nanosecond	5 ns rise	< 50 ns	
1.1.2 Microsecond	1 µs rise	50 ns – 1 ms	
1.1.3 Millisecond	0.1 ms rise	> 1 ms	
1.2 Oscillatory			
1.2.1 Low frequency	< 5 kHz	0.3–50 ms	0–4 pu[a]
1.2.2 Medium frequency	5–500 kHz	20 µs	0–8 pu
1.2.3 High frequency	0.5–5 MHz	5 µs	0–4 pu
2.0 Short-duration root-mean-square (rms) variations			
2.1 Instantaneous			
2.1.1 Sag		0.5–30 cycles	0.1–0.9 pu
2.1.2 Swell		0.5–30 cycles	1.1–1.8 pu
2.2 Momentary			
2.2.1 Interruption		0.5 cycles – 3 s	< 0.1 pu
2.2.2 Sag		30 cycles – 3 s	0.1–0.9 pu
2.2.3 Swell		30 cycles – 3 s	1.1–1.4 pu
2.3 Temporary			
2.3.1 Interruption		>3 s – 1 min	< 0.1 pu
2.3.2 Sag		>3 s – 1 min	0.1–0.9 pu
2.3.3 Swell		>3 s – 1 min	1.1–1.2 pu
3.0 Long duration rms variations			
3.1 Interruption, sustained		> 1 min	0.0 pu
3.2 Undervoltages		> 1 min	0.8–0.9 pu
3.3 Overvoltages		> 1 min	1.1–1.2 pu
3.4 Current overload		> 1 min	
4.0 Imbalance			
4.1 Voltage		steady state	0.5–2%
4.2 Current		steady state	1.0–30%
5.0 Waveform distortion			
5.1 DC offset		steady state	0–0.1%
5.2 Harmonics	0–9 kHz	steady state	0–20%
5.3 Interharmonics	0–9 kHz	steady state	0–2%
5.4 Notching		steady state	
5.5 Noise	broadband	steady state	0–1%
6.0 Voltage fluctuations	< 25 Hz	intermittent	0.1–7% 0.2–2 P_{st} [b]
7.0 Power frequency variations		< 10 s	± 0.10 Hz

Appendix B: Adama Spinning Factory Electrical Installation Layout (Finally revised on July, 2004)

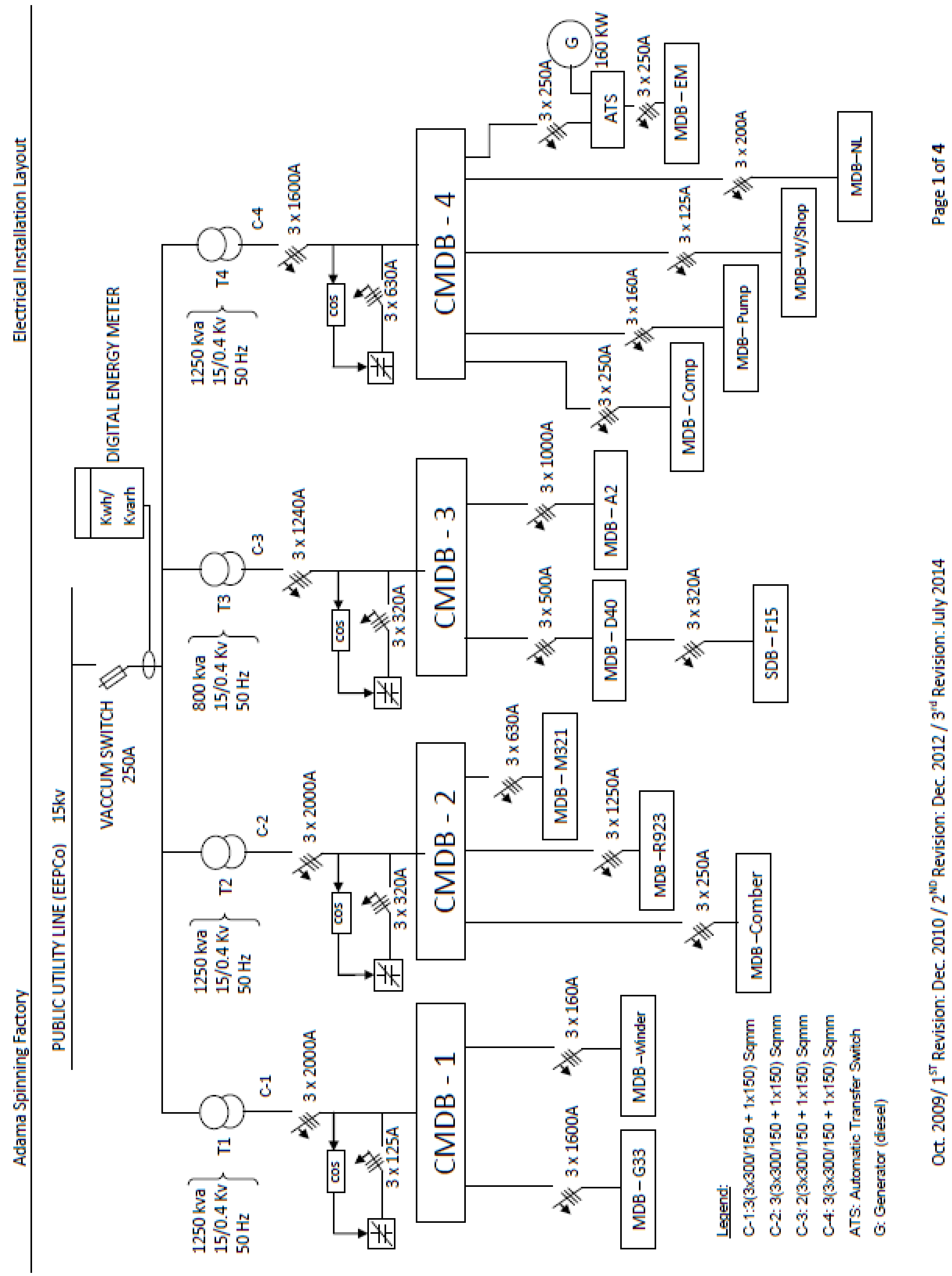

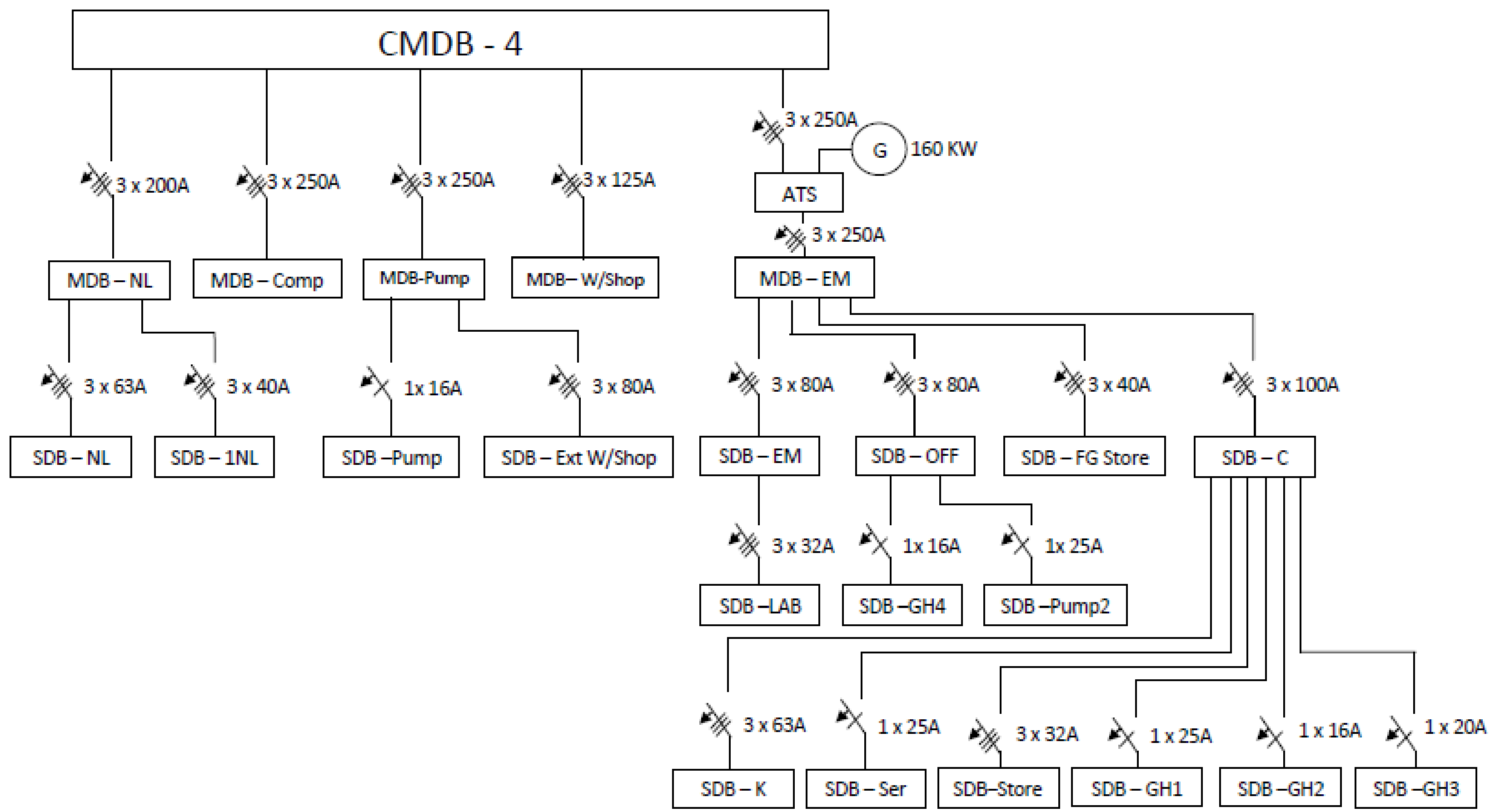
CMDB - 4
3 x 200A
3 x 250A
3 x 250A
3 x 125A
3 x 250A
G
160 KW
ATS
3 x 250A
MDB – NL
MDB – Comp
MDB-Pump
MDB– W/Shop
MDB – EM
3 x 63A
3 x 40A
1x 16A
3 x 80A
3 x 80A
3 x 80A
3 x 40A
3 x 100A
SDB – NL
SDB – 1NL
SDB –Pump
SDB – Ext W/Shop
SDB – EM
SDB – OFF
SDB – FG Store
SDB – C
3 x 32A
1x 16A
1x 25A
SDB –LAB
SDB –GH4
SDB –Pump2
3 x 63A
1 x 25A
3 x 32A
1 x 25A
1 x 16A
1 x 20A
SDB – K
SDB – Ser
SDB–Store
SDB – GH1
SDB –GH2
SDB –GH3

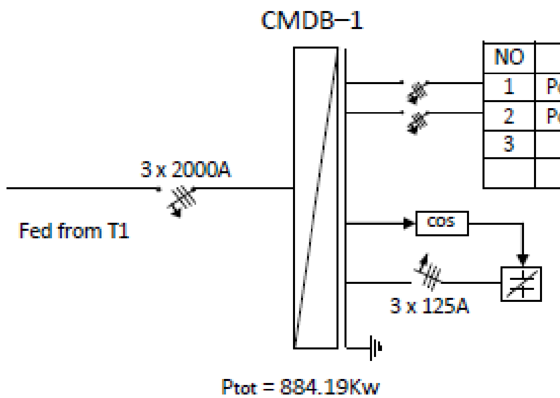

NO	Description	A(mm²)	I (A)	Load (KW)
1	Power to MDB – G33	5(3x150/70 + 1x70)	3 x 1600	652.80
2	Power to MDB - Winder	2(3x120/70 + 1x70)	3 x 630	231.39
3				

Automatic Power Factor
regulator (3 steps) 40 Kvar
2x10 Kvar
1x20 Kvar

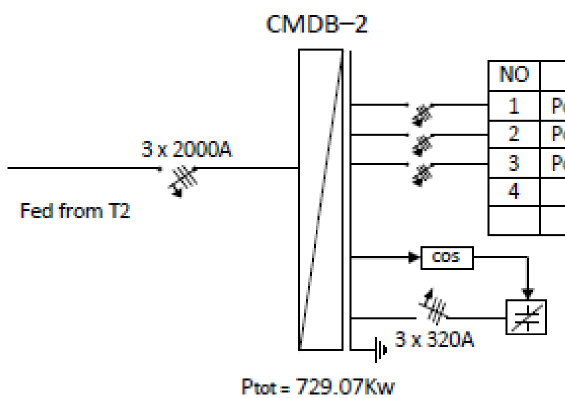

NO	Description	A(mm²)	I (A)	Load (KW)
1	Power to MDB – R923	4(3x150/70 + 1x70)	3 x 1250	392.00
2	Power to MDB – M321	2(3x150/70 + 1x70)	3 x 630	255.00
3	Power to MDB – Comber	3x120/70 + 1x70	3 x 250	82.07
4				

Automatic Power Factor
regulator (5 steps) 162.5 Kvar
1x12.5 Kvar
2x25 Kvar
2x50 Kvar

CMDB–3

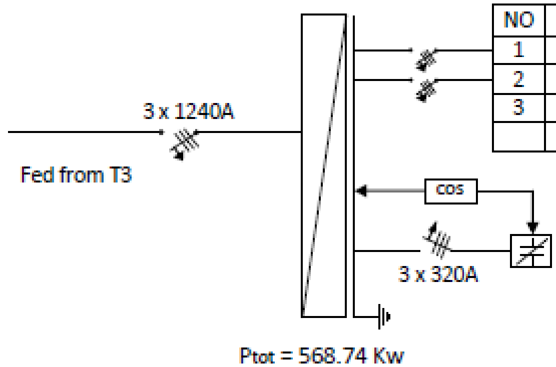

NO	Description	A(mm²)	I (A)	Load (KW)
1	Power to MDB – A2	4(3x120/70 + 1x70)	3 x 1000	368.16
2	Power to MDB – D40	2(3x120/70 + 1x70)	3 x 500	200.58
3				

Automatic Power Factor
regulator (5 steps) 150Kvar
2x12.5 Kvar
1x25 Kvar
2x50 Kvar

CMDB–4

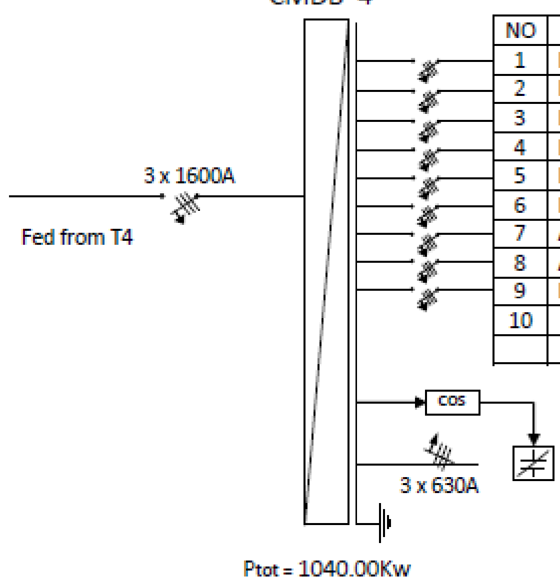

NO	Description	A(mm²)	I (A)	Load (KW)
1	Power to SDB - Comp	2(3 x 35/25)	3 x 250	95.60
2	Power to SDB - Workshop	3x35 + 1x16	3 x 125	40.8
3	Power to SDB - Pump	4x70	3 x 160	210.65
4	Power to MDB - NL	4x120	3 x 200	67
5	Power to MDB - EM	4x120	3 x 250	202.45
6	Bale Press	3x6 + 1x6	3 x 32	8.5
7	AC 1 and 2	2(4x150)	3 x 630	261
8	AC 3 and 4	2(4x95)	3 x 400	154
9	Reserve	-	3 x 63	-
10				

Automatic Power Factor
regulator (5 steps) 162.5 Kvar
1x12.5 Kvar
2x25 Kvar
2x50 Kvar

Appendix C: Adama Spinning Factory monthly energy consumption report of the last 26 months (January, 2016 - February, 2018)

	Company Name:	Document No:	
	ADAMA DEVELOPMENT PLC **Adama Spinning Factory**	**ADSF- OF- 367**	
Title	**Annual Electric Energy Consumption**	Revision No: **0**	Page : **1 of 1**

SPINNING **Fiscal Year: 2016-2018**

Meter Constant(KWh/KVARh):	6000	Contract No.:	5497013027374822764644
Power Factor Penality Block Rate(Birr):	68.37	Tariff Category:	41-ICS-INDUSTRIAL
Active Energy Block Rate(Birr/KWh):	0.5778	Meter Number:	ECE000064/516776
Service Charge(Birr):	53.57		

S/N	Consumption period			Active Energy		Reactive Energy		Max. Demand		Power Factor	PF Penality (Birr)	Active Energy Cost (Birr)	Total Payment (Birr)
	Month	Days	Reading Date	Reading	KWh	Reading	KVARh	Reading	MD (KWh)				
1	Jan, 2016	29	28-Jan-16	4266	408000	1849	186000	0.183	1098	0.90991	0.00	235,742.4	235,795.97
2	Feb, 2016	32	29-Feb-16	4359	558000	1890	246000	0.185	1110	0.91502	0.00	322,412.4	322,465.97
3	Mar, 2016	30	30-Mar-16	4444	510000	1926	216000	0.165	990	0.92082	0.00	294,678.0	294,731.57
4	Apr, 2016	28	27-Apr-16	4525	486000	1960	204000	0.193	1158	0.92206	0.00	280,810.8	280,864.37
5	May, 2016	33	30-May-16	4623	588000	2003	258000	0.21	1260	0.91573	0.00	339,746.4	339,799.97
6	Jun, 2016	29	28-Jun-16	4719	576000	2045	252000	0.19	1140	0.91616	0.00	332,812.8	332,866.37
7	Jul, 2016	30	28-Jul-16	4770	306000	2067	132000	0.18	1080	0.91821	0.00	176,806.8	176,860.37
8	Aug, 2016	32	29-Aug-16	4851	486000	2101	204000	0.18	1080	0.92206	0.00	280,810.8	280,864.37
9	Sep, 2016	35	3-Oct-16	4932	486000	2144	258000	0.170	1020	0.88326	1167.62	280,810.8	282,031.99
10	Oct, 2016	26	29-Oct-16	5007	450000	2185	246000	0.19	1140	0.87745	1757.74	260,010.0	261,821.31
11	Nov, 2016	33	1-Dec-16	5109	612000	2236	306000	0.18	1080	0.89443	411.49	353,613.6	354,078.66
12	Dec, 2016	27	28-Dec-16	5201	552000	2282	276000	0.19	1140	0.89443	434.35	318,945.6	319,433.52
13	Jan, 2017	33	30-Jan-17	5304	618000	2337	330000	0.18	1080	0.88212	1320.57	357,080.4	358,454.54
14	Feb, 2017	28	27-Feb-17	5400	576000	2390	318000	0.188	1128	0.87544	1893.74	332,812.8	334,760.11
15	Mar, 2017	30	29-Mar-17	5506	636000	2447	342000	0.213	1278	0.88074	1683.07	367,480.8	369,217.44
16	Apr, 2017	30	28-Apr-17	5610	624000	2503	336000	0.214	1284	0.88047	1714.39	360,547.2	362,315.16
17	May, 2017	31	29-May-17	5724	684000	2566	378000	0.278	1668	0.87524	2823.48	395,215.2	398,092.25
18	Jun, 2017	29	27-Jun-17	5827	618000	2622	336000	0.194	1164	0.87855	1707.31	357,080.4	358,841.28
19	Jul, 2017	30	27-Jul-17	5939	672000	2685	378000	0.198	1188	0.87158	2308.74	388,281.6	390,643.91
20	Aug, 2017	30	26-Aug-17	6057	708000	2750	390000	0.2	1200	0.8759	1977.07	409,082.4	411,113.04
21	Sep, 2017	34	29-Sep-17	6176	714000	2815	390000	0.200	1200	0.87761	1836.67	412,549.2	414,439.44
22	Oct, 2017	31	30-Oct-17	6305	774000	2885	420000	0.21	1260	0.87894	1814.67	447,217.2	449,085.44
23	Nov, 2017	29	28-Nov-17	6424	714000	2945	360000	0.204	1224	0.89292	592.37	412,549.2	413,195.14
24	Dec, 2017	31	29-Dec-17	6554	780000	3013	408000	0.218	1308	0.8861	1243.21	450,684.0	451,980.78
25	Jan, 2018	31	29-Jan-18	6674	720000	3075	372000	0.207	1242	0.88843	982.82	416,016.0	417,052.39
26	Feb, 2018	31	1-Mar-18	6796	732000	3137	372000	0.204	1224	0.89149	712.56	422,949.6	423,715.73

Appendix D: Measurement data taken from CMDB-1, 2, 3 and 4.

Table D.1: Measured data on CMDB-1.

CMDB-1																		
					Harmonic Distortion Current							Harmonic Distortion Voltage						
Date	Time	Cos φ	I-Sec.	V_{l-n}	THD-I	1st	3rd	5th	7th	9th	11th	THD-V	1st	3rd	5th	7th	9th	11th
17/3/2017	8:25AM	0.93	0.81	224	26.7	0.8	0.02	0.18	0.1	0	0.04	26.4	223	0	5	2	0	1
17/3/2017	11:34AM	0.94	0.93	219	25.8	0.92	0.02	0.2	0.1	0	0.04	2.3	220	0	3	2	0	1
17/3/2017	1:10PM	0.92	0.71	225	29.6	0.65	0.01	0.06	0.09	0	0.03	1.9	224	0	2	3	0	0
17/3/2017	1:40PM	0.93	0.72	224	28.6	0.7	0.01	0.17	0.09	0	0.03	2	223	0	2	3	0	0
17/3/2017	4:40PM	0.94	0.78	224	28.7	0.69	0.01	0.17	0.1	0	0.03	1.8	224	0	2	3	0	0
17/3/2017	5:00PM	0.94	0.62	227	29.9	0.6	0.02	0.15	0.08	0	0.03	1.9	227	0	3	2	0	0
20/3/2018	8:10AM	0.96	0.49	230	41.8	0.45	0.02	0.16	0.09	0	0.02	1.9	231	0	3	2	0	0
20/3/2018	8:30AM	0.96	0.65	226	33.8	0.61	0.02	0.17	0.1	0	0.03	2.4	225	0	4	2	0	1
20/3/2018	1:05PM	0.95	0.72	227	33.8	0.69	0.01	0.2	0.1	0	0.04	2.3	226	0	3	3	0	1
20/3/2018	2:00PM	0.95	0.77	226	34.1	0.73	0.02	0.22	0.1	0	0.04	2.5	227	0	3	3	0	1
20/3/2018	4:55PM	0.96	0.64	228	37.1	0.62	0.02	0.19	0.1	0	0.03	2.3	229	0	4	4	0	1
20/3/2018	5:05PM	0.96	0.46	230	38.1	0.49	0.01	0.17	0.09	0	0.02	2	231	0	3	3	0	1
22/3/2018	6:00PM	0.93	0.47	230	43.4	0.44	0.02	0.16	0.08	0	0.02	1.7	230	0	2	3	0	0
22/3/2018	7:00PM	0.96	0.51	229	38.6	0.47	0.02	0.18	0.09	0	0.03	2.3	231	0	4	3	0	1
22/3/2018	8:00PM	0.91	0.75	230	28.5	0.71	0.03	0.17	0.09	0	0.03	2.1	231	0	4	2	0	1
22/3/2018	9:00PM	0.92	0.69	229	29.6	0.66	0.03	0.17	0.09	0	0.03	2	229	0	3	2	0	1
22/3/2018	10:50PM	0.96	0.47	230	43.8	0.43	0.02	0.16	0.09	0	0.02	1.6	231	0	3	2	0	0
23/3/2018	3:30AM	0.95	0.48	228	34.7	0.45	0.02	0.12	0.06	0	0.02	2.4	228	0	5	2	0	0
23/3/2018	6:30AM	0.97	0.15	228	--	0.13	0.01	0.06	0.03	0	0	1.3	228	0	2	0	0	0
23/3/2018	8:15AM	0.91	0.08	227	--	0.07	0	0.03	0.02	0	0	0.6	232	0	0	1	0	0
23/3/2018	8:55AM	0.94	0.55	224	26	0.54	0.01	0.11	0.07	0	0.03	1.7	224	0	3	2	0	0
23/3/2018	1:00PM	0.93	0.63	226	26.9	0.61	0.01	0.16	0.08	0	0.03	1.7	226	0	2	3	0	0
23/3/2018	1:20PM	0.94	0.54	223	30.9	0.52	0.01	0.14	0.07	0	0.02	1.4	223	0	2	2	0	0
23/3/2018	5:00PM	0.95	0.58	225	28.2	0.55	0.01	0.13	0.07	0	0.02	1.6	227	0	3	1	0	0
23/3/2018	6:00PM	0.93	0.68	228	29.2	1.9	0.65	0.01	0.17	0.08	0	1.9	228	0	3	3	0	0
23/3/2018	7:00PM	0.97	0.47	233	37.2	0.34	0.01	0.11	0.06	0	0.02	1.5	233	0	2	2	0	0
23/3/2018	8:00PM	0.97	0.2	233	--	0.19	0.01	0.07	0.04	0	0.01	1	233	0	1	1	0	0
23/3/2018	9:00PM	0.95	0.72	229	34.7	0.68	0.02	0.2	0.09	0	0.04	2.3	230	0	2	2	0	1

Note: "--"is displayed when the actual values are very small and outside the measuring range of the device. The shaded boxes represent a value which has a very high variation from the mean of all the recorded data.

Table D.2: Measured data on CMDB-2.

CMDB-2																		
					Harmonic Distortion Current							**Harmonic Distortion Voltage**						
Date	**Time**	**Cos φ**	**I-Sec.**	**$V_{l\text{-}n}$**	**THD-I**	**1^{st}**	**3^{rd}**	**5^{th}**	**7^{th}**	**9^{th}**	**11^{th}**	**THD-V**	**1^{st}**	**3^{rd}**	**5^{th}**	**7^{th}**	**9^{th}**	**11^{th}**
3/4/2018	10:45AM	0.84	0.91	215	14.2	0.91	0	0.11	0.05	0	0.02	1.3	216	0	1	2	0	1
3/4/2018	11:05AM	0.84	0.89	215	12.9	0.88	0	0.09	0.06	0	0.01	1.1	215	0	1	1	0	0
3/4/2018	1:50PM	0.84	0.98	217	16.8	0.96	0.01	0.11	0.06	0	0.02	1.4	218	0	1	1	0	0
3/4/2018	2:50PM	0.84	0.8	216	15.1	0.79	0.01	0.1	0.06	0	0.02	1.4	217	0	2	1	0	0
3/4/2018	4:00PM	0.84	0.82	216	17.5	0.82	0.01	0.12	0.06	0	0.02	1.4	217	0	2	2	0	0
3/4/2018	4:20PM	0.86	0.96	213	14.4	0.96	0.01	0.11	0.06	0	0.02	1.4	213	0	2	1	0	0
3/4/2018	7:00PM	0.84	0.95	214	14.8	0.93	0.02	0.13	0.06	0	0.02	1.5	215	0	2	2	0	0
3/4/2018	9:00PM	0.82	0.98	221	15.8	0.96	0.01	0.13	0.06	0	0.02	1.5	221	0	1	2	0	0
3/4/2018	11:00PM	0.83	0.96	220	15	0.96	0.02	0.12	0.06	0	0.02	1.5	220	0	2	2	0	0
4/4/2018	3:00AM	0.83	0.94	219	13	0.91	0.02	0.12	0.06	0	0.02	1.5	220	0	2	2	0	0
4/4/2018	10:20AM	0.86	0.95	212	12.5	0.92	0.01	0.08	0.06	0	0.02	1.4	213	0	2	1	0	0
4/4/2018	10:40AM	0.85	0.95	213	14.1	0.98	0.01	0.11	0.06	0	0.02	1.3	214	0	2	1	0	0
4/4/2018	2:00PM	0.81	0.93	219	16.6	0.92	0	0.13	0.06	0	0.02	1.3	219	0	1	2	0	0
4/4/2018	2:40PM	0.82	0.94	218	16.1	0.92	0.01	0.13	0.06	0	0.02	1.4	218	0	1	2	0	0
4/4/2018	4:35PM	0.85	1.09	215	12.4	0.97	0	0.11	0.06	0	0.02	1.3	215	0	1	2	0	0
5/4/2018	1:35PM	0.84	0.93	214	14.6	0.94	0.01	0.11	0.06	0	0.02	1.5	214	0	2	1	0	0
5/4/2018	2:00PM	0.85	0.94	215	14.2	0.9	0.01	0.11	0.06	0	0.02	1.3	215	0	2	1	0	0
5/4/2018	3:20PM	0.85	0.94	215	14.2	0.94	0	0.11	0.06	0	0.02	1.2	215	0	2	1	0	0
5/4/2018	4:00PM	0.83	0.95	218	16.7	0.94	0	0.13	0.06	0	0.02	1.2	218	0	1	2	0	1
5/4/2018	6:30PM	0.84	0.94	216	16.4	0.94	0.01	0.11	0.06	0	0.02	1.2	215	0	2	1	0	1
5/4/2018	7:50PM	0.84	0.93	218	15.2	0.92	0	0.11	0.06	0	0.02	1.3	215	0	1	2	0	1
6/4/2018	11:10AM	--	0.01	227	--	0.01	0	0	0	0	0	0.7	0.01	0	0	0	0	0
7/4/2018	8:00AM	--	0.01	226	--	0.01	0	0	0	0	0	0.5	226	0	0	0	0	0.5
7/4/2018	10:30AM	0.95	0.03	225	--	0.03	0	0	0	0	0	0.7	225	0	0	1	0	1
7/4/2018	1:00PM	0.95	0.03	225	--	0.03	0	0	0	0	0	0.7	225	0	0	1	0	1
9/4/2018	5:00AM	0.95	0.03	228	--	0.03	0	0	0	0	0	0.7	225	0	0	1	0	1
10/4/2018	7:00AM	0.91	0.35	222	13.2	0.35	0	0.03	0.02	0	0	0.5	222	0	1	0	0	0.5

Note: "--"is displayed when the actual values are very small and outside the measuring range of the device.

Table D.3: Measured data on CMDB-3.

CMDB-3																		
					Harmonic Distortion Current							Harmonic Distortion Voltage						
Date	Time	Cos φ	I-Sec.	V_{l-n}	THD-I	1st	3rd	5th	7th	9th	11th	THD-V	1st	3rd	5th	7th	9th	11th
10/4/2018	9:45AM	0.87	0.7	217	17.6	0.57	0.01	0.08	0.06	0	0.01	1.1	218	1	1	2	0	0
10/4/2018	10:45AM	0.86	1.05	216	20.9	1.06	0.01	0.18	0.08	0	0.02	1.5	218	0	1	2	0	1
10/4/2018	2:00PM	0.82	0.99	217	22.6	0.99	0.01	0.18	0.09	0	0.02	1.6	216	0	1	2	0	0
10/4/2018	2:25PM	0.8	0.84	220	22.1	0.82	0.01	0.15	0.09	0	0.02	1.5	220	0	2	2	0	0
10/4/2018	3:05PM	0.83	1.1	216	21.9	1	0.02	0.19	0.1	0	0.02	1.8	216	0	3	2	0	1
10/4/2018	4:10PM	0.85	0.79	218	21.7	0.83	0.01	0.16	0.08	0	0.01	1.2	218	0	1	2	0	0
10/4/2018	6:00PM	0.86	0.81	219	19.9	0.83	0.01	0.14	0.08	0	0.01	1.2	219	0	1	2	0	0
10/4/2018	6:30PM	0.84	0.82	220	20.4	0.68	0.01	0.12	0.07	0	0.01	1.2	219	0	1	2	0	0
10/4/2018	9:00PM	0.87	0.42	220	22.8	0.38	0.01	0.06	0.03	0	0.01	1.2	220	0	1	2	0	0
10/4/2018	9:30PM	0.81	0.61	221	22.5	0.55	0.01	0.11	0.05	0	0.01	1.4	221	0	1	2	0	0
11/4/2018	10:18AM	--	0.01	228	--	0.01	0	0	0	0	0	0.7	227	0	0	0	0	0
11/4/2018	10:50AM	0.9	0.08	220	--	0.03	0	0	0	0	0	0.7	221	0	0	1	0	0
11/4/2018	2:10PM	0.88	0.55	217	23.1	0.54	0.01	0.1	0.07	0	0.01	1.3	216	0	1	2	0	0
11/4/2018	3:50PM	0.84	0.99	216	23.2	0.99	0.02	0.19	0.1	0	0.01	2.1	216	0	4	2	0	1
11/4/2018	7:30PM	0.81	0.6	220	24.6	0.66	0.02	0.12	0.06	0	0.01	1.8	220	1	2	3	0	0
11/4/2018	2:00PM	0.85	0.92	220	23.1	0.9	0.01	0.16	0.07	0	0.01	1.8	220	0	2	3	0	0
11/4/2018	9:00PM	0.81	0.65	220	20.9	0.71	0.01	0.13	0.07	0	0.01	1.7	219	0	1	3	0	0
11/4/2018	9:30PM	0.82	0.75	221	18.9	0.72	0.01	0.14	0.07	0	0.01	1.5	221	0	0	3	0	0
11/4/2018	10:00PM	0.86	0.6	221	23.1	0.56	0.02	0.14	0.07	0	0.01	1.7	218	1	2	3	0	0
12/4/2018	12:00AM	0.86	0.71	223	22.8	0.65	0.01	0.18	0.09	0	0.02	1.6	218	0	1	2	0	0
12/4/2018	2:00AM	0.85	0.9	222	23.1	0.66	0.02	0.16	0.08	0	0.01	1.5	220	1	1	3	0	1
12/4/2018	4:05AM	0.85	0.76	223	20.9	0.82	0.01	0.19	0.06	0	0.02	1.8	221	0	1	2	0	1
12/4/2018	6:00AM	0.85	0.72	219	22.6	0.74	0.01	0.18	0.07	0	0.02	1.8	222	1	1	2	0	1

Note: "--"is displayed when the actual values are very small and outside the measuring range of the device.

Table D.4: Measured data on CMDB-4.

CMDB-4																		
					Harmonic Distortion Current							Harmonic Distortion Voltage						
Date	**Time**	**Cos φ**	**I-Sec.**	**V_{l-n}**	**THD-I**	**1st**	**3rd**	**5th**	**7th**	**9th**	**11th**	**THD-V**	**1st**	**3rd**	**5th**	**7th**	**9th**	**11th**
12/4/2018	9:20AM	0.91	2.37	218	2.1	2.43	0.03	0.03	0.01	0	0.01	1.3	218	0	2	1	0	0
12/4/2018	1:00PM	0.89	2.51	224	1.7	2.43	0.02	0.01	0.02	0	0.01	1.1	224	0	2	1	0	0
12/4/2018	10:15PM	0.91	2.68	219	1.8	2.65	0.02	0.02	0.03	0	0.01	1.5	220	0	2	1	0	0
12/4/2018	6:00PM	0.89	2.57	222	1.8	2.65	0.02	0.03	0.03	0	0.01	1.4	222	0	2	1	0	0
12/4/2018	9:25PM	0.89	2.68	224	1.7	2.53	0.03	0.02	0.02	0	0.01	1.3	220	0	2	1	0	0
12/4/2018	10:00PM	0.87	2.29	227	2.6	2.12	0.04	0.03	0.02	0	0.01	1.2	227	0	2	2	0	1
12/4/2018	10:33PM	0.87	2.24	227	2.6	2.19	0.04	0.02	0.02	0	0.01	0.01	228	0	1	2	0	0
12/4/2018	10:55PM	0.88	2.32	224	2.5	2.22	0.04	0.01	0.02	0	0.01	0.08	225	0	1	1	0	0
12/4/2018	11:58PM	0.89	2.18	224	2.4	2.13	0.04	0	0.01	0	0.02	1.2	224	0	2	1	0	1
13/4/2018	1:30AM	0.87	2.18	225	2.7	2.32	0.03	0.03	0.01	0	0.01	2.4	225	0	3	1	0	1
13/4/2018	2:30AM	0.87	2.26	226	2.6	2.24	0.04	0.03	0	0	0.01	2.7	226	0	2	0	0	0
13/4/2018	5:00AM	0.88	2.12	226	2.2	2.12	0.04	0.01	0.01	0	0	0.8	226	0	1	1	0	0
13/4/2018	6:00AM	0.87	2.06	224	2	2.17	0.04	0.01	0	0	0	0.07	224	0	1	1	0	0
13/4/2018	7:00AM	0.88	2.24	222	2.2	2.11	0.03	0.02	0.01	0	0	1.1	222	0	2	1	0	0
13/4/2018	9:55AM	0.9	2.45	221	1.2	2.46	0.03	0.03	0.01	0.01	0	0.9	221	0	1	2	0	6
13/4/2018	1:00PM	0.9	2.43	224	2.1	2.43	0.03	0.03	0.02	0	0	0.8	224	0	1	1	0	0
13/4/2018	3:25PM	0.9	2.57	222	2.1	2.57	0.03	0.03	0.02	0	0.01	0.6	223	0	0	1	0	0
14/4/2018	4:30PM	0.89	2.3	222	2.3	2.2	0.03	0.03	0.02	0	0	0.4	223	0	0	0	0	0
14/4/2018	5:00PM	0.9	2.48	221	2	2.45	0.03	0.02	0.02	0	0.01	0.7	221	0	1	1	0	0
14/4/2018	8:00PM	0.89	2.35	221	2.5	2.35	0.04	0.03	0.01	0	0	0.7	222	0	0	1	0	0
14/4/2018	8:30PM	0.89	2.34	222	2.5	2.33	0.04	0.03	0.02	0	0	0.7	222	0	0	1	0	0
14/4/2018	9:00PM	0.89	2.38	223	2.8	2.41	0.04	0.04	0.02	0	0	0.9	223	0	0	2	0	0
14/4/2018	9:30PM	0.88	2.23	224	2.7	2.32	0.04	0.03	0.01	0	0	0.8	224	0	0	1	0	0
14/4/2018	10:00PM	0.87	2.23	225	2.9	2.21	0.04	0.04	0.01	0	0	0.07	226	0	1	1	0	0
14/4/2018	11:00PM	0.88	2.18	226	2	2.17	0.04	0.04	0.01	0	0	0.8	227	0	0	2	0	0
15/4/2018	2:00AM	0.87	2.23	228	2.5	2.18	0.04	0.02	0	0	0	0.08	228	0	0	1	0	0
15/4/2018	5:00AM	0.88	2.11	226	2.2	2.09	0.04	0.01	0	0	0	0.07	226	0	0	1	0	0
15/4/2018	6:00AM	0.88	2.24	226	2.2	2.22	0.04	0.01	0	0	0	0.07	226	0	0	1	0	0
15/4/2018	7:00AM	0.87	2.19	227	2	2.12	0.04	0.01	0	0	0	0.05	227	0	0	1	0	0

Note: The shaded boxes represent a value which has a very high variation from the mean of all the recorded data.